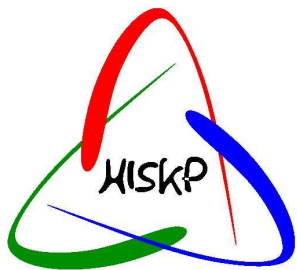


Nucleon resonances extracted from Bonn-Gatchina coupled channel analysis

A. Sarantsev



Petersburg
Nuclear
Physics
Institute

HISKP (Bonn), PNPI (Russia)

NSTAR 2011

17-20 May 2011, JLAB, USA

Bonn-Gatchina partial wave analysis group:

A. Anisovich, E. Klempt, V. Nikonov, A. Srantsev, U. Thoma

<http://pwa.hiskp.uni-bonn.de/>



Bonn-Gatchina Partial Wave Analysis



Address: Nussallee 14-16, D-53115 Bonn Fax: (+49) 228 / 73-2505

<u>Data Base</u>	<u>Meson Spectroscopy</u>	<u>Baryon Spectroscopy</u>	<u>NN-interaction</u>	<u>Formalism</u>
<p>Analysis of Other Groups</p> <ul style="list-style-type: none"> • SAID • MAID • Giessen Uni 		<p>BG PWA</p> <ul style="list-style-type: none"> • Publications • Talks • Contacts 		<p>Useful Links</p> <ul style="list-style-type: none"> • SPIRES • PDG Homepage • Durham Data Base • Bonn Homepage
<p>CB-ELSA Homepage</p>				

Responsible: Dr. V. Nikonov, E-mail: nikonov@hiskp.uni-bonn.de
 Last changes: January 26th, 2010.

Search for baryon states

1. Analysis of single meson and double meson photoproduction reactions.

$\gamma p \rightarrow \pi N, \eta N, K \Lambda, K \Sigma, \pi \pi N, \pi \eta N$, CB-ELSA, CLAS, GRAAL, LEPS.

2. Analysis of single meson and double meson pion-induced reactions.

$\pi N \rightarrow \pi N, \eta N, K \Lambda, K \Sigma, \pi \pi N$.

Search for meson states

1. Analysis of the $p\bar{p}$ annihilation at rest and $\pi\pi$ interaction data.
2. Analysis of the $p\bar{p}$ annihilation in flight into two and three meson final state.
3. Analysis of the J/Ψ decays (BES III collaboration).

Analysis of NN interaction

1. Analysis of single and double meson production $NN \rightarrow \pi NN$ and $\pi\pi NN$
2. Analysis of hyperon production $NN \rightarrow K \Lambda p$

Energy dependent approach

In many cases an unambiguous partial wave decomposition at fixed energies is impossible. Then the energy and angular parts should be analyzed together:

$$A(s, t) = \sum_{\beta\beta'n} A_n^{\beta\beta'}(s) Q_{\mu_1 \dots \mu_n}^{(\beta)+} F_{\nu_1 \dots \nu_n}^{\mu_1 \dots \mu_n} Q_{\nu_1 \dots \nu_n}^{(\beta')}$$

1. C. Zemach, Phys. Rev. 140, B97 (1965); 140, B109 (1965).
2. S.U.Chung, Phys. Rev. D 57, 431 (1998).
3. A.V. Anisovich *et al.* J. Phys. G 28 15 (2002)
 V. V. Anisovich, M. A. Matveev, V. A. Nikonov, J. Nyiri and A. V. Sarantsev,
Hackensack, USA: World Scientific (2008) 580 p
 1. Correlations between angular part and energy part are under control.
 2. Unitarity and analyticity can be introduced from the beginning.
 3. Parameters are be fixed from combined fit of many reactions.

πN vertices

$$N_{\mu_1 \dots \mu_n}^+ = X_{\mu_1 \dots \mu_n}^{(n)} \quad N_{\mu_1 \dots \mu_n}^- = i\gamma_\nu \gamma_5 X_{\nu \mu_1 \dots \mu_n}^{(n+1)} \quad (1)$$

γN vertices

$$\begin{aligned} Q_{\alpha_1 \dots \alpha_n}^{(1+)\mu} &= \gamma_\mu i\gamma_5 X_{\alpha_1 \dots \alpha_n}^{(n)} , & Q_{\alpha_1 \dots \alpha_n}^{(1-)\mu} &= \gamma_\xi \gamma_\mu O_{\xi \alpha_1 \dots \alpha_n}^{(n+1)} , \\ Q_{\alpha_1 \dots \alpha_n}^{(2+)\mu} &= \gamma_\nu i\gamma_5 X_{\mu \nu \alpha_1 \dots \alpha_n}^{(n+2)} , & Q_{\alpha_1 \dots \alpha_n}^{(2-)\mu} &= X_{\mu \alpha_1 \dots \alpha_n}^{(n+1)} , \\ Q_{\alpha_1 \dots \alpha_n}^{(3+)\mu} &= \gamma_\nu i\gamma_5 X_{\nu \alpha_1 \dots \alpha_n}^{(n+1)} g_{\mu \alpha_n}^\perp , & Q_{\alpha_1 \dots \alpha_n}^{(3-)\mu} &= X_{\alpha_2 \dots \alpha_n}^{(n-1)} g_{\alpha_1 \mu}^\perp . \end{aligned}$$

Fermion propagator for $J = N + \frac{1}{2}$

$$F_{\nu_1 \dots \nu_L}^{\mu_1 \dots \mu_L}(p) = (m + \hat{p}) O_{\alpha_1 \dots \alpha_L}^{\mu_1 \dots \mu_L} \frac{L+1}{2L+1} \left(g_{\alpha_1 \beta_1}^\perp - \frac{L}{L+1} \sigma_{\alpha_1 \beta_1} \right) \prod_{i=2}^L g_{\alpha_i \beta_i} O_{\nu_1 \dots \nu_L}^{\beta_1 \dots \beta_L}$$

$$\sigma_{\alpha_i \alpha_j} = \frac{1}{2} (\gamma_{\alpha_i} \gamma_{\alpha_j} - \gamma_{\alpha_j} \gamma_{\alpha_i})$$

Combined analysis of pion- and photo-production data:

For pion induced reactions:

$$A_{1i} = K_{1j}(I - i\rho K)_{ji}^{-1}$$

and

$$K_{ij} = \sum_{\alpha} \frac{g_i^{\alpha} g_j^{\alpha}}{M_{\alpha}^2 - s} + f_{ij}(s) \quad f_{ij} = \frac{f_{ij}^{(1)} + f_{ij}^{(2)} \sqrt{s}}{s - s_0^{ij}}.$$

where f_{ij} is nonresonant transition part.

For the photoproduction:

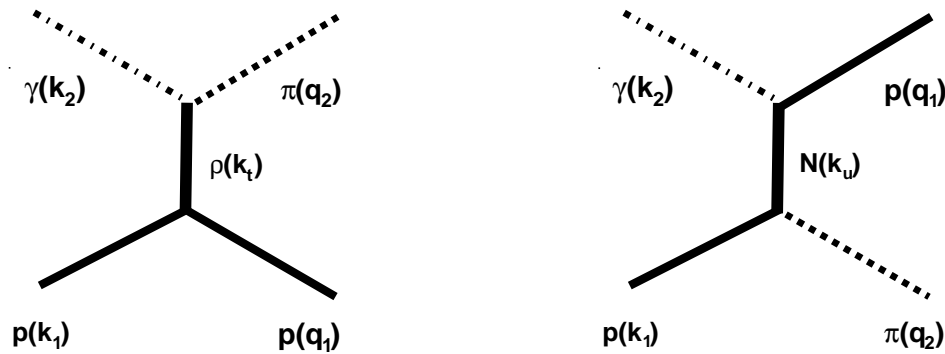
$$A_k = P_j(I - i\rho K)_{jk}^{-1}$$

The vector of the initial interaction has the form:

$$P_j = \sum_{\alpha} \frac{\Lambda^{\alpha} g_j^{\alpha}}{M_{\alpha}^2 - s} + F_j(s)$$

Here F_j is nonresonant production of the final state j .

Reggeized exchanges:



The amplitude for t-channel exchange:

$$A = g_1(t)g_2(t)R(\xi, \nu, t) = g_1(t)g_2(t) \frac{1 + \xi \exp(-i\pi\alpha(t))}{\sin(\pi\alpha(t))} \left(\frac{\nu}{\nu_0}\right)^{\alpha(t)} \quad \nu = \frac{1}{2}(s - u).$$

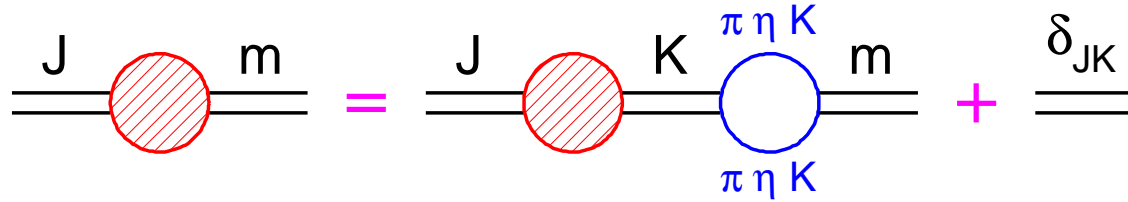
Here $\alpha(t)$ is Reggion trajectory, and ξ is its signature:

$$R(+, \nu, t) = \frac{e^{-i\frac{\pi}{2}\alpha(t)}}{\sin(\frac{\pi}{2}\alpha(t))\Gamma\left(\frac{\alpha(t)}{2}\right)} \left(\frac{\nu}{\nu_0}\right)^{\alpha(t)},$$

$$R(-, \nu, t) = \frac{ie^{-i\frac{\pi}{2}\alpha(t)}}{\cos(\frac{\pi}{2}\alpha(t))\Gamma\left(\frac{\alpha(t)}{2} + \frac{1}{2}\right)} \left(\frac{\nu}{\nu_0}\right)^{\alpha(t)}.$$

N/D based analysis of the data

In the case of resonance contributions only we have factorization and Bethe-Salpeter equation can be easily solved:



$$A_{jm} = A_{jk} \sum_{\alpha} B_{\alpha}^{km}(s) \frac{1}{M_m - s} + \frac{\delta_{jm}}{M_j^2 - s} \quad B_{\alpha}^{km}(s) = \int_{4m_{\alpha}^2}^{\infty} \frac{ds'}{\pi} \frac{g_{\alpha}^{(k)}(s') \rho_{\alpha}(s') g_{\alpha}^{(m)}(s')}{s' - s - i0}$$

$$\hat{A} = \hat{\kappa}(I - \hat{B}\hat{\kappa})^{-1} \quad \kappa_{ij} = \frac{\delta_{ij}}{M_i^2 - s} \quad B^{ij} = \sum_{\alpha} B_{\alpha}^{km}(s)$$

There is no factorization for non-resonant contributions: for every non-resonant transition to introduce a vertices and propagator (e.g. $R = 1$).

$$B_{\alpha}^{km}(s) = B_{\alpha}^{km}(M_s^2) + (s - M_s^2) \int_{4m_{\alpha}^2}^{\infty} \frac{ds'}{\pi} \frac{g_{\alpha}^{(k)}(s') \rho_{\alpha}(s') g_{\alpha}^{(m)}(s')}{(s' - s - i0)(s' - M_s^2)}$$

Data Base

Pion induced reactions (χ^2 analysis).

Observable	N_{data}	$\frac{\chi^2}{N_{\text{data}}}$		Observable	N_{data}	$\frac{\chi^2}{N_{\text{data}}}$	
$N_{1/2-}^*$ S ₁₁ ($\pi N \rightarrow \pi N$)	112	2.05	SAID (2.10)	$\Delta_{1/2-}$ S ₃₁ ($\pi N \rightarrow \pi N$)	112	2.31	SAID (2.10)
$N_{1/2+}^*$ P ₁₁ ($\pi N \rightarrow \pi N$)	112	2.49	SAID (2.10)	$\Delta_{1/2+}$ P ₃₁ ($\pi N \rightarrow \pi N$)	104	3.81	SAID (2.10)
$N_{3/2+}^*$ P ₁₃ ($\pi N \rightarrow \pi N$)	112	1.33	SAID (2.20)	$\Delta_{3/2+}^*$ P ₃₃ ($\pi N \rightarrow \pi N$)	120	2.79	SAID (2.20)
$N_{3/2-}^*$ D ₁₃ ($\pi N \rightarrow \pi N$)	108	2.55	SAID (2.20)	$\Delta_{3/2-}^*$ D ₃₃ ($\pi N \rightarrow \pi N$)	108	2.47	SAID (2.10)
$N_{5/2-}^*$ D ₁₅ ($\pi N \rightarrow \pi N$)	140	2.37	SAID (2.40)	$N_{7/2-}^*$ G ₁₇ ($\pi N \rightarrow \pi N$)	102	2.54	SAID (2.40)
$N_{5/2+}^*$ F ₁₅ ($\pi N \rightarrow \pi N$)	88	1.72	SAID (2.20)	$\Delta_{5/2+}$ F ₃₅ ($\pi N \rightarrow \pi N$)	62	1.45	SAID (2.10)
$N_{7/2+}^*$ F ₁₇ ($\pi N \rightarrow \pi N$)	82	1.98	SAID (2.50)	$\Delta_{7/2+}$ F ₃₇ ($\pi N \rightarrow \pi N$)	72	2.75	SAID (2.10)
$N_{9/2-}^*$ G ₁₉ ($\pi N \rightarrow \pi N$)	74	2.82	SAID (2.50)	$N_{9/2+}^*$ H ₁₉ ($\pi N \rightarrow \pi N$)	86	2.56	SAID (2.50)
$d\sigma/d\Omega(\pi^- p \rightarrow n\eta)$	70	1.58	Richards <i>et al.</i>	$d\sigma/d\Omega(\pi^- p \rightarrow n\eta)$	84	2.73	CBALL
$d\sigma/d\Omega(\pi^- p \rightarrow K\Lambda)$	598	1.67	RAL	$P(\pi^- p \rightarrow K\Lambda)$	355	1.67	RAL+ANL
				$\beta(\pi^- p \rightarrow K\Lambda)$	72	1.04	RAL
$d\sigma/d\Omega(\pi^+ p \rightarrow K^+\Sigma)$	609	1.25	RAL	$P(\pi^+ p \rightarrow K^+\Sigma)$	307	1.43	RAL
				$\beta(\pi^+ p \rightarrow K^+\Sigma)$	7	2.08	RAL
$d\sigma/d\Omega(\pi^- p \rightarrow K^0\Sigma^0)$	259	0.88	RAL	$P(\pi^- p \rightarrow K^0\Sigma^0)$	95	1.35	RAL

Data Base

π and η photoproduction reactions (χ^2 analysis).

Observable	N_{data}	$\frac{\chi^2}{N_{\text{data}}}$		Observable	N_{data}	$\frac{\chi^2}{N_{\text{data}}}$	
$d\sigma/d\Omega(\gamma p \rightarrow p\pi^0)$	1106	1.56	CB-ELSA	$d\sigma/d\Omega(\gamma p \rightarrow p\pi^0)$	861	1.58	GRAAL
$d\sigma/d\Omega(\gamma p \rightarrow p\pi^0)$	592	1.27	CLAS	$d\sigma/d\Omega(\gamma p \rightarrow p\pi^0)$	1692	2.00	TAPS@MAMI
$\Sigma(\gamma p \rightarrow p\pi^0)$	540	0.71	CB-ELSA	$\Sigma(\gamma p \rightarrow p\pi^0)$	1492	2.48	SAID db
$E(\gamma p \rightarrow p\pi^0)$	140	1.14	A2-GDH				
$P(\gamma p \rightarrow p\pi^0)$	607	2.98	SAID db	$T(\gamma p \rightarrow p\pi^0)$	389	3.15	SAID db
$H(\gamma p \rightarrow p\pi^0)$	71	1.17	SAID db	$G(\gamma p \rightarrow p\pi^0)$	75	1.70	SAID db
$O_x(\gamma p \rightarrow p\pi^0)$	7	1.14	SAID db	$O_z(\gamma p \rightarrow p\pi^0)$	7	0.27	SAID db
$d\sigma/d\Omega(\gamma p \rightarrow n\pi^+)$	484	1.45	CLAS	$d\sigma/d\Omega(\gamma p \rightarrow n\pi^+)$	1583	1.53	SAID db
$d\sigma/d\Omega(\gamma p \rightarrow n\pi^+)$	408	0.55	A2-GDH				
$\Sigma(\gamma p \rightarrow n\pi^+)$	899	2.95	SAID db	$E(\gamma p \rightarrow n\pi^+)$	231	1.52	A2-GDH
$P(\gamma p \rightarrow n\pi^+)$	252	2.00	SAID db	$T(\gamma p \rightarrow n\pi^+)$	661	2.87	SAID db
$H(\gamma p \rightarrow p\pi^+)$	71	4.20	SAID db	$G(\gamma p \rightarrow p\pi^+)$	86	5.67	SAID db
$d\sigma/d\Omega(\gamma p \rightarrow p\eta)$	680	1.23	CB-ELSA	$d\sigma/d\Omega(\gamma p \rightarrow p\eta)$	100	2.26	TAPS
$\Sigma(\gamma p \rightarrow p\eta)$	51	1.90	GRAAL 98	$\Sigma(\gamma p \rightarrow p\eta)$	100	2.43	GRAAL 07
$T(\gamma p \rightarrow p\eta)$	50	1.39	Phoenics				

Data Base

Kaon photoproduction (χ^2 analysis).

Observable	N_{data}	$\frac{\chi^2}{N_{\text{data}}}$		Observable	N_{data}	$\frac{\chi^2}{N_{\text{data}}}$	
$d\sigma/d\Omega(\gamma p \rightarrow \Lambda K^+)$	1320	0.78	CLAS09	$d\sigma/d\Omega(\gamma p \rightarrow \Sigma^0 K^+)$	1280	1.98	CLAS
$P(\gamma p \rightarrow \Lambda K^+)$	1270	1.75	CLAS09	$P(\gamma p \rightarrow \Sigma^0 K^+)$	95	1.53	CLAS
$C_x(\gamma p \rightarrow \Lambda K^+)$	160	1.44	CLAS	$C_x(\gamma p \rightarrow \Sigma^0 K^+)$	94	2.36	CLAS
$C_z(\gamma p \rightarrow \Lambda K^+)$	160	1.53	CLAS	$C_z(\gamma p \rightarrow \Sigma^0 K^+)$	94	1.62	CLAS
$\Sigma(\gamma p \rightarrow \Lambda K^+)$	66	3.32	GRAAL	$\Sigma(\gamma p \rightarrow \Sigma^0 K^+)$	42	1.80	GRAAL
$\Sigma(\gamma p \rightarrow \Lambda K^+)$	45	2.34	LEP	$\Sigma(\gamma p \rightarrow \Sigma^0 K^+)$	45	1.31	LEP
$T(\gamma p \rightarrow \Lambda K^+)$	66	1.35	GRAAL 09	$d\sigma/d\Omega(\gamma p \rightarrow \Sigma^+ K^0)$	48	3.41	CLAS
$O_x(\gamma p \rightarrow \Lambda K^+)$	66	1.70	GRAAL 09	$d\sigma/d\Omega(\gamma p \rightarrow \Sigma^+ K^0)$	72	0.67	CB-ELSA 10
$O_z(\gamma p \rightarrow \Lambda K^+)$	66	1.66	GRAAL 09	$P(\gamma p \rightarrow \Sigma^+ K^0)$	24	1.17	CB-ELSA 10
$P(\gamma p \rightarrow \Lambda K^+)$	84	0.60	GRAAL	$\Sigma(\gamma p \rightarrow \Sigma^+ K^0)$	15	1.39	CB-ELSA 10

Data Base

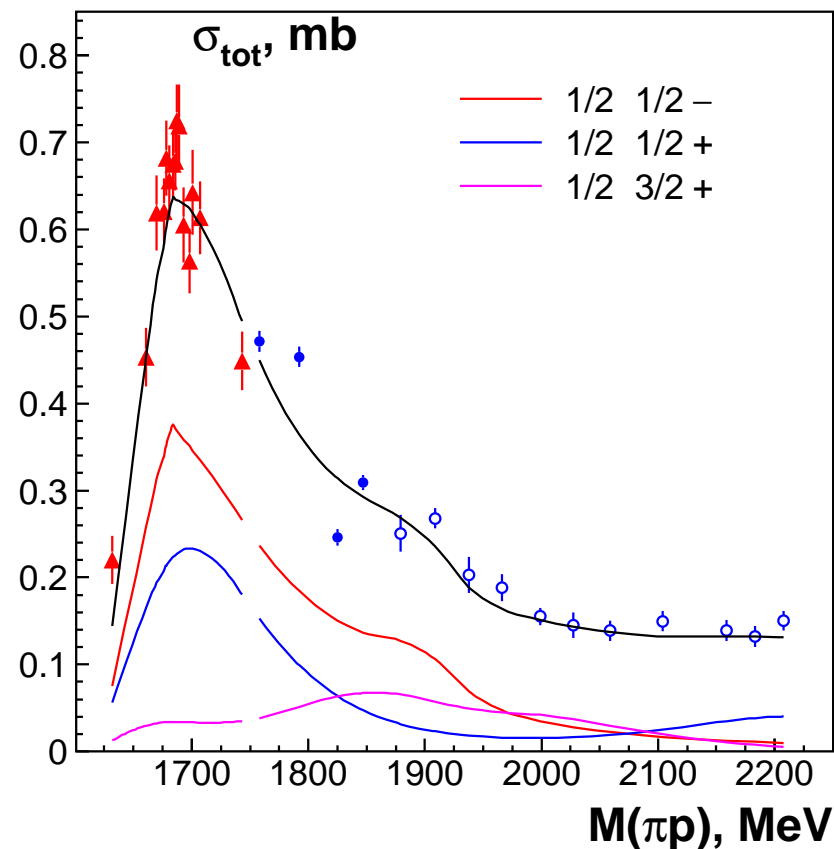
Multi-meson final states (maximum likelihood analysis).

$d\sigma/d\Omega(\pi^- p \rightarrow n\pi^0\pi^0)$	CBALL				
$d\sigma/d\Omega(\gamma p \rightarrow p\pi^0\pi^0)$	CB-ELSA (1.4 GeV)	$E(\gamma p \rightarrow p\pi^0\pi^0)$	16	1.91	MAMI
$d\sigma/d\Omega(\gamma p \rightarrow p\pi^0\eta)$	CB-ELSA (3.2 GeV)	$\Sigma(\gamma p \rightarrow p\pi^0\eta)$	180	2.37	GRAAL
$d\sigma/d\Omega(\gamma p \rightarrow p\pi^0\pi^0)$	CB-ELSA (3.2 GeV)	$\Sigma(\gamma p \rightarrow p\pi^0\pi^0)$	128	0.96	GRAAL
$d\sigma/d\Omega(\gamma p \rightarrow p\pi^0\eta)$	CB-ELSA (3.2 GeV)	$\Sigma(\gamma p \rightarrow p\pi^0\eta)$	180	2.37	GRAAL
$I_c(\gamma p \rightarrow p\pi^0\eta)$	CB-ELSA (3.2 GeV)	$I_s(\gamma p \rightarrow p\pi^0\eta)$			CB-ELSA (3.2 GeV)

The fit of the the $\pi^- p \rightarrow K \Lambda$ reaction

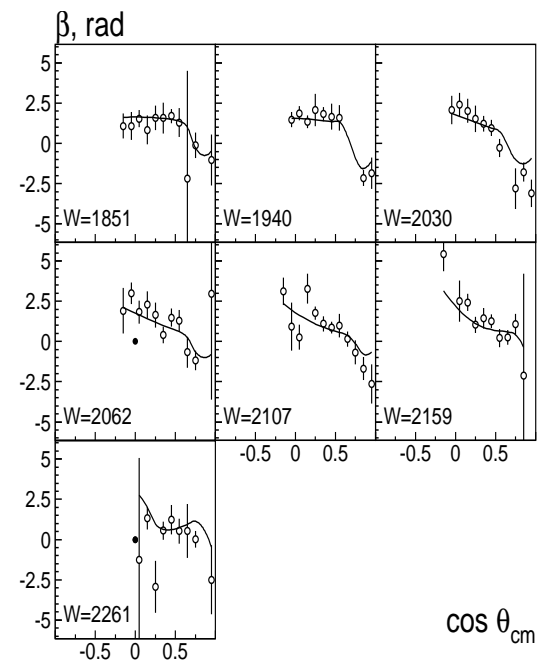
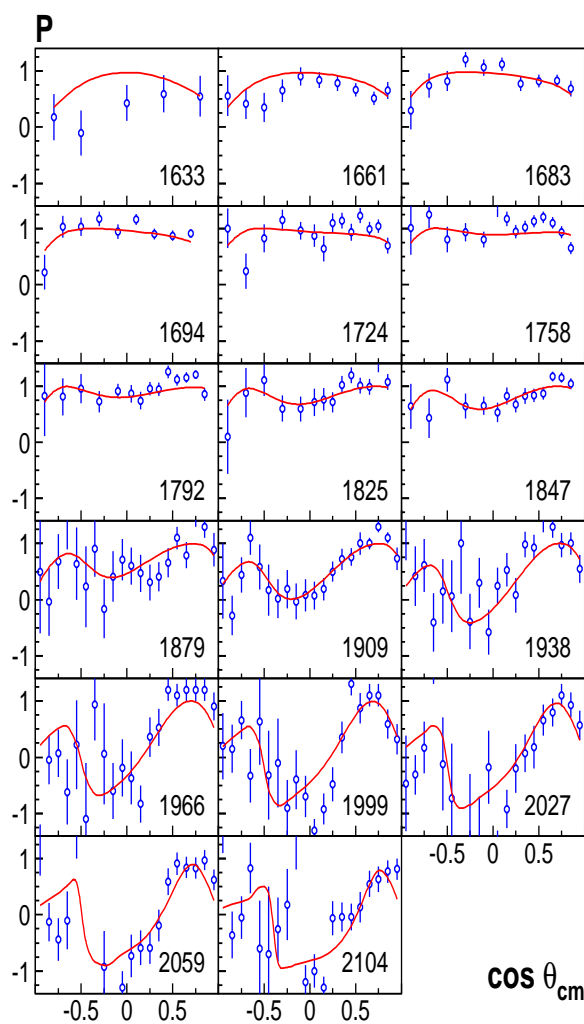
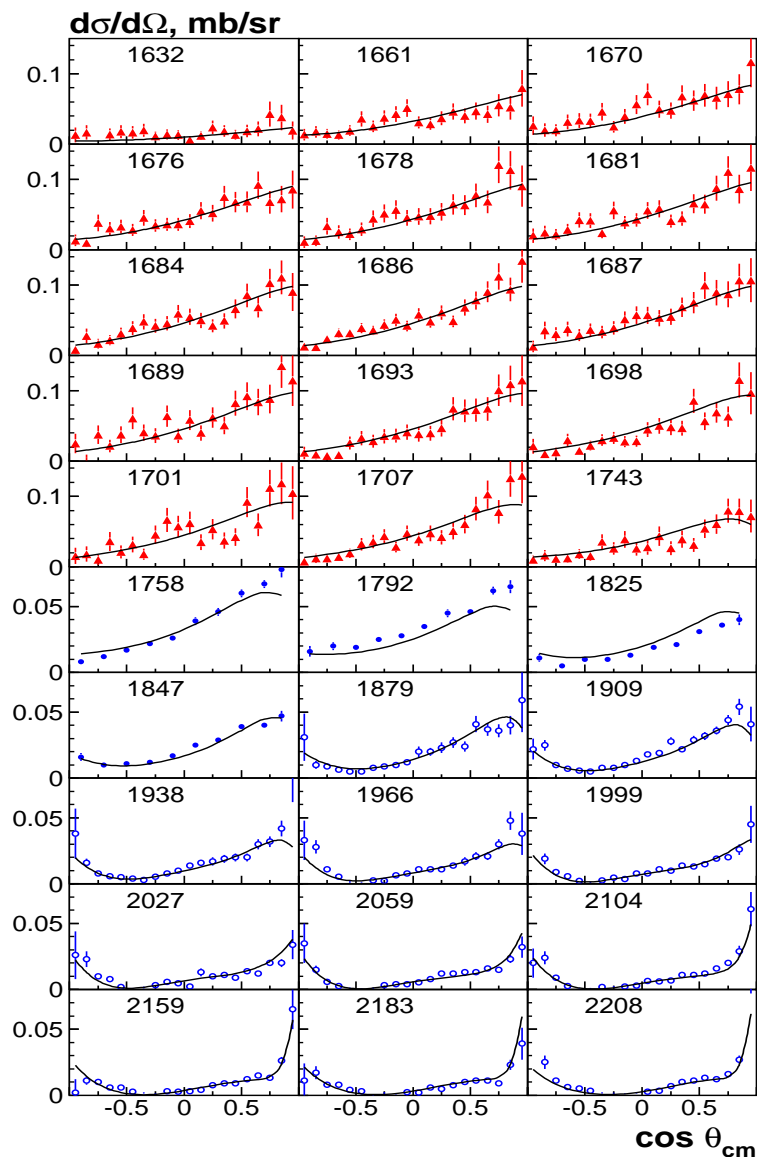
Full experiment for $\pi N \rightarrow K \Lambda$:
differential cross section, analyzing
power, rotation parameter.

**A clear evidence for resonances which
are hardly seen (or not seen) in
the elastic reactions:** $N(1710)P_{11}$,
 $N(1900)P_{13}$,

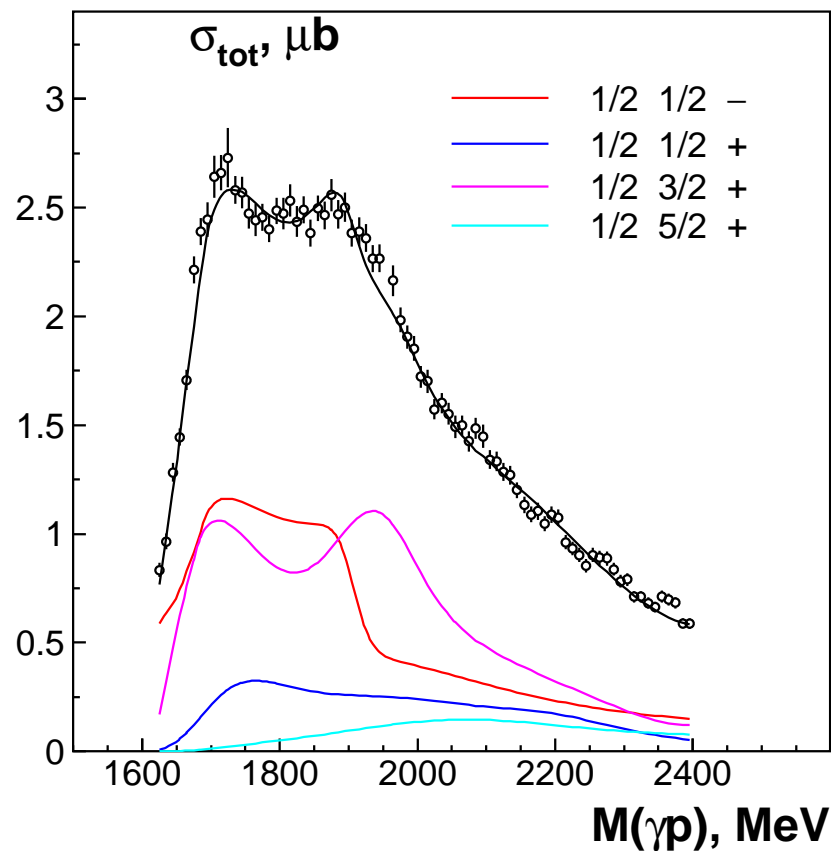
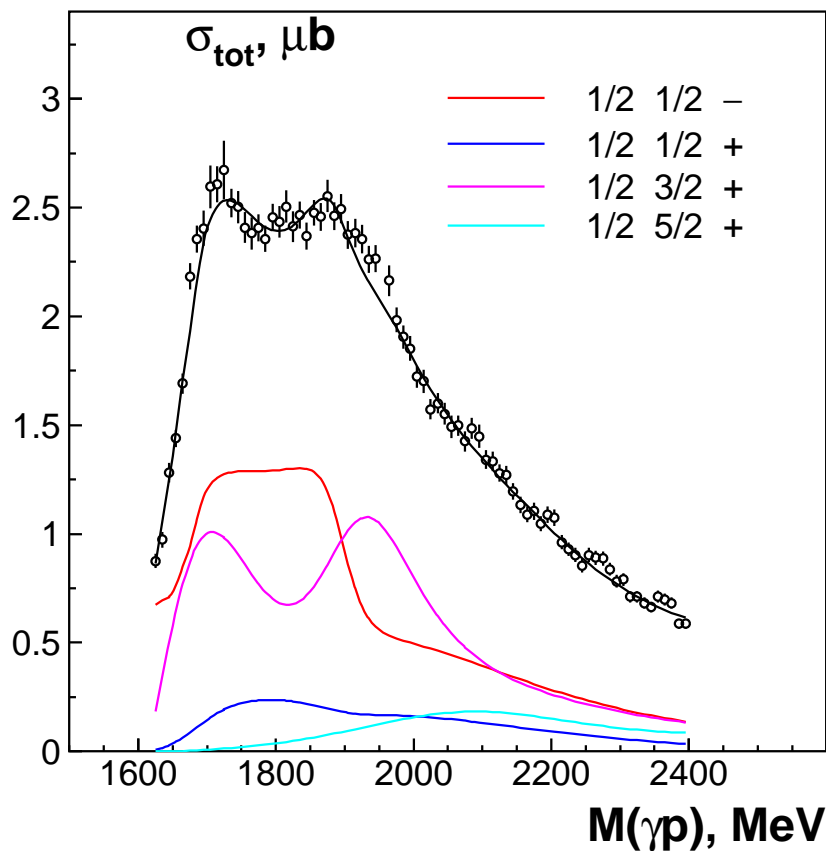


The total cross section for the reaction
 $\pi^- p \rightarrow K^0 \Lambda$ and contributions from
leading partial waves.

$$\pi^- p \rightarrow K \Lambda (d\sigma/d\Omega, P, \beta)$$

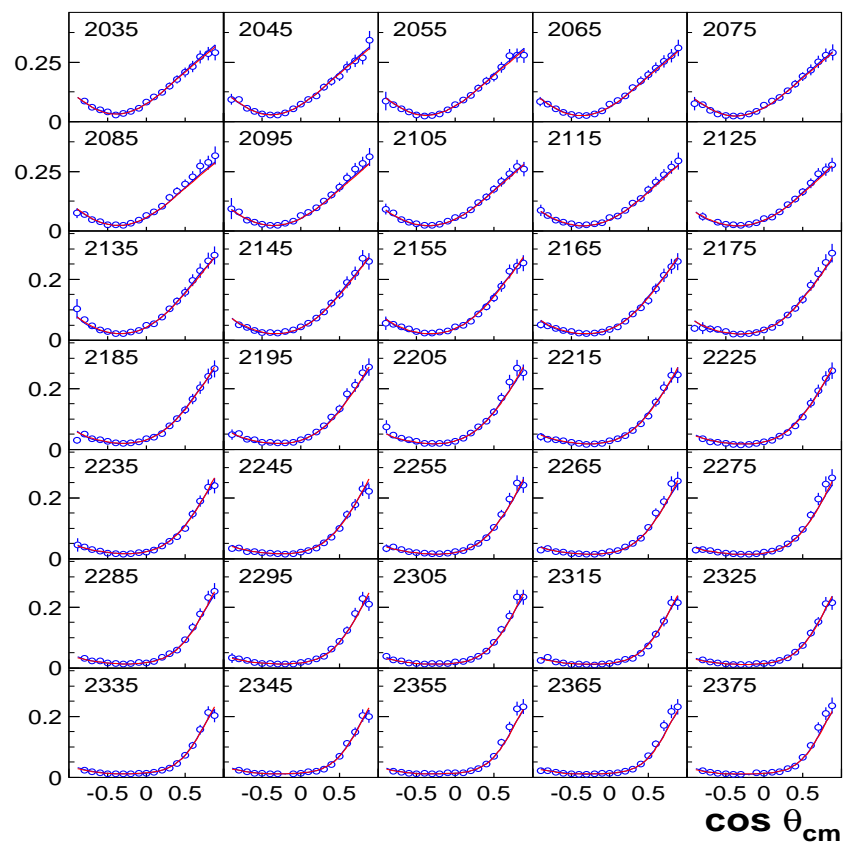
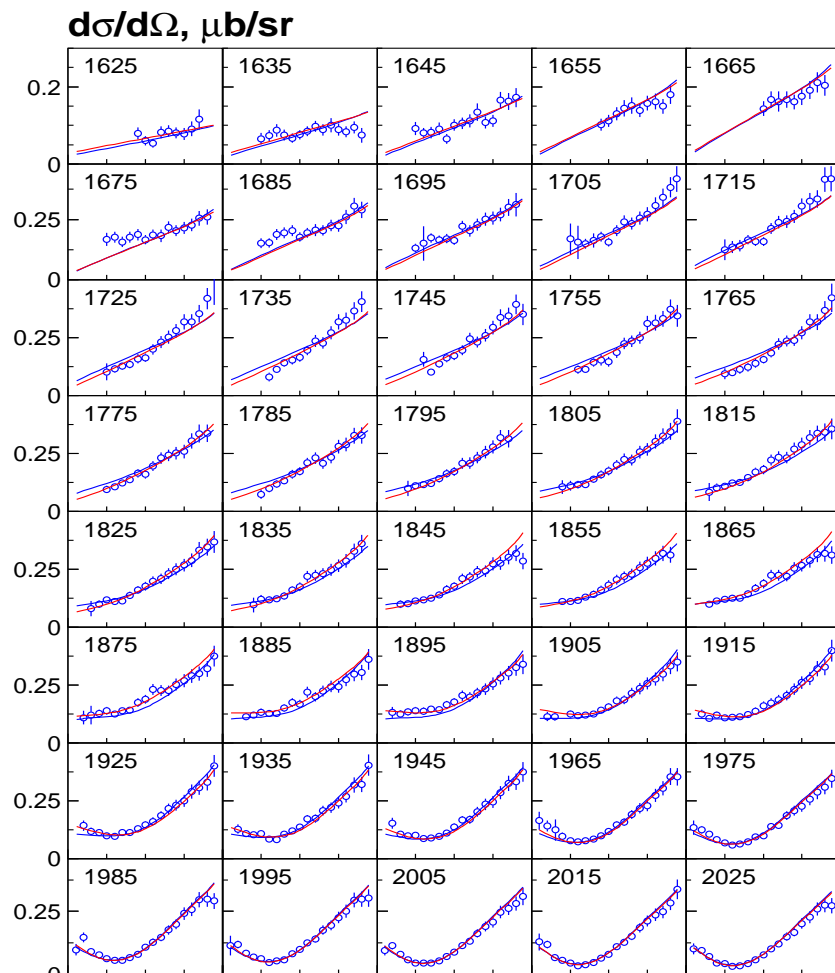


The $\gamma p \rightarrow K \Lambda$ reaction (CLAS 2009)

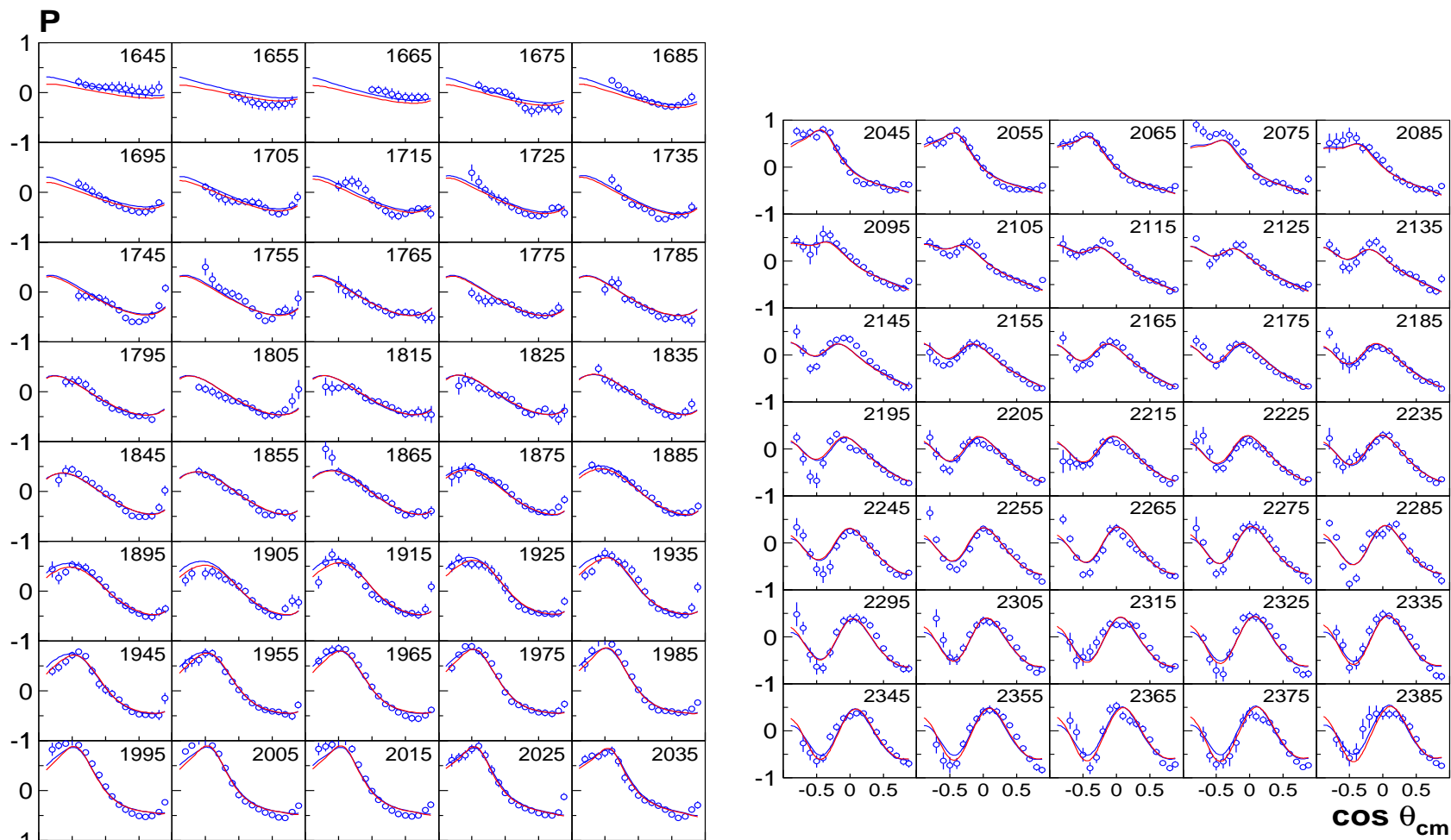


The fit of the $\gamma p \rightarrow K \Lambda$ differential cross section

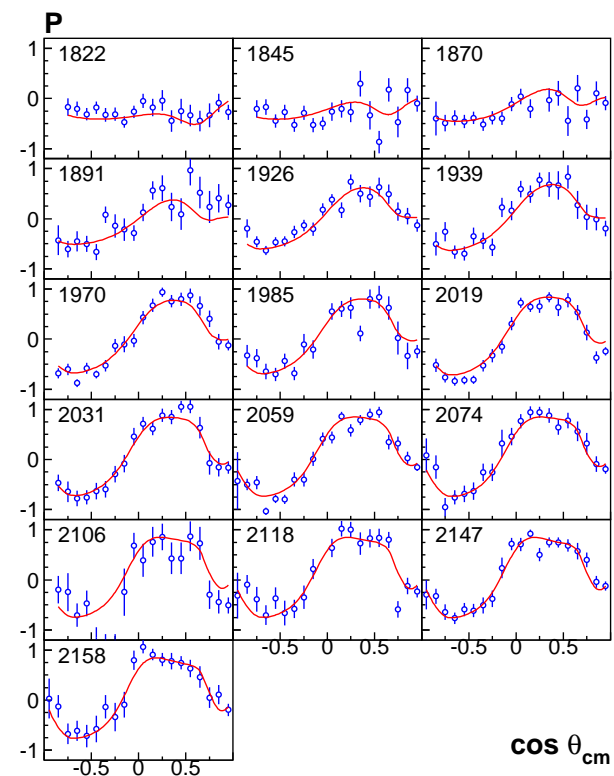
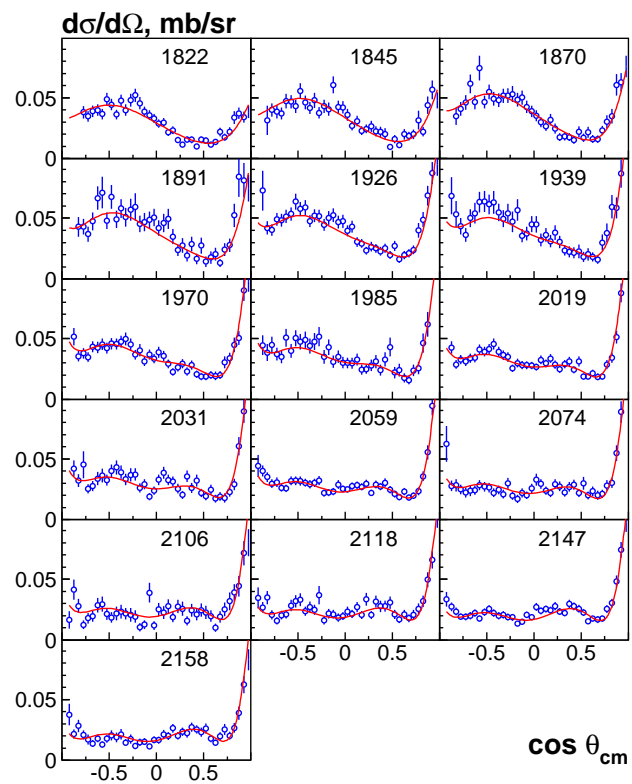
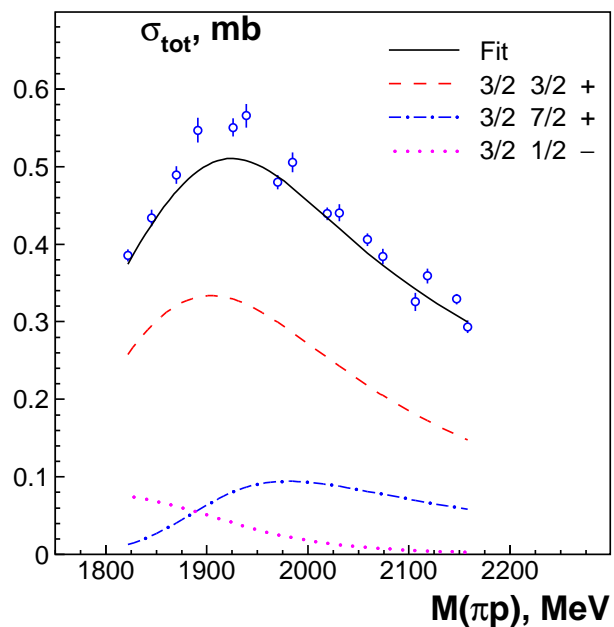
(CLAS 2009)



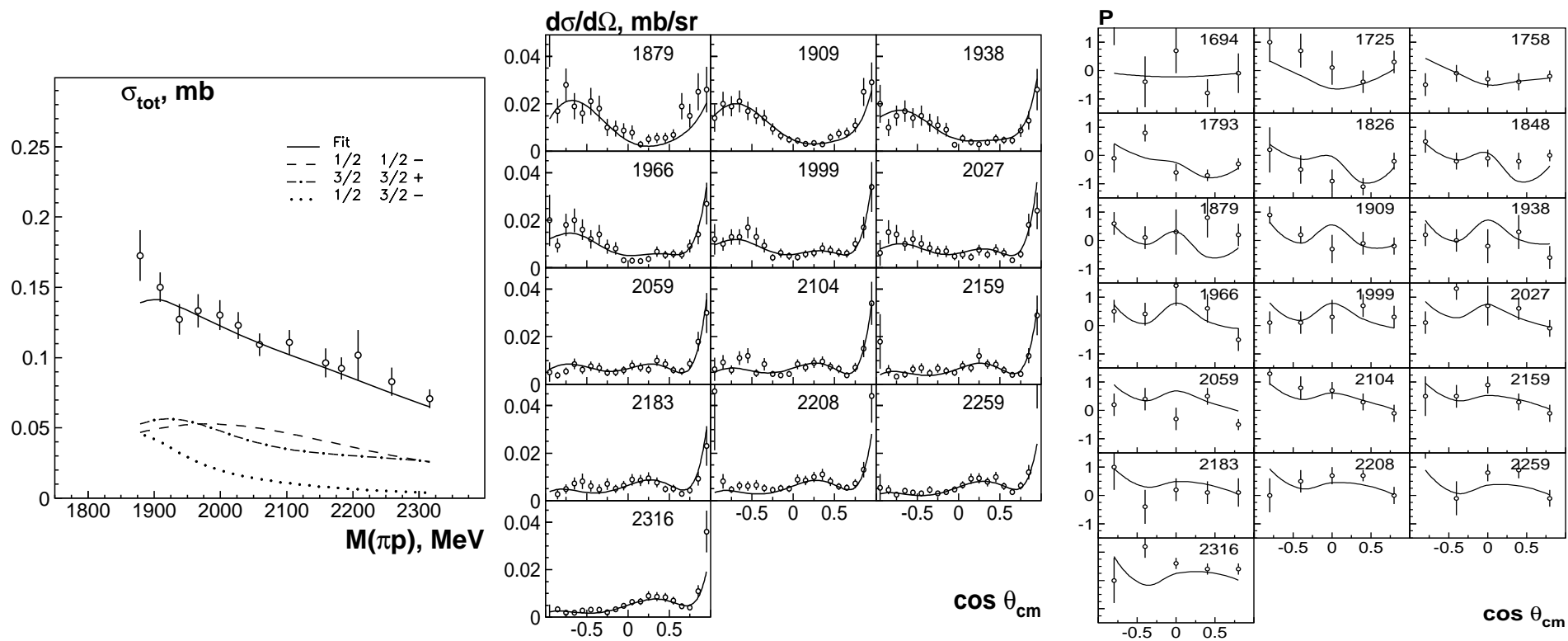
The fit of the $\gamma p \rightarrow K \Lambda$ recoil asymmetry
(CLAS 2009)

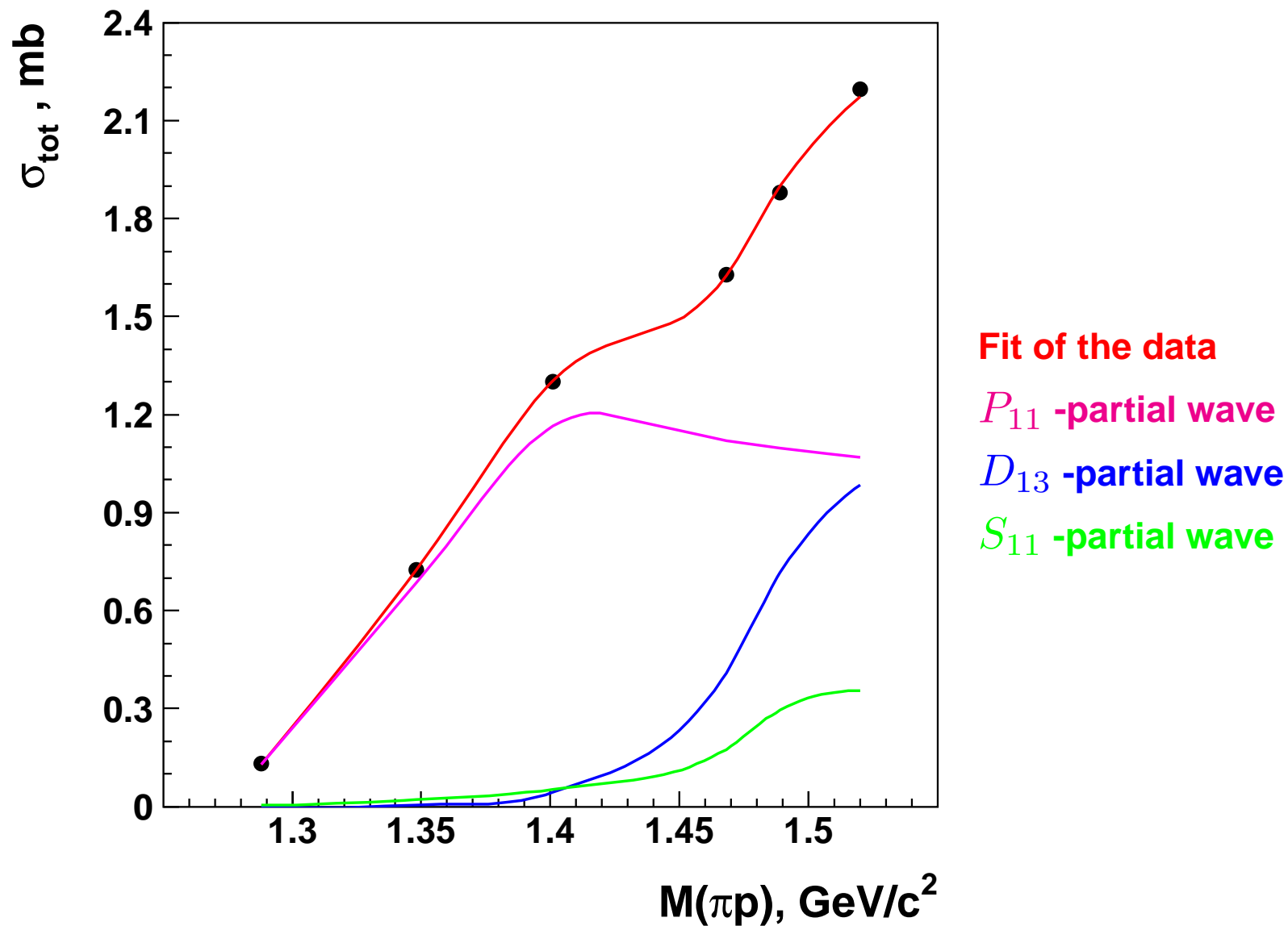


The fit of the the $\pi^+ p \rightarrow K^+ \Sigma^+$ reaction



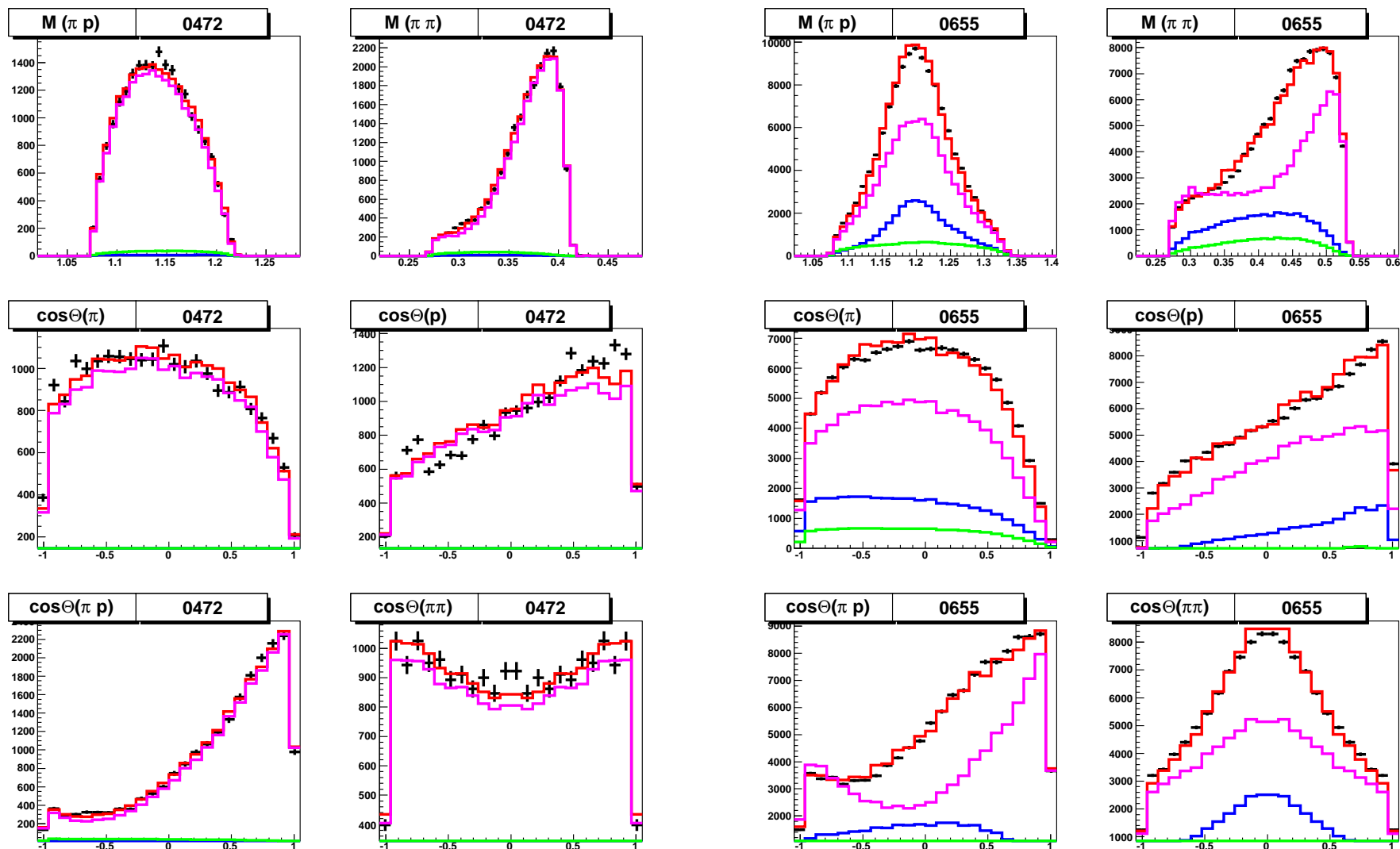
The fit of the the $\pi^- p \rightarrow K^0 \Sigma^0$ reaction



$\pi^- p \rightarrow n\pi^0\pi^0$ (Crystal Ball) total cross section

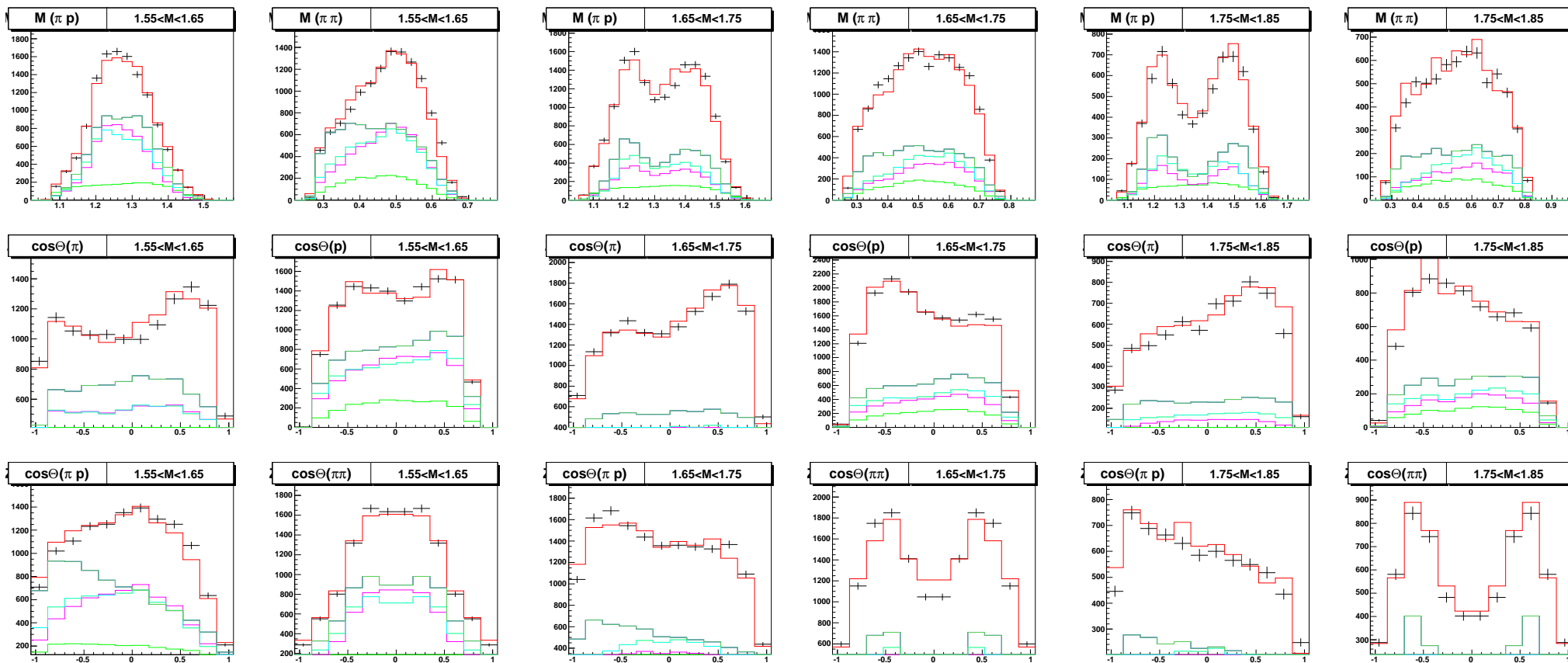
$$\pi^- p \rightarrow n \pi^0 \pi^0 \text{ (Crystal Ball)}$$

Differential cross sections for 472 and 665 MeV/c data.



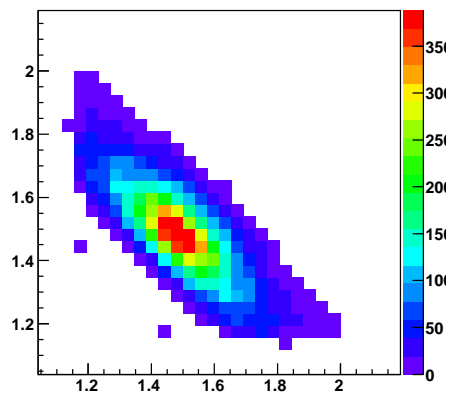
$$\gamma p \rightarrow p\pi^0\pi^0 \text{ (Crystal Barrel)}$$

Differential cross sections.

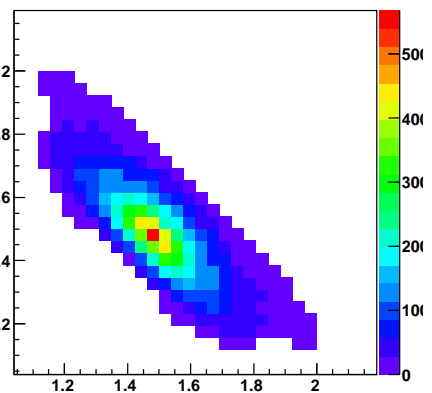


$\gamma p \rightarrow p\pi^0\pi^0$ (Crystal Barrel)Dalitz plots $W=1.5, 1.6, 1.7, 1.8$ GeV.

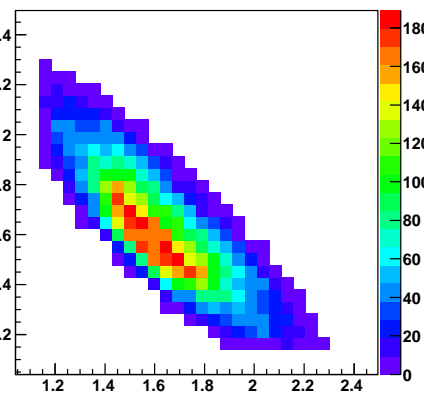
Dp(13 vs 23)M(123)-1.50



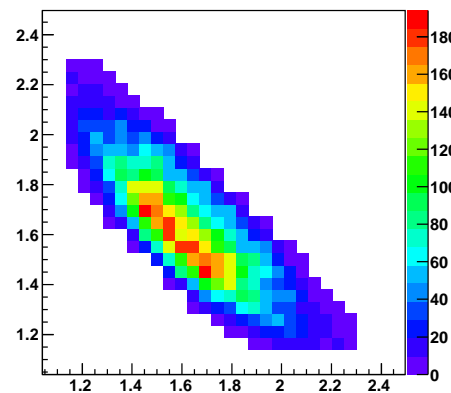
Dp(13 vs 23)M(123)-1.50



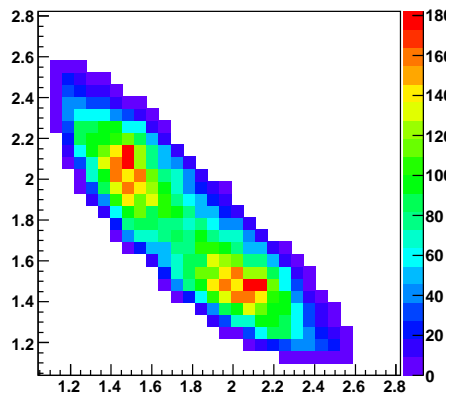
Dp(13 vs 23)M(123)-1.60



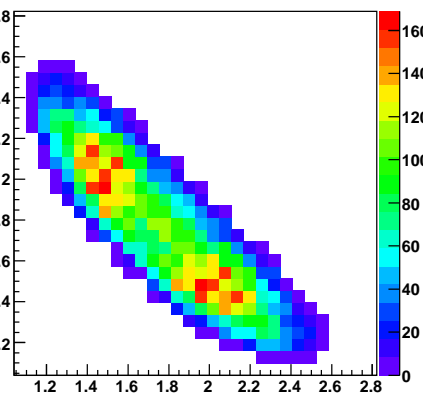
Dp(13 vs 23)M(123)-1.60



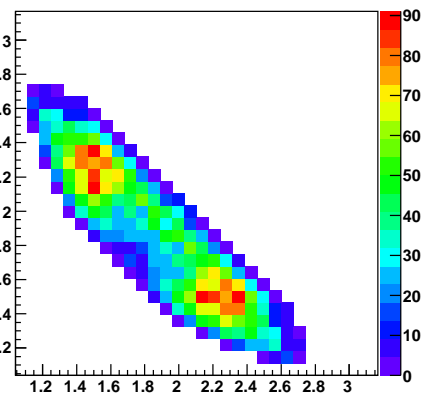
Dp(13 vs 23)M(123)-1.70



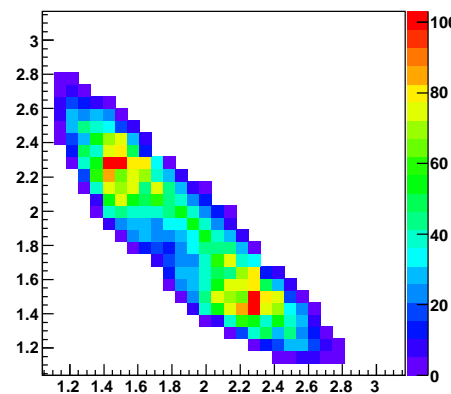
Dp(13 vs 23)M(123)-1.70



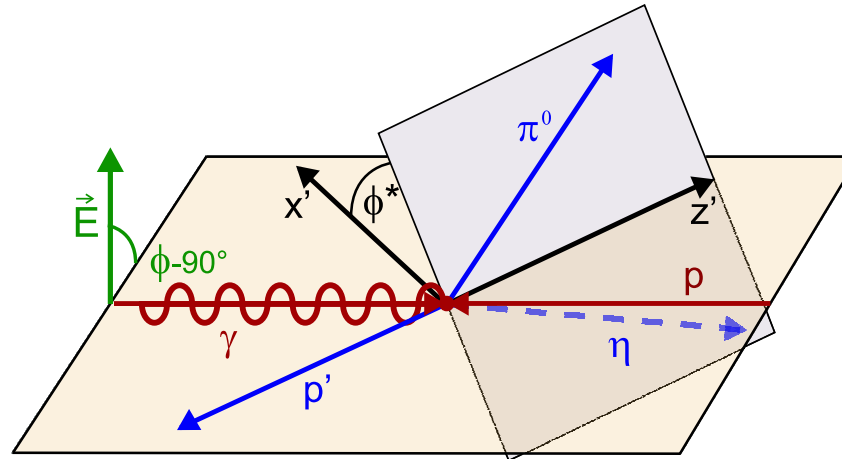
Dp(13 vs 23)M(123)-1.80



Dp(13 vs 23)M(123)-1.80



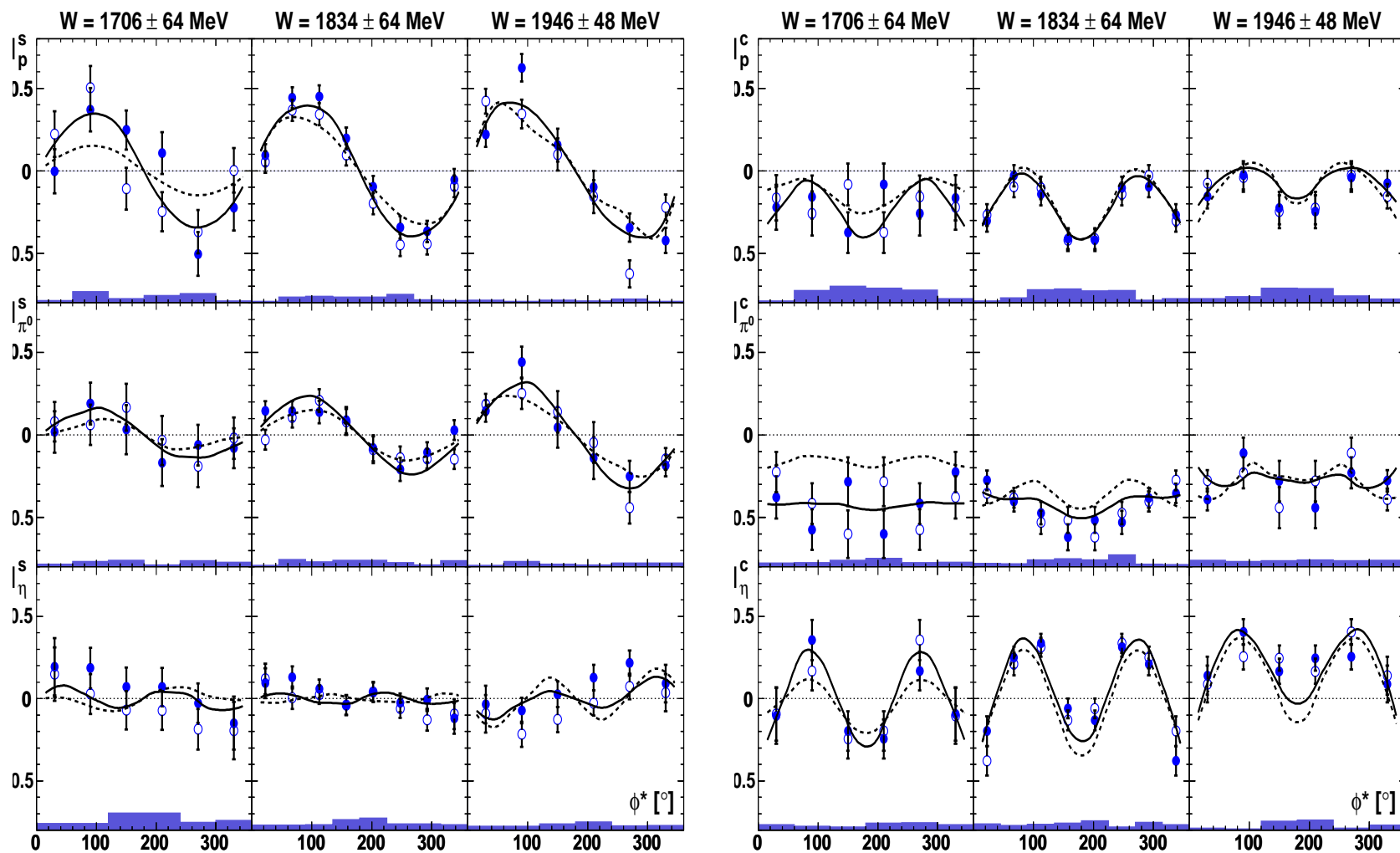
$\gamma p \rightarrow p \pi^0 \eta$ (CB-ELSA) with linear polarized photon



$$\frac{d\sigma}{d\Omega} = \left(\frac{d\sigma}{d\Omega} \right)_0 \{1 + \delta_l [I^s \sin(2\phi) + I^c \cos(2\phi)]\}, \quad (2)$$

$$\Sigma = \int_0^{2\pi} I^c d\phi^*$$

I^c and I^s for $\gamma p \rightarrow p\pi^0\eta$ (CB-ELSA)

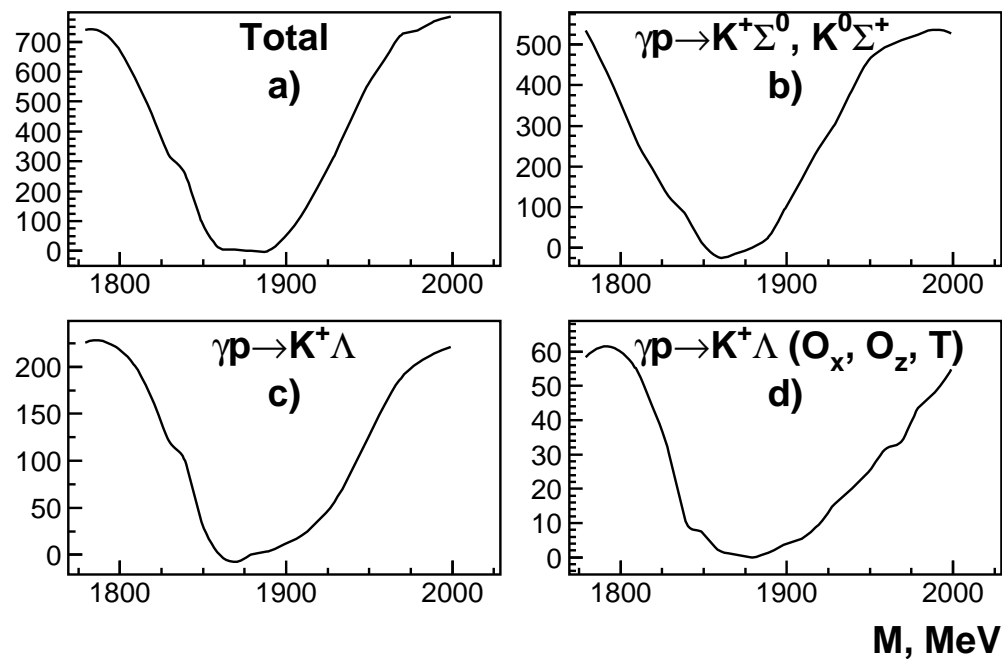
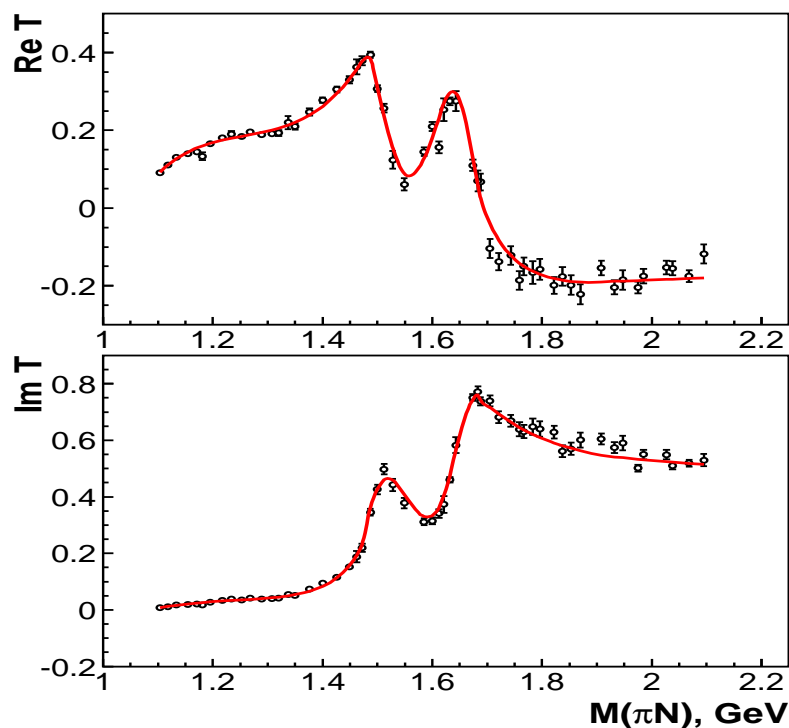


Pole position of baryon states (Re and -2Im) in the mass region 1900-2300 MeV

State		Solution 1	Solution 2	Arndt	Hoehler	Cutcosky
$N(1875) \frac{1}{2}^+$	Re	1860 ± 20	1850^{+20}_{-50}		1885 ± 30 (Manley)	
*	-2Im	110^{+30}_{-10}	360 ± 40		113 ± 44 (Manley)	
$N(1890) \frac{1}{2}^-$	Re	1895 ± 8		—	1880 ± 20	—
*	-2Im	82 ± 10		—	95 ± 30	—
$N(1880) \frac{3}{2}^-$	Re	1860 ± 12		—	—	1880 ± 100
*	-2Im	185 ± 16		—	—	180 ± 60
$N(2130) \frac{3}{2}^-$	Re	2130 ± 45		—	2081 ± 20	2050 ± 70
**	-2Im	340 ± 45		—	265 ± 40	200 ± 60
$N(1900) \frac{3}{2}^+$	Re	1910 ± 40	1920 ± 50	—	—	—
**	-2Im	270 ± 50	300 ± 60	—	—	—
$N(2000) \frac{5}{2}^+$	Re	$1800 - 1950$		1807	1882 ± 10	—
**	-2Im	$100 - 300$		109	95 ± 20	—
$N(2100) \frac{5}{2}^+$	Re	2100 ± 25		—	—	—
	-2Im	550 ± 40		—	—	—
$N(2070) \frac{5}{2}^-$	Re	2060 ± 8		—	—	2100 ± 60
	-2Im	370 ± 15		—	—	360 ± 80
$N(1990) \frac{7}{2}^+$	Re	1975 ± 15	2090 ± 15	—	~ 1935	1900 ± 30
**	-2Im	170 ± 50	260 ± 20	—	~ 260	260 ± 60
$N(2190) \frac{7}{2}^-$	Re	2160 ± 20		2070	2042	2100 ± 50
***	-2Im	310 ± 25		520	480	400 ± 160

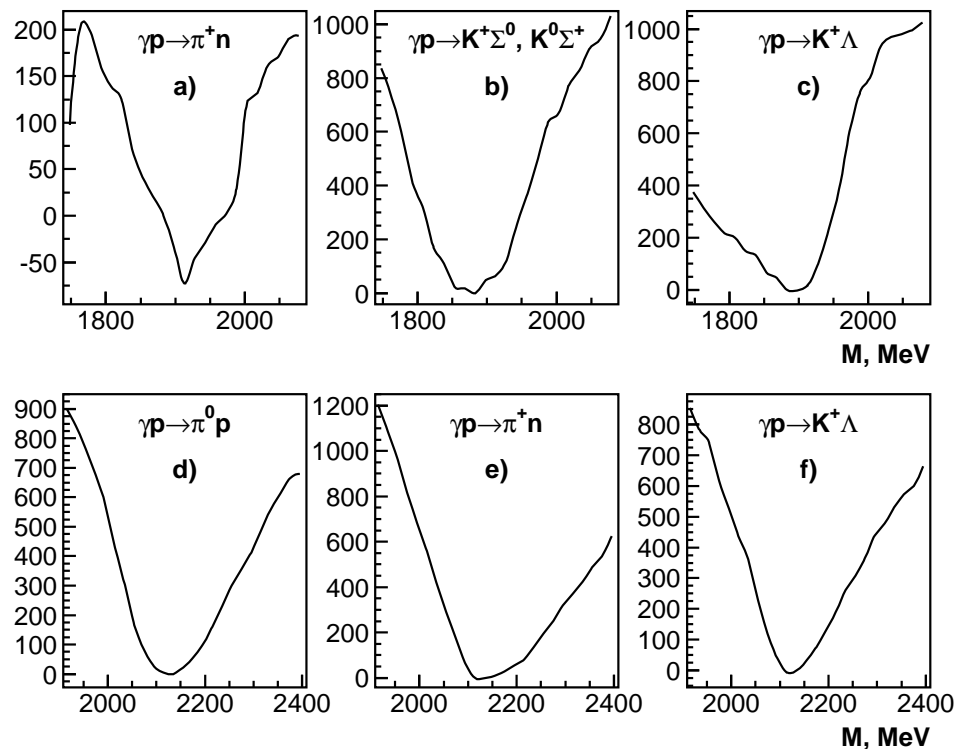
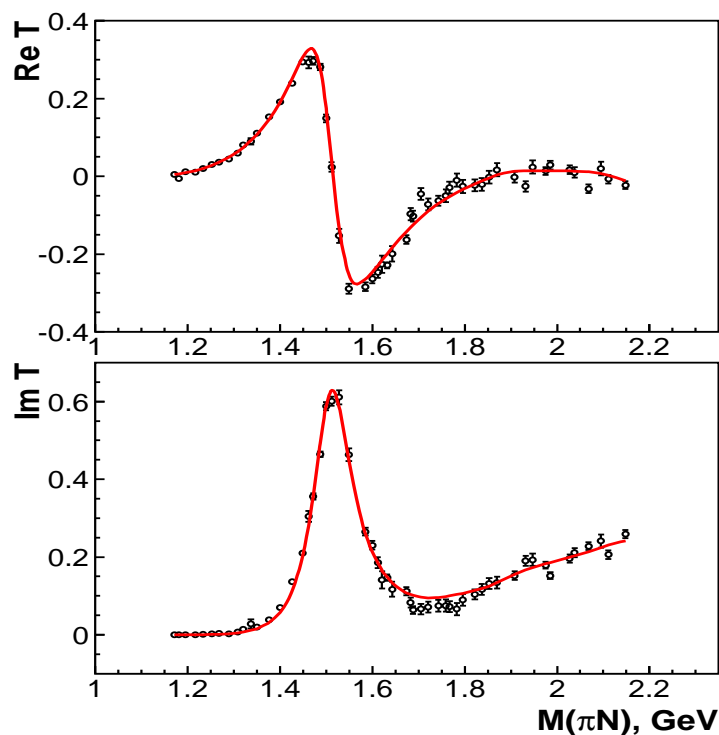
S_{11} : pole position and Breit-Wigner parameters

State		Solution 1	Solution 2	Arndt	Hoehler	Cutcosky
$N(1890) \frac{1}{2}^-$	Re	1895 ± 8				
*	-2Im	82 ± 10				
BW	M	1900 ± 10			1880 ± 20	
parameters	Γ	77 ± 15			95 ± 30	



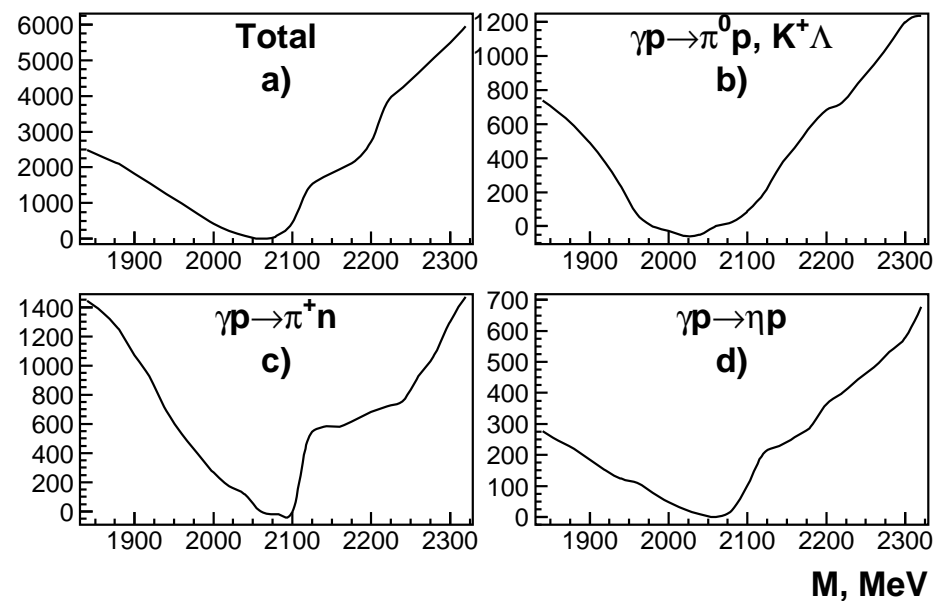
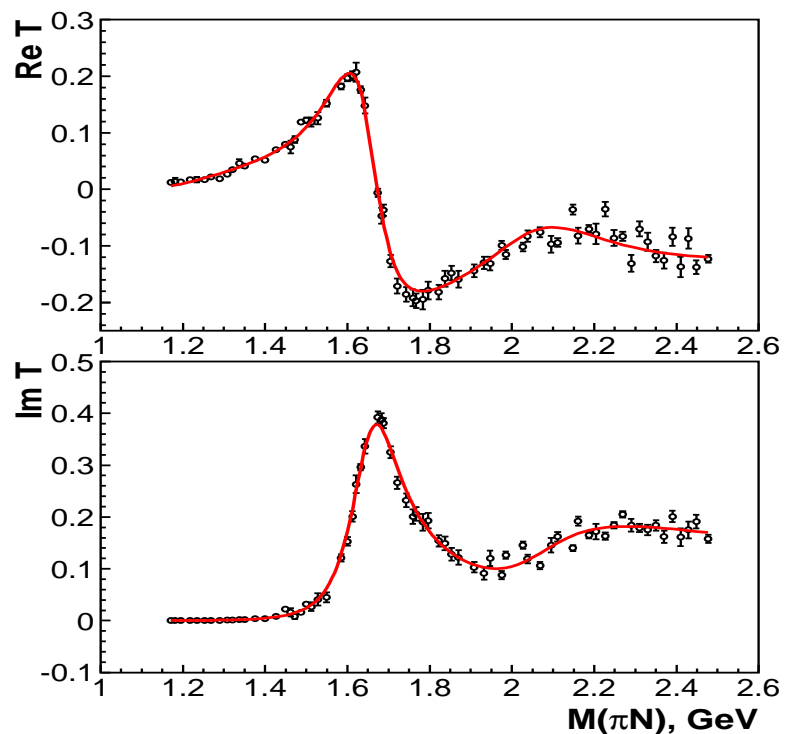
D_{13} : pole positions

State		Solution 1	Solution 2	Arndt	Hoehler	Cutcosky
$N(1880) \frac{3}{2}^-$	Re	1860 ± 12	—	—	—	1880 ± 100
*	-2Im	185 ± 16	—	—	—	180 ± 60
$N(2130) \frac{3}{2}^-$	Re	2130 ± 45	—	—	2081 ± 20	2050 ± 70
**	-2Im	340 ± 45	—	—	265 ± 40	200 ± 60



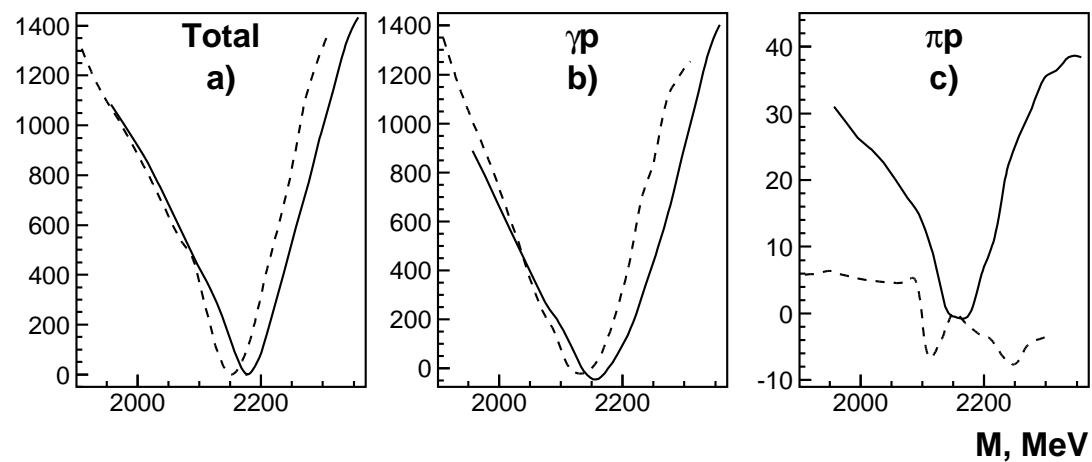
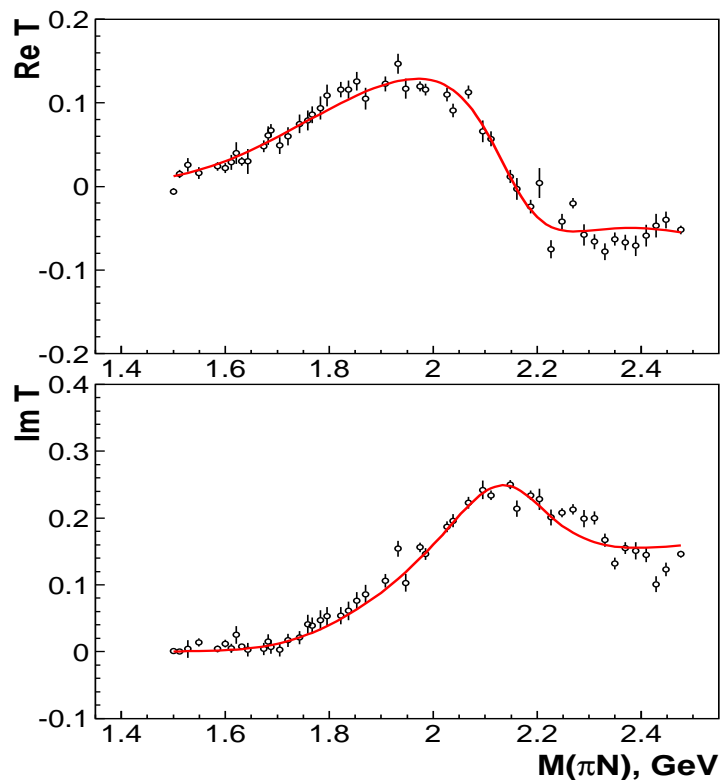
D_{15} : pole position and Breit-Wigner parameters

State		Solution 1	Solution 2	Arndt	Hoehler	Cutcosky
$N(2070) \frac{5}{2}^-$	Re	2060 ± 8		—	—	2100 ± 60
	-2Im	370 ± 15		—	—	360 ± 80
BW parameters	M	2075 ± 12			2228 ± 30	2180 ± 80
	Γ	365 ± 20			310 ± 50	400 ± 100



G_{17} : pole position and Breit-Wigner parameters

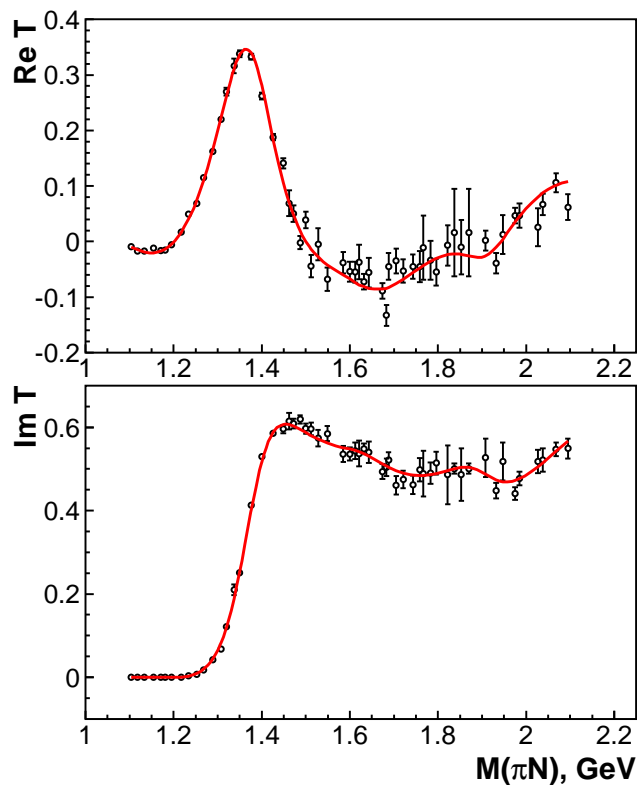
State		Solution 1	Solution 2	Arndt	Hoehler	Cutcosky
$N(2190) \frac{7}{2}^-$	Re	2160 ± 20		2070	2042	2100 ± 50
** ** *	-2Im	310 ± 25		520	480	400 ± 160
BW	M	2185 ± 20		2152.4 ± 1.4	2140 ± 12	2200 ± 70
parameters	Γ	290 ± 40		484 ± 13	390 ± 30	500 ± 150



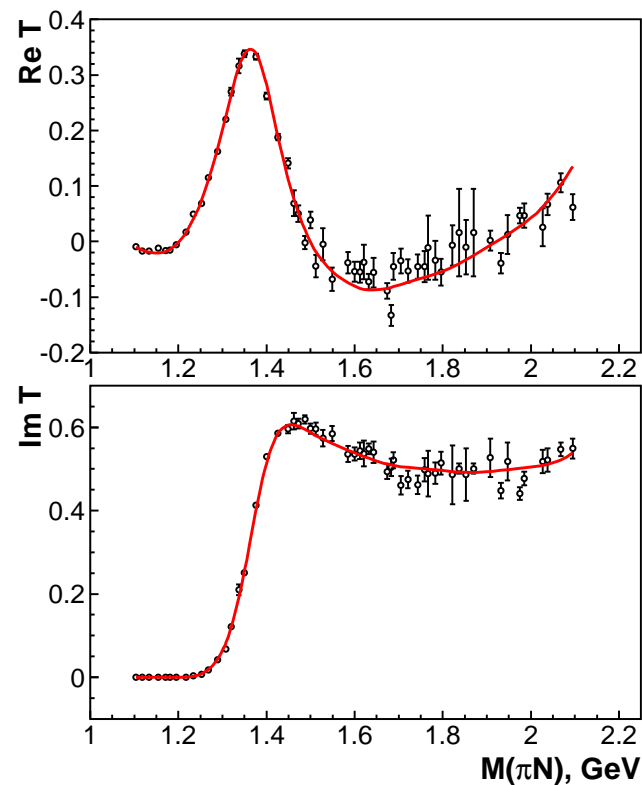
P_{11} : pole position and Breit-Wigner parameters

State		Solution 1	Solution 2	Manley
$N(1875) \frac{1}{2}^+$	Re	1860 ± 20	1850^{+20}_{-50}	1885 ± 30
*	-2Im	110^{+30}_{-10}	360 ± 40	113 ± 44
BW	M	1864 ± 10	1863 ± 20	
parameters	Γ	115 ± 20	320 ± 30	

BG2011-01



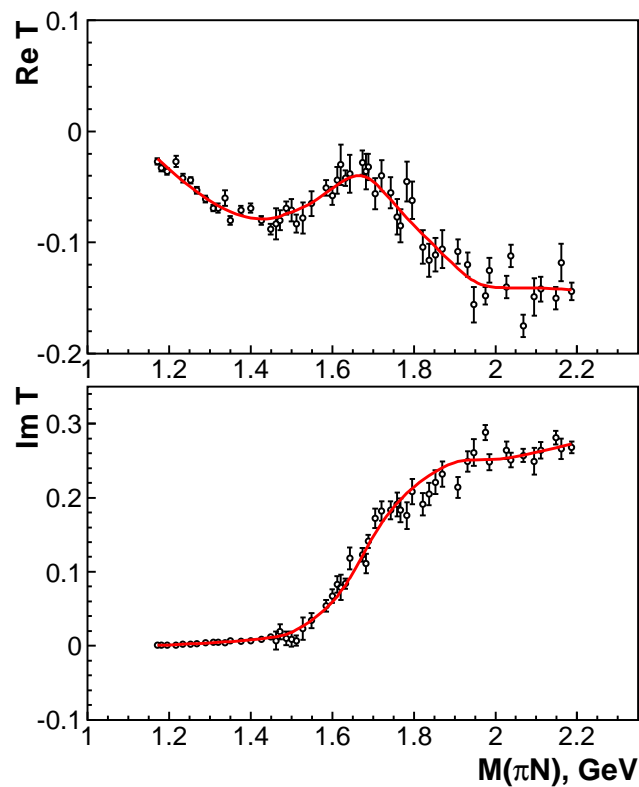
BG2011-02



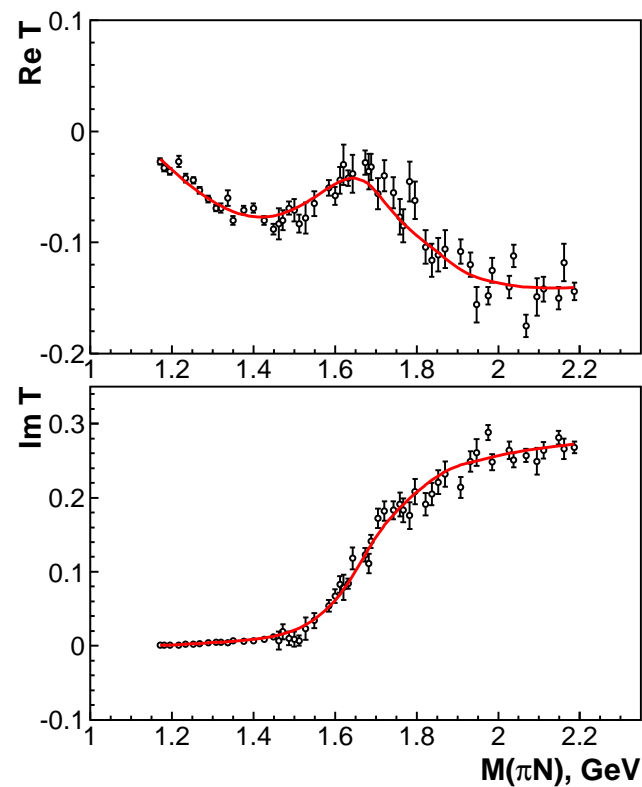
P_{13} : pole position and Breit-Wigner parameters

State		Solution 1	Solution 2	Arndt	Hoehler	Cutcosky
$N(1900) \frac{3}{2}^+$	Re	1920 ± 50	1890 ± 50	—	—	—
**	-2Im	300 ± 60	270^{+180}_{-100}	—	—	—
$N(1900) \frac{3}{2}^+$	Re	-	1970 ± 25	—	—	—
**	-2Im	-	250 ± 60	—	—	—

BG2011-01

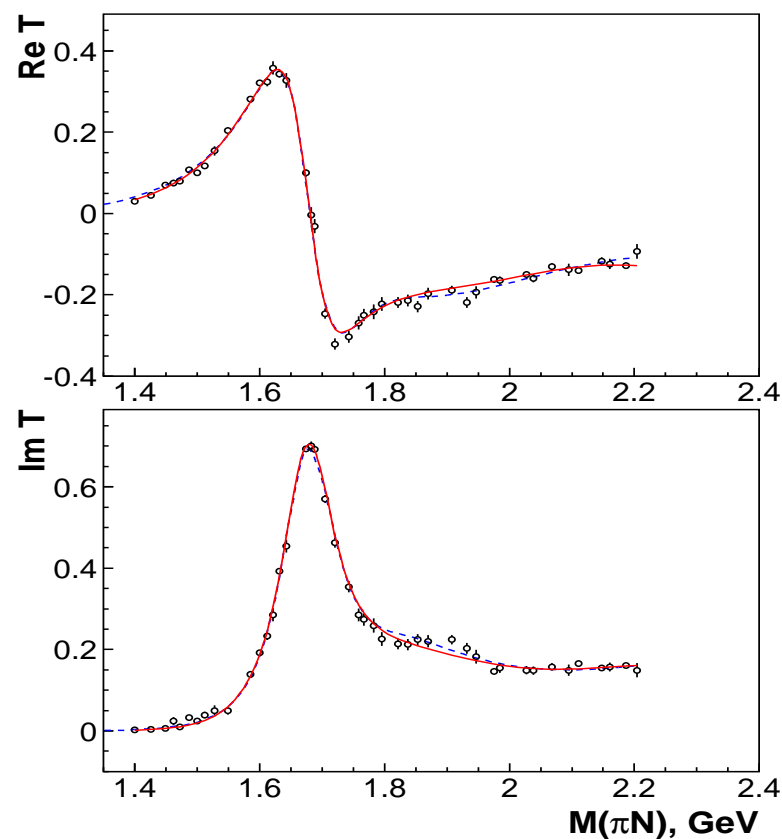
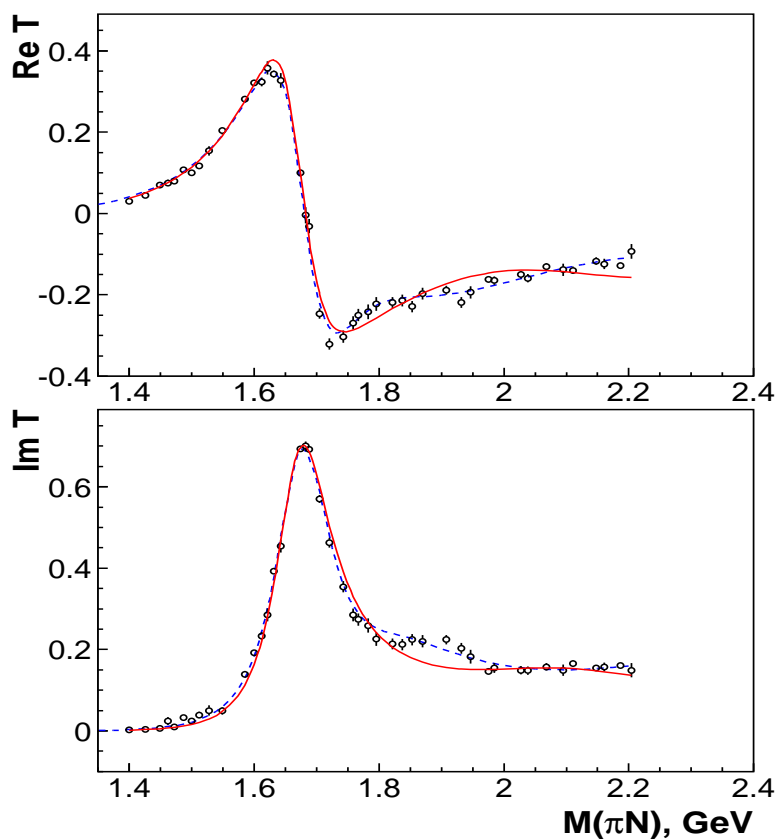


BG2011-02



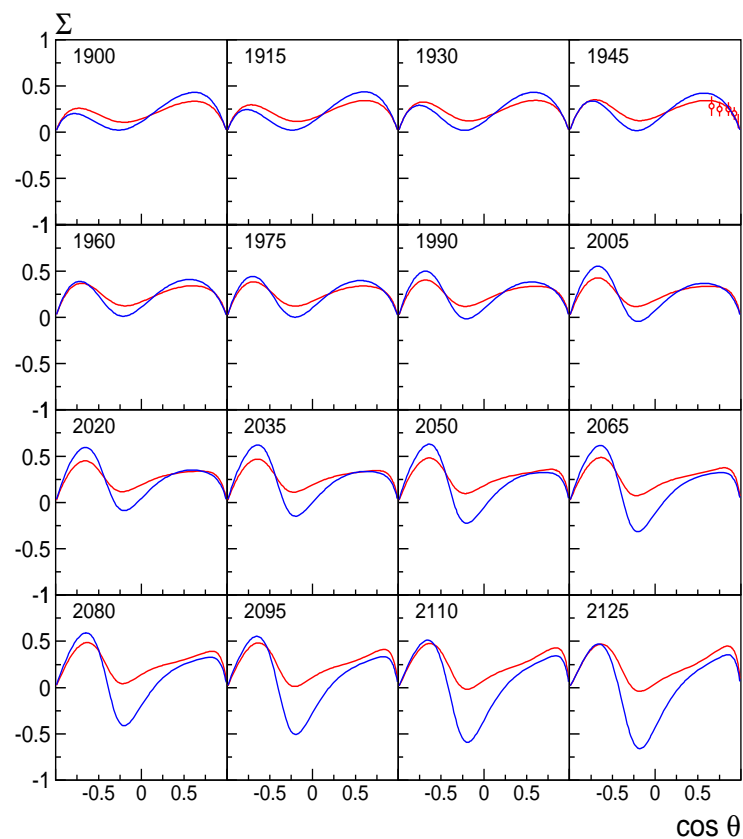
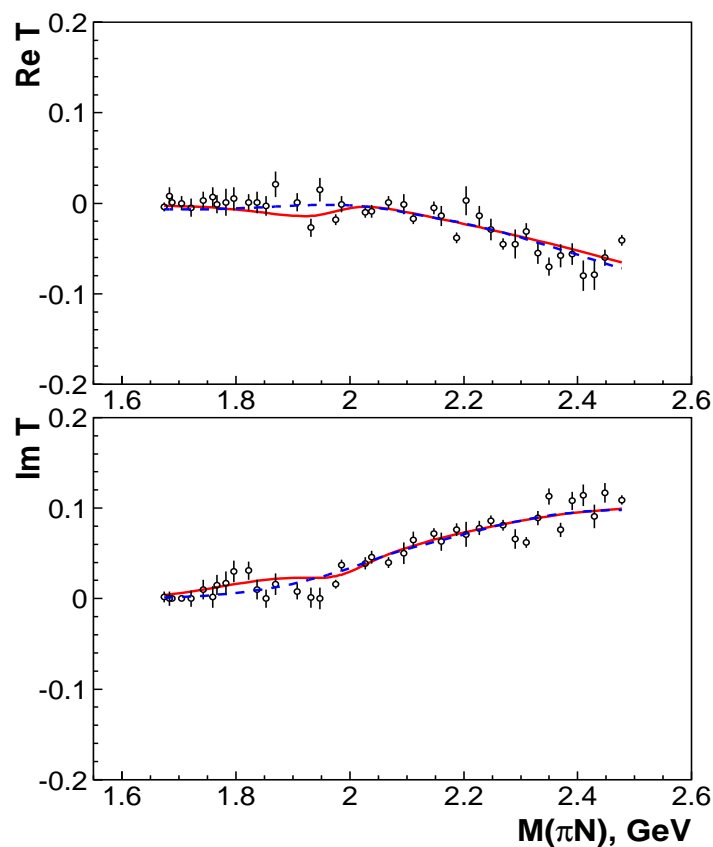
Pole position of F_{15} : two and three pole solution

State		Solution 1	Solution 2	Arndt	Hoehler	Cutcosky
$N(2000) \frac{5}{2}^+$	Re	1800 – 1950	1800 – 1950	1807	1882 ± 10	—
	-2Im	100 – 300	100 – 300	109	95 ± 20	—
$N(2100) \frac{5}{2}^+$	Re	2090^{+20}_{-40}	2110^{+20}_{-80}	—	—	—
	-2Im	560 ± 100	540 ± 100	—	—	—



Pole position of F_{17} and helicity couplings (absolute value ($10^{-3} \text{ GeV}^{\frac{1}{2}}$)/phase (degrees))

State		Solution 1	$A(\frac{1}{2})/A(\frac{3}{2})$	Solution 2	$A(\frac{1}{2})/A(\frac{3}{2})$
$N(1990) \frac{7}{2}^+$	Re	1980 ± 25	$15/14^\circ$	2100 ± 30	$76/50^\circ$
**	-2Im	180 ± 30	$28/3^\circ$	300 ± 60	$78/45^\circ$



Holographic QCD (AdS/QCD)

L, S, N	κ_{gd}	Resonance					Pred.
$0, \frac{1}{2}, 0$	$\frac{1}{2}$	$N(940)$				input:	0.94
$0, \frac{3}{2}, 0$	0	$\Delta(1232)$					1.27
$0, \frac{1}{2}, 1$	$\frac{1}{2}$	$N(1440)$					1.40
$1, \frac{1}{2}, 0$	$\frac{1}{4}$	$N(1535)$	$N(1520)$				1.53
$1, \frac{3}{2}, 0$	0	$N(1650)$	$N(1700)$	$N(1675)$			1.64
$1, \frac{1}{2}, 0$	0	$\Delta(1620)$	$\Delta(1700)$		$L, S, N=0, \frac{3}{2}, 1:$	$\Delta(1600)$	1.64
$2, \frac{1}{2}, 0$	$\frac{1}{2}$	$N(1720)$	$N(1680)$		$L, S, N=0, \frac{1}{2}, 2:$	$N(1710)$	1.72
$1, \frac{1}{2}, 1$	$\frac{1}{4}$	$N(1890)$	$N(1880)$				1.82
$1, \frac{3}{2}, 1$	0	$\Delta(1900)$	$\Delta(1940)$	$\Delta(1930)$			1.92
$2, \frac{3}{2}, 0$	0	$\Delta(1910)$	$\Delta(1920)$	$\Delta(1905)$	$\Delta(1950)$		1.92
$2, \frac{3}{2}, 0$	0	$N(1875)$	$N(1900)$	$N(1880)$	$N(1980)$		1.92
$0, \frac{1}{2}, 3$	$\frac{1}{2}$	$N(????)$					2.03
$3, \frac{1}{2}, 0$	$\frac{1}{4}$	$N(2075)$	$N(2185)$	$L, S, N=1, \frac{1}{2}, 2:$	$N(????)$	$N(????)$	2.12
$3, \frac{3}{2}, 0$	0	$N(2200)$	$N(2250)$	$L, S, N=1, \frac{1}{2}, 2:$	$\Delta(2223)$	$\Delta(2200)$	2.20
$4, \frac{1}{2}, 0$	$\frac{1}{2}$	$N(2220)$					2.27
$4, \frac{3}{2}, 0$	0	$\Delta(2390)$	$\Delta(2300)$	$\Delta(2420)$	$ L, N=3, 1:$	$\Delta(2400)$	2.43
$5, \frac{1}{2}, 0$	$\frac{1}{4}$	$N(2600)$				$\Delta(2350)$	2.57

Parity doublets of N and Δ resonances at high mass region

Parity doublets must not interact by pion emission

and could have a small coupling to πN .

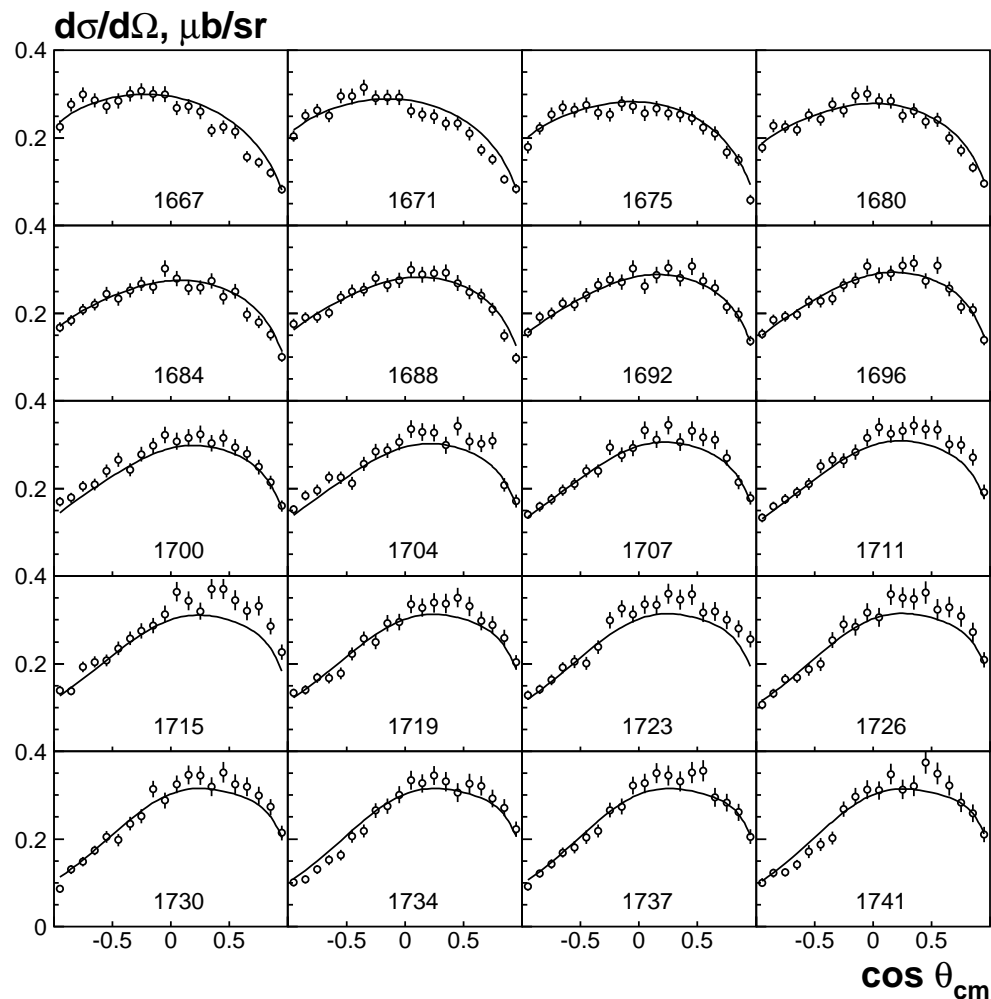
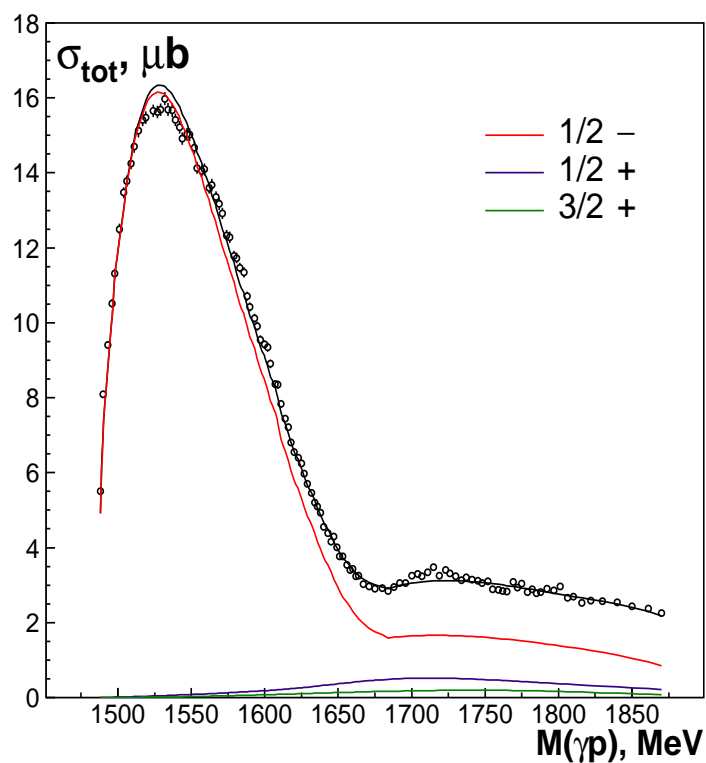
$J=\frac{1}{2}$	$\mathbf{N}_{1/2+}$ (1880) *	$\mathbf{N}_{1/2-}$ (1890) *	$\Delta_{1/2+}$ (1910) ****	$\Delta_{1/2-}$ (1900) ^a **
$J=\frac{3}{2}$	$\mathbf{N}_{3/2+}$ (1900) **	$\mathbf{N}_{3/2-}$ (1875) **	$\Delta_{3/2+}$ (1940) ^a ***	$\Delta_{3/2-}$ (1990) ^a *
$J=\frac{5}{2}$	$\mathbf{N}_{5/2+}$ (1880) **	$\mathbf{N}_{5/2-}$ (2070)	$\Delta_{5/2+}$ (1940) ****	$\Delta_{5/2-}$ (1930) ^a ***
$J=\frac{7}{2}$	$\mathbf{N}_{7/2+}$ (1980) **	$\mathbf{N}_{7/2-}$ (2170) ****	$\Delta_{7/2+}$ (1920) ****	$\Delta_{7/2-}$ (2200) *
$J=\frac{9}{2}$	$\mathbf{N}_{9/2+}$ (2220) ****	$\mathbf{N}_{9/2-}$ (2250) ****	$\Delta_{9/2+}$ (2300) **	$\Delta_{9/2-}$ (2400) ^a **
$J=\frac{5}{2}$	$\mathbf{N}_{5/2+}$ (2100) **	$\mathbf{N}_{5/2-}$ (2070)	$\Delta_{5/2+}$ (1940) ****	$\Delta_{5/2-}$ (1930) ^a ***
$J=\frac{7}{2}$	$\mathbf{N}_{7/2+}$ (2100) **	$\mathbf{N}_{7/2-}$ (2160) ****	$\Delta_{7/2+}$ (1920) ****	$\Delta_{7/2-}$ (2200) *
$J=\frac{9}{2}$	$\mathbf{N}_{9/2+}$ (2220) ****	$\mathbf{N}_{9/2-}$ (2250) ****	$\Delta_{9/2+}$ (2300) **	$\Delta_{9/2-}$ (2400) ^a **

Summary

- The analysis of (almost) all available data for production of baryons in the pion and photo induced reaction is completed.
- We have observed a set of new states in the region 1800-2150 MeV, however, this number is much less than that predicted by the classical quark model.
- The low spin states in this mass region fit very well the AdS/QCD prediction as well as with the idea about chiral restoration at high energies.
- There are two solutions for the $N_{\frac{7}{2}^+}$ lowest state which should be distinguished from analysis of beam asymmetry data on photoproduction of hyperon-kaon final states.
- The situation for $N(\frac{5}{2}^+)$ can be resolved with reanalysis of πN elastic data and an analysis of new data on double pion photoproduction (with charged pions).
- The search for the chiral partner of $\Delta_{7/2^+}(1920)$ state is the main subject in our current analysis of double pion and $\pi^0\eta$ photoproduction data.

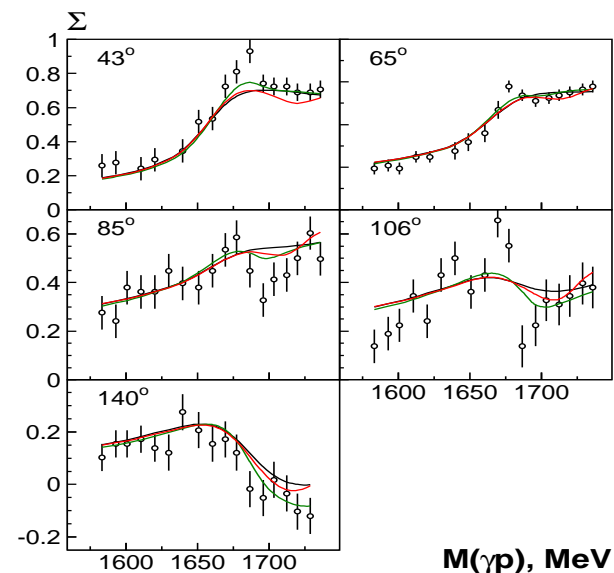
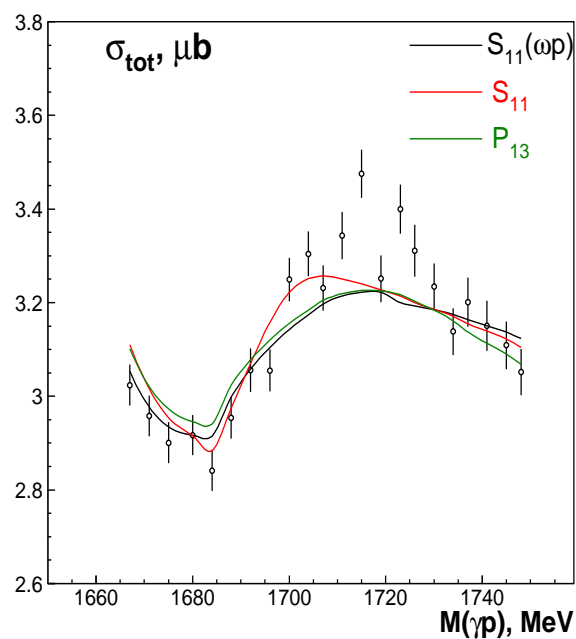
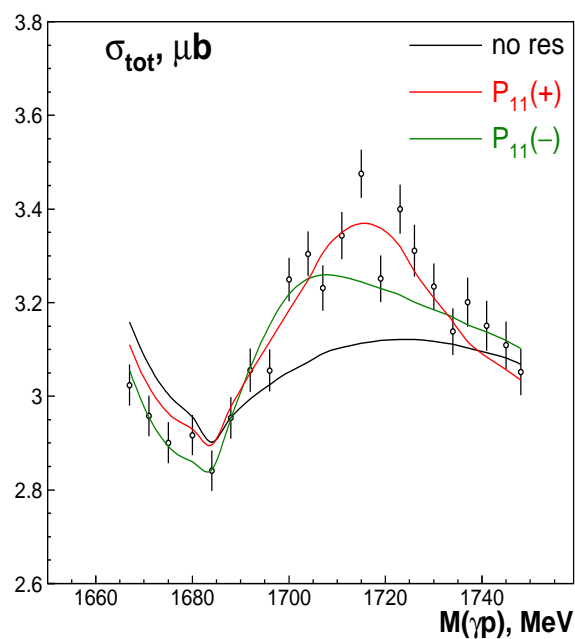
MAMI data on $\gamma p \rightarrow \eta p$. A narrow state at 1700 MeV?

E. F. McNicoll *et al.*, Phys. Rev. C 82 (2010) 035208 [arXiv:1007.0777 [nucl-ex]]

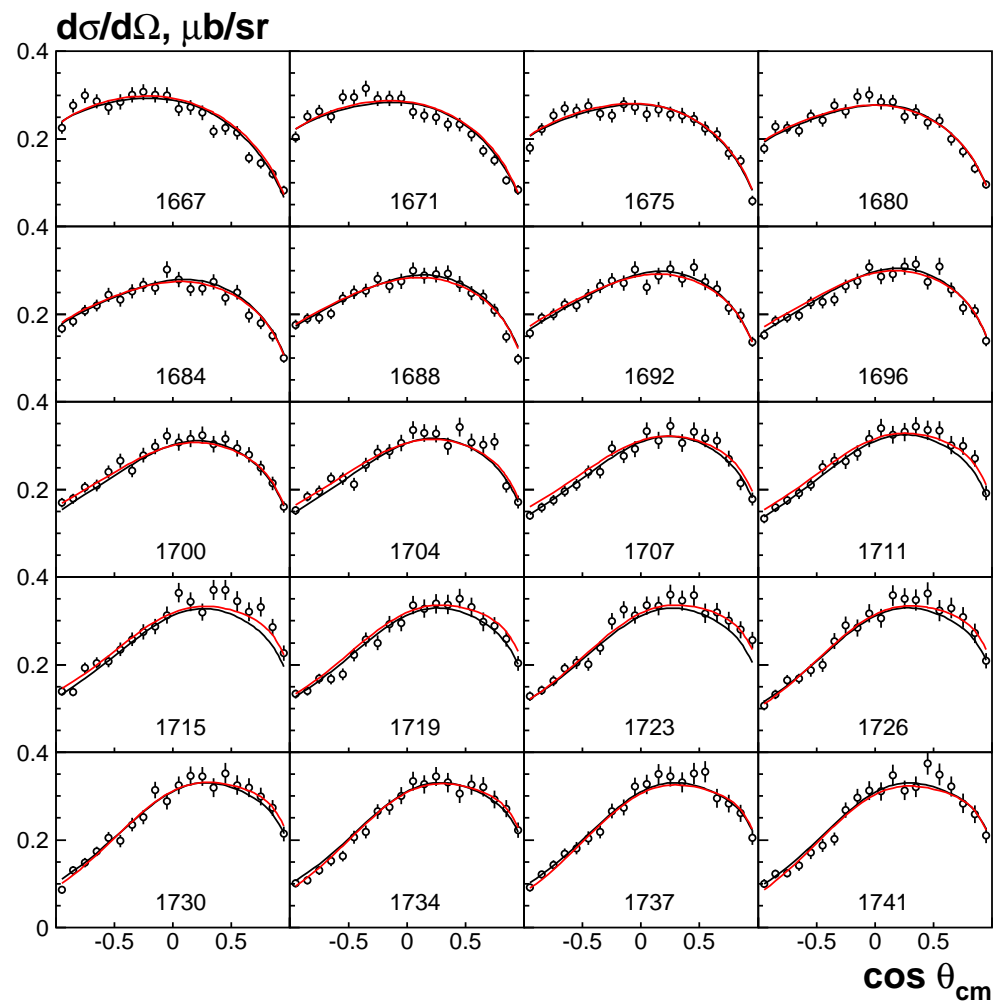
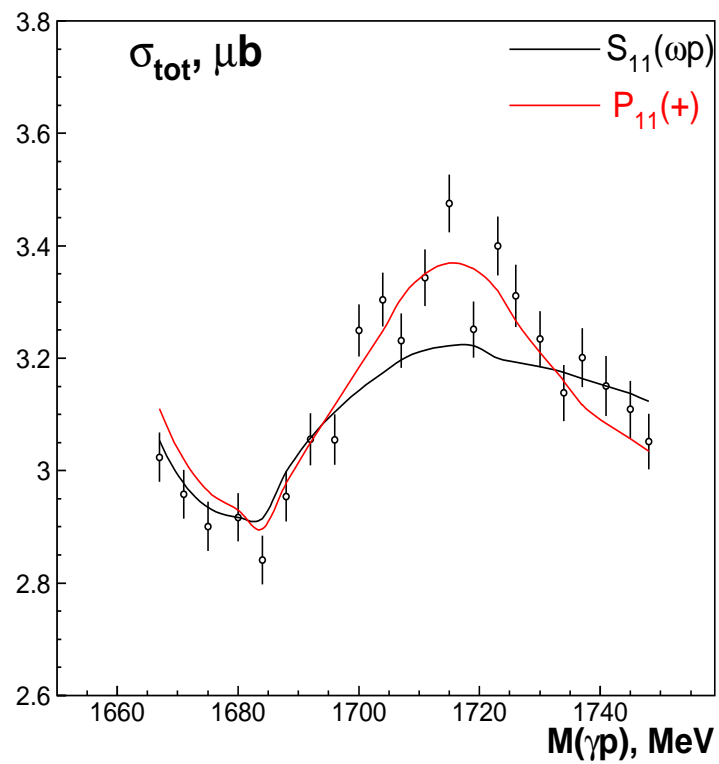


Fits with narrow states or ωp photoproduction

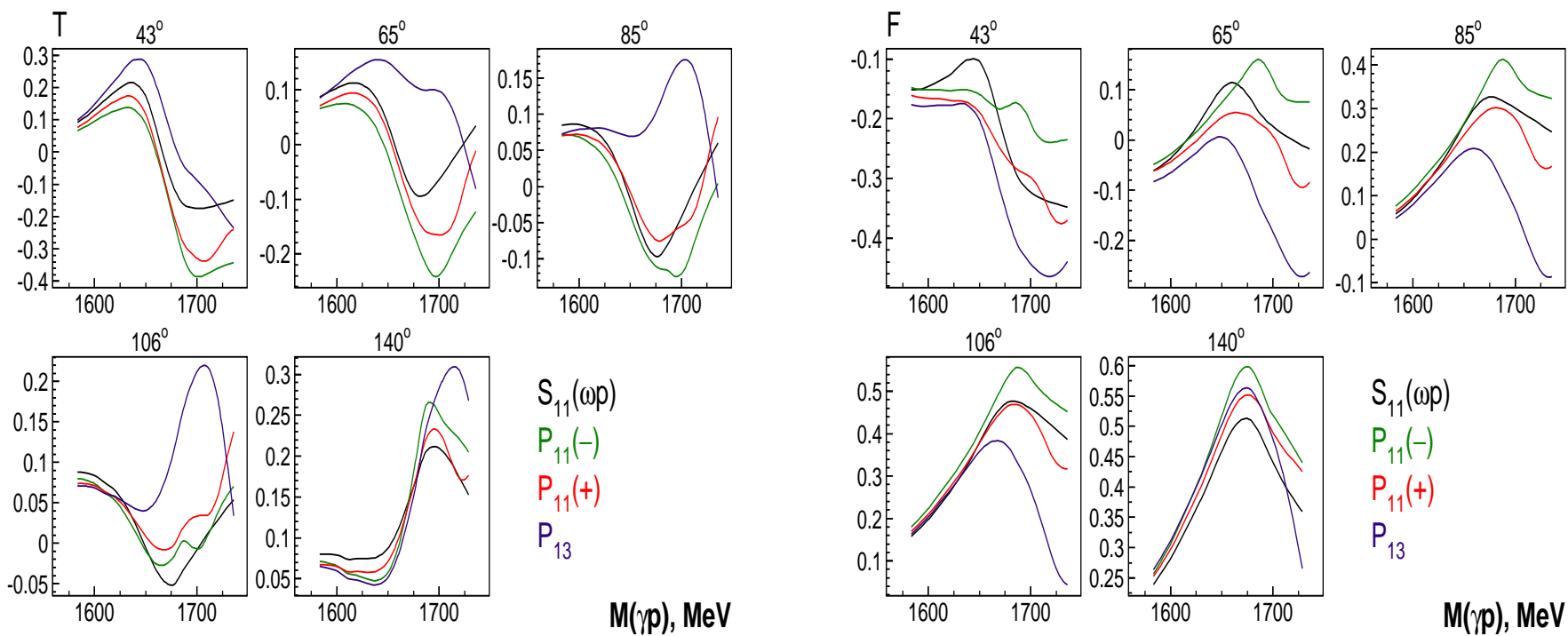
Resonance	Mass MeV	Γ_{tot} MeV	$\sqrt{\text{Br}_{\eta N} A_{1/2}^p}$ $10^{-3} \text{GeV}^{1/2}$	$\sqrt{\text{Br}_{\eta N} A_{3/2}^p}$ $10^{-3} \text{GeV}^{1/2}$	$\chi_{\text{tot}}^2/N_{\text{dat}}$	$\chi_{\text{sel}}^2/N_{\text{dat}}$	$\chi_{\Sigma}^2/N_{\text{dat}}$
no res.	-	-	-	-	1.13	1.21	1.46
$P_{11}(+)$	1719	41	3.1	-	1.07	0.93	1.51
$P_{11}(-)$	1694	35	2.9	-	1.11	0.91	1.11
P_{13}	1728	72	2.6	4.7	1.02	0.93	1.47
S_{11}	1685	30	0.8	-	1.12	1.12	1.47
$S_{11}(\omega p)$	-	-	-	-	1.12	0.93	1.41



Solutions $S_{11}(\omega p)$ and $P_{11}(+)$

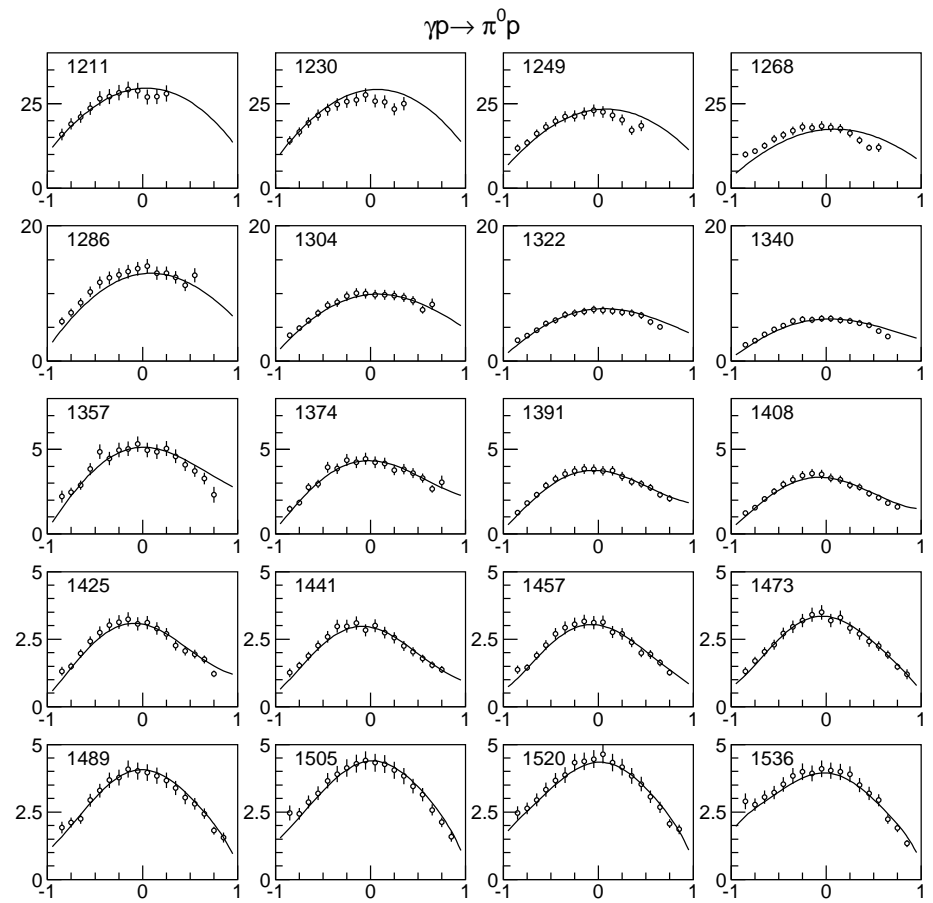
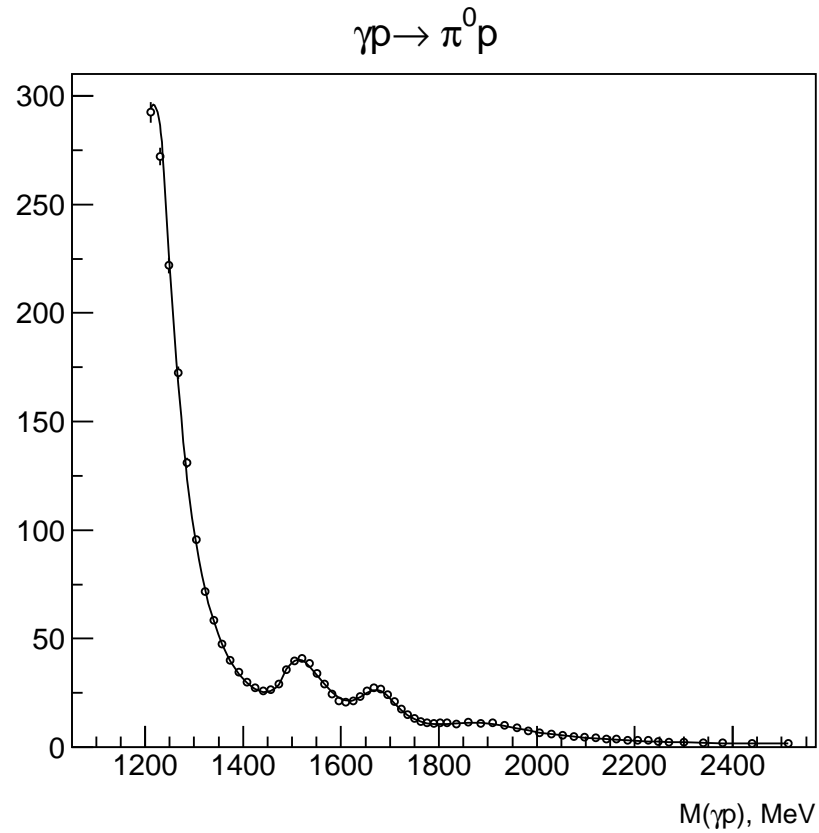


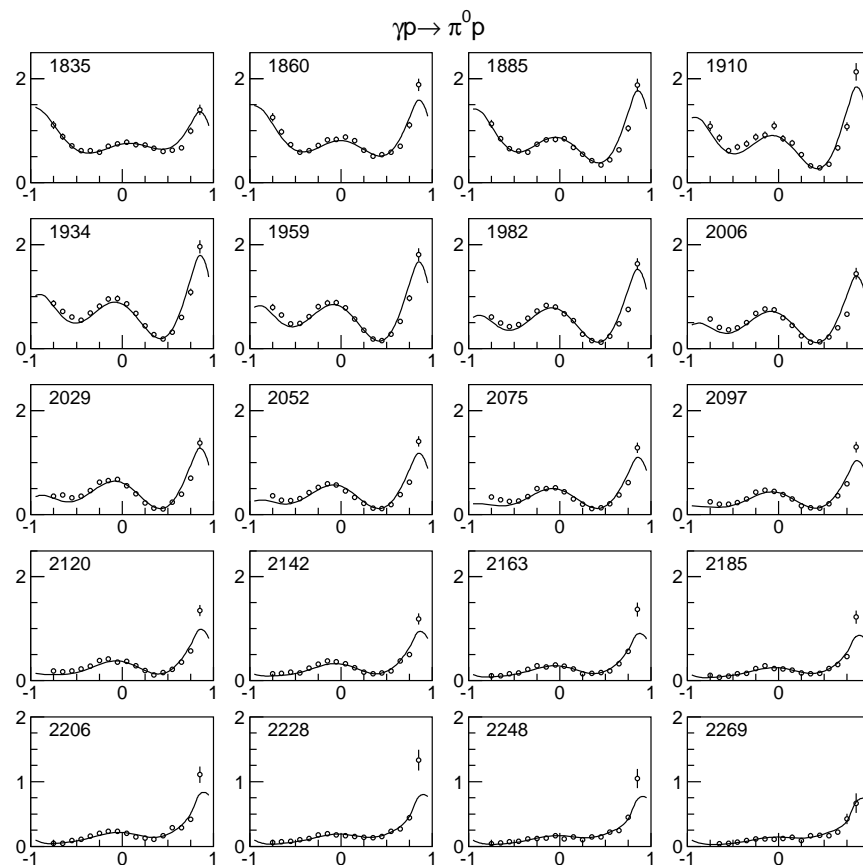
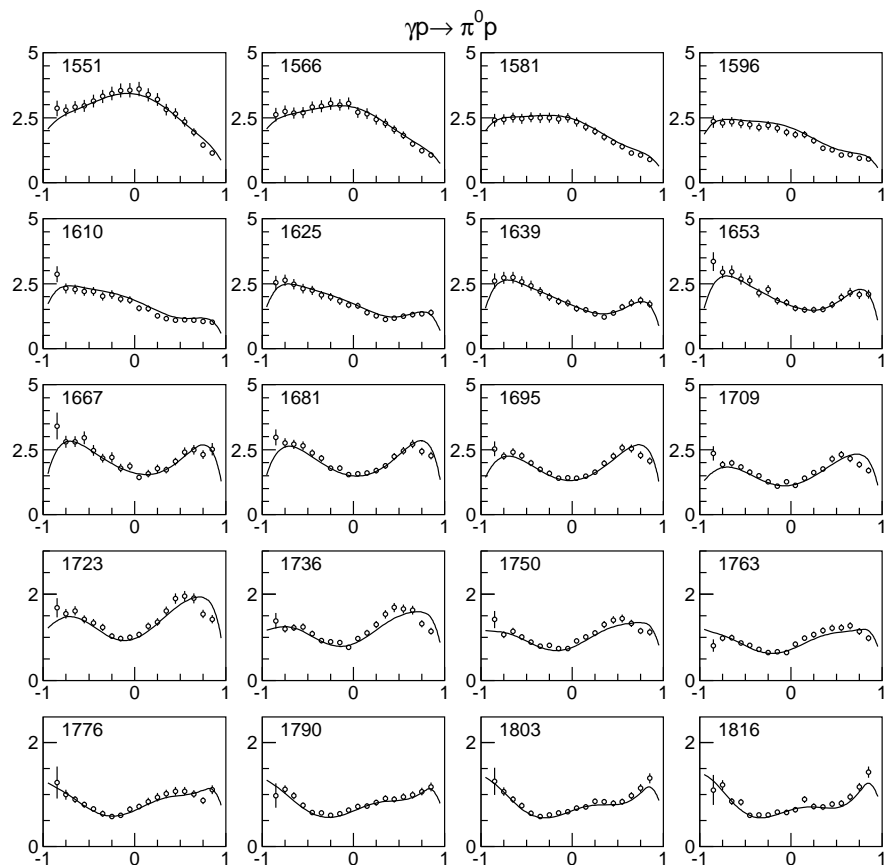
Prediction for polarization observables



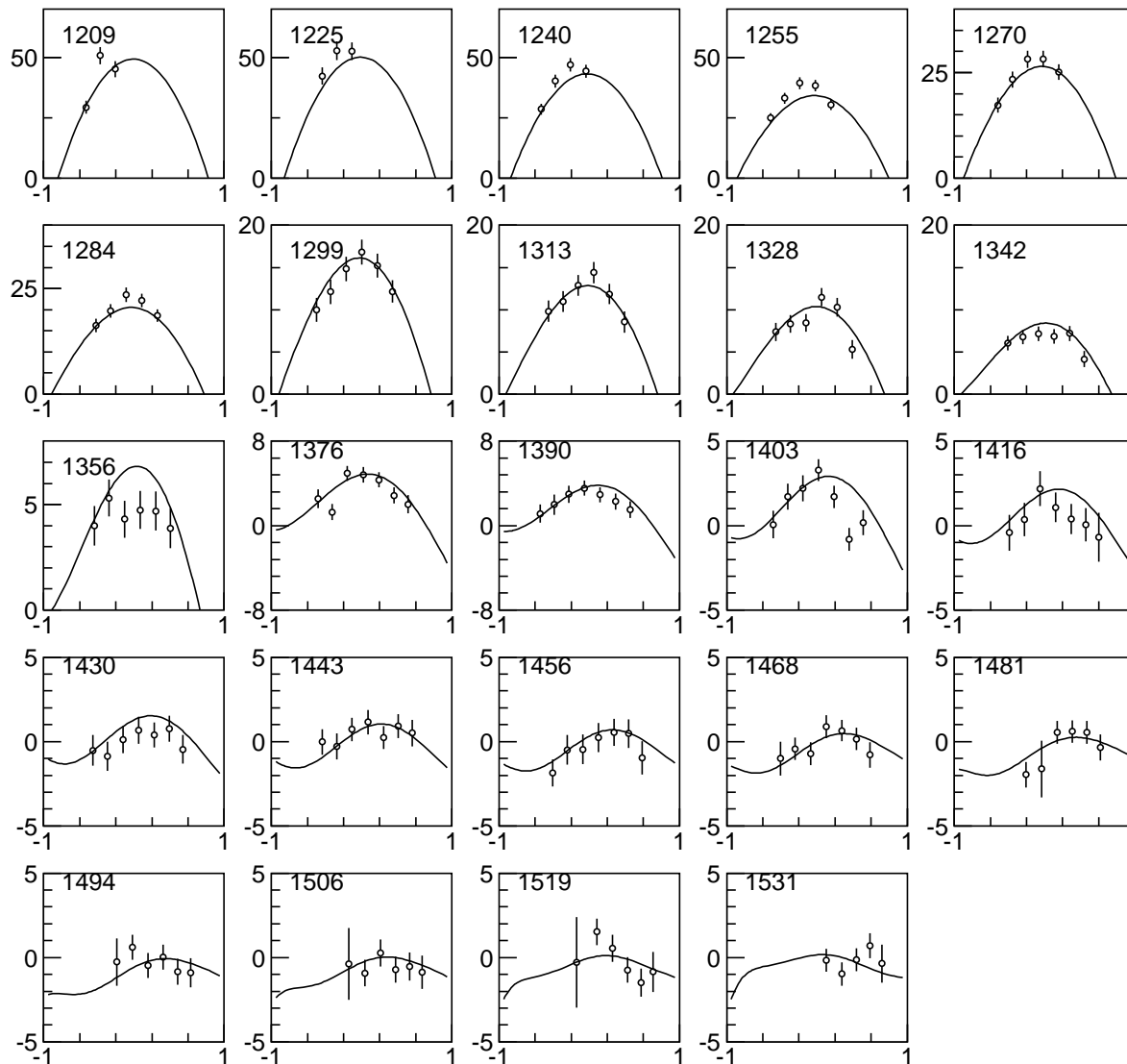
Summary

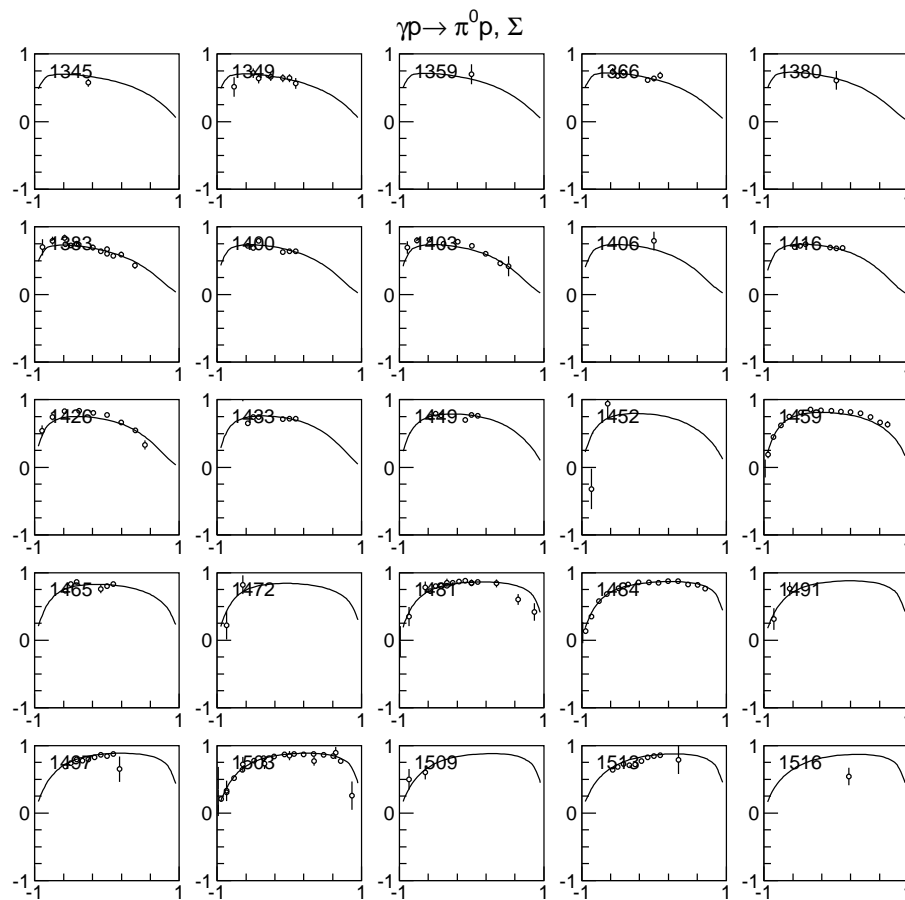
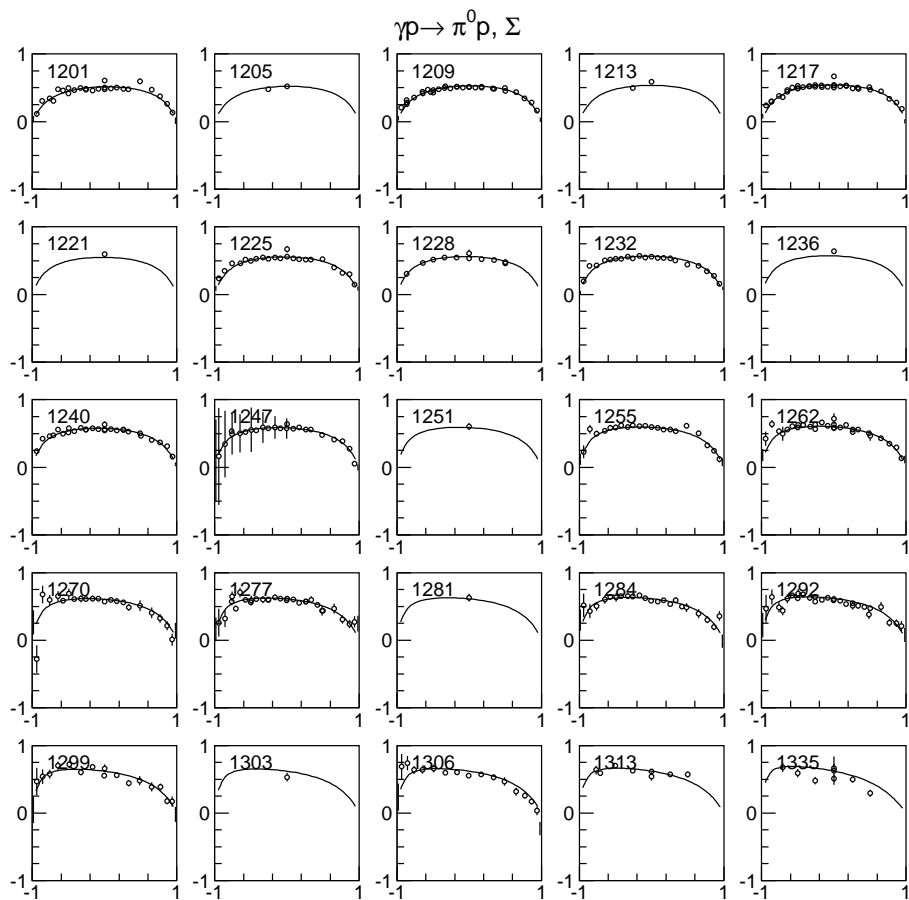
- **New high precision data on $\gamma p \rightarrow \eta p$ show a narrow structure in the mass region 1650-1750 MeV.**
- **The structure can be explained either with a narrow state (in the S_{11} , P_{11} or P_{13} partial wave) or as an effect from photoproduction of ωp channel in the S_{11} partial wave.**
- **The beam asymmetry data [2] favor the solution $P_{11}(-)$ with mass 1694 MeV and width 35 MeV.**
- **High statistical data on beam asymmetry and beam-target polarization observables will determine which partial wave is responsible for the narrow structure. Such data can also help to distinguish between $P_{11}(+)$ and $P_{11}(-)$ solutions.**

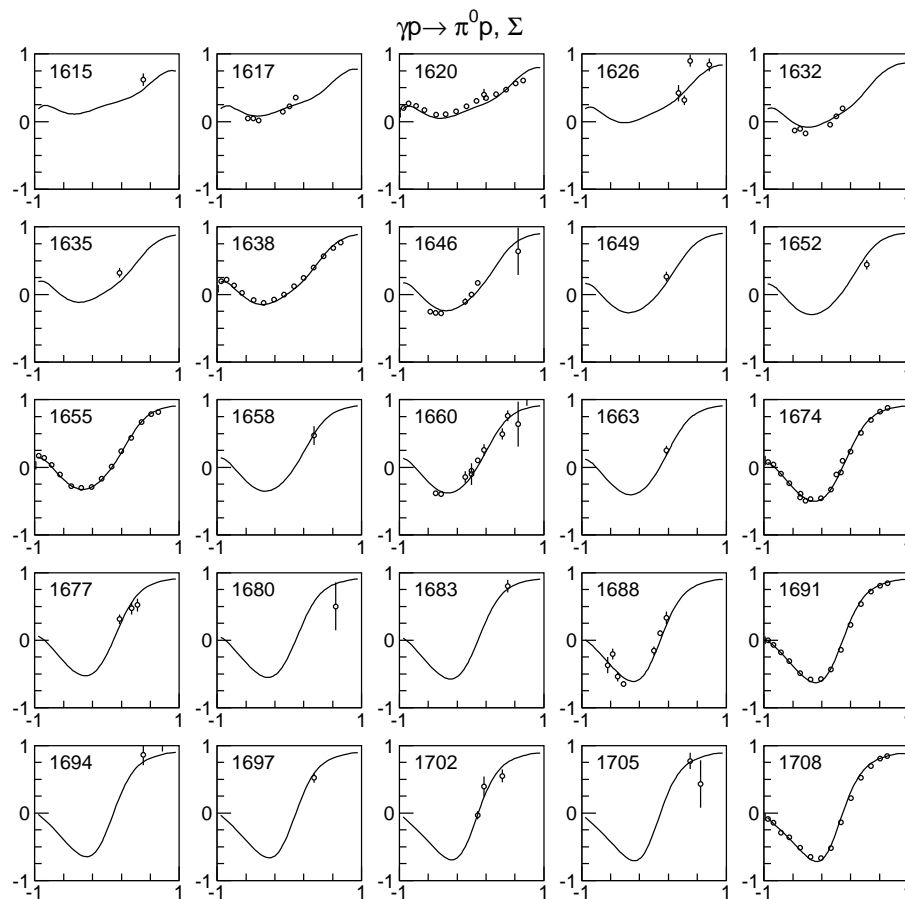
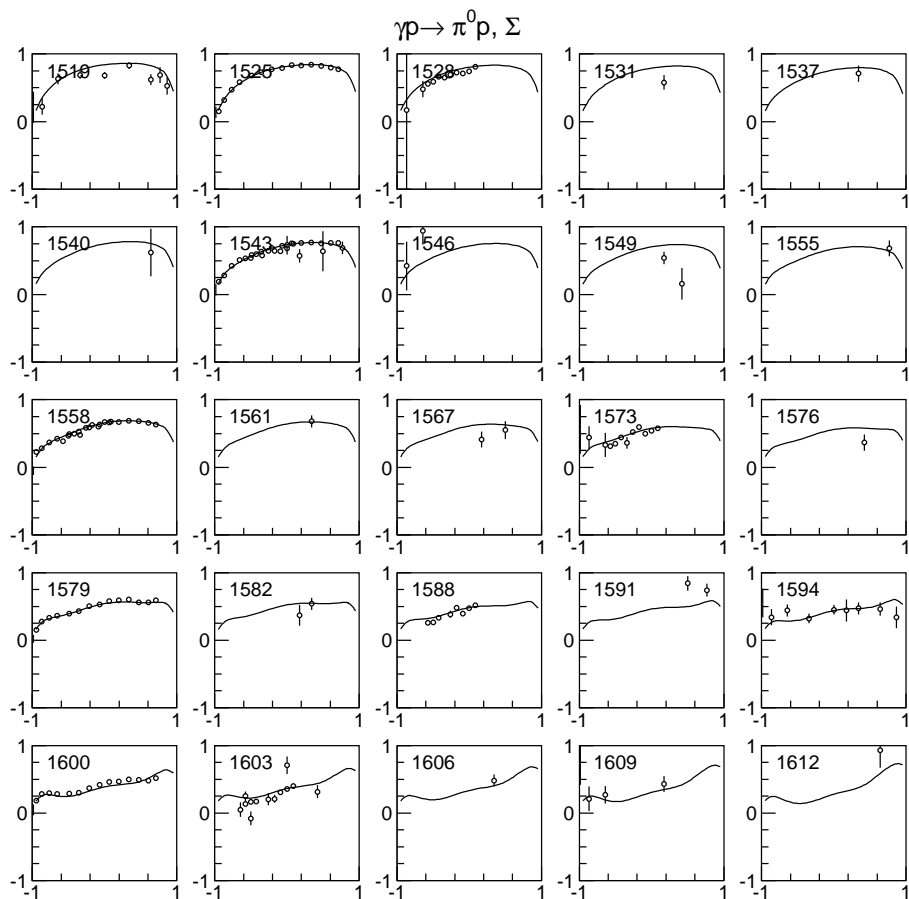


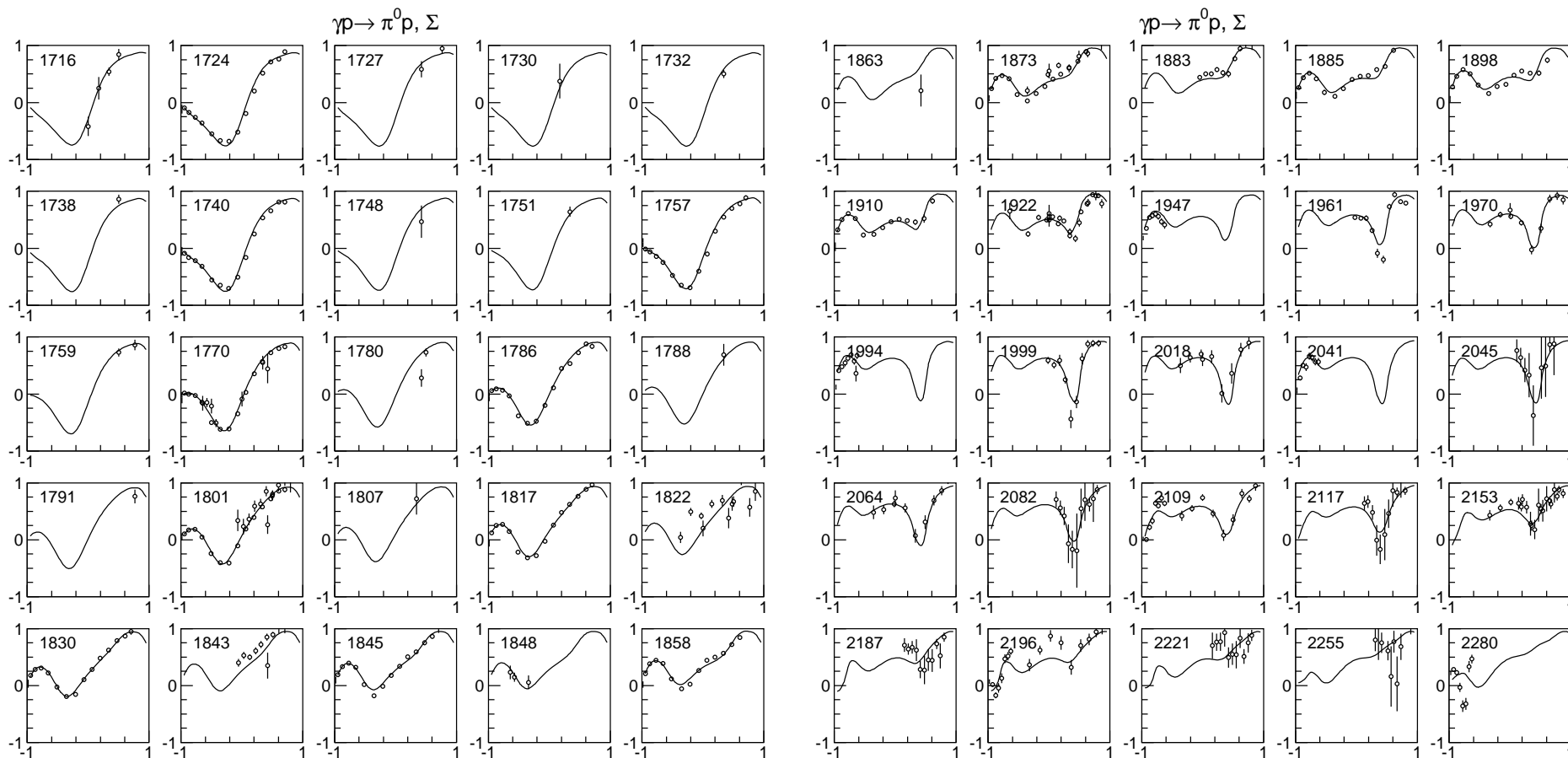


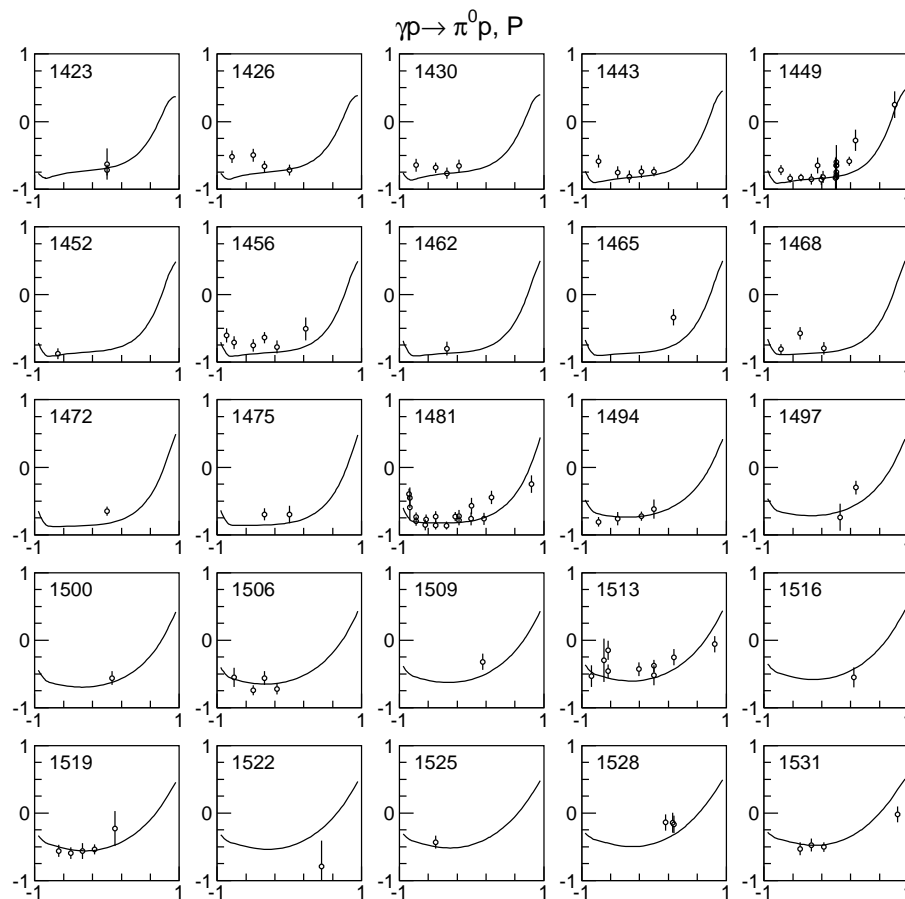
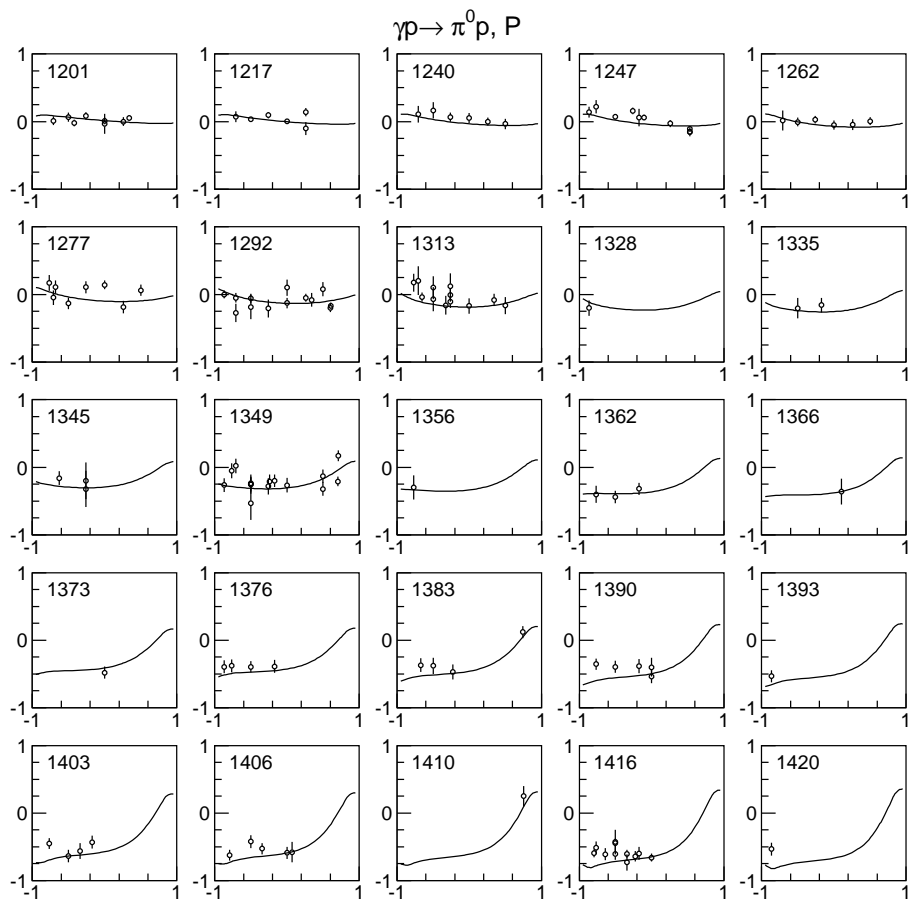
$\gamma p \rightarrow \pi^0 p, 3/2-1/2$

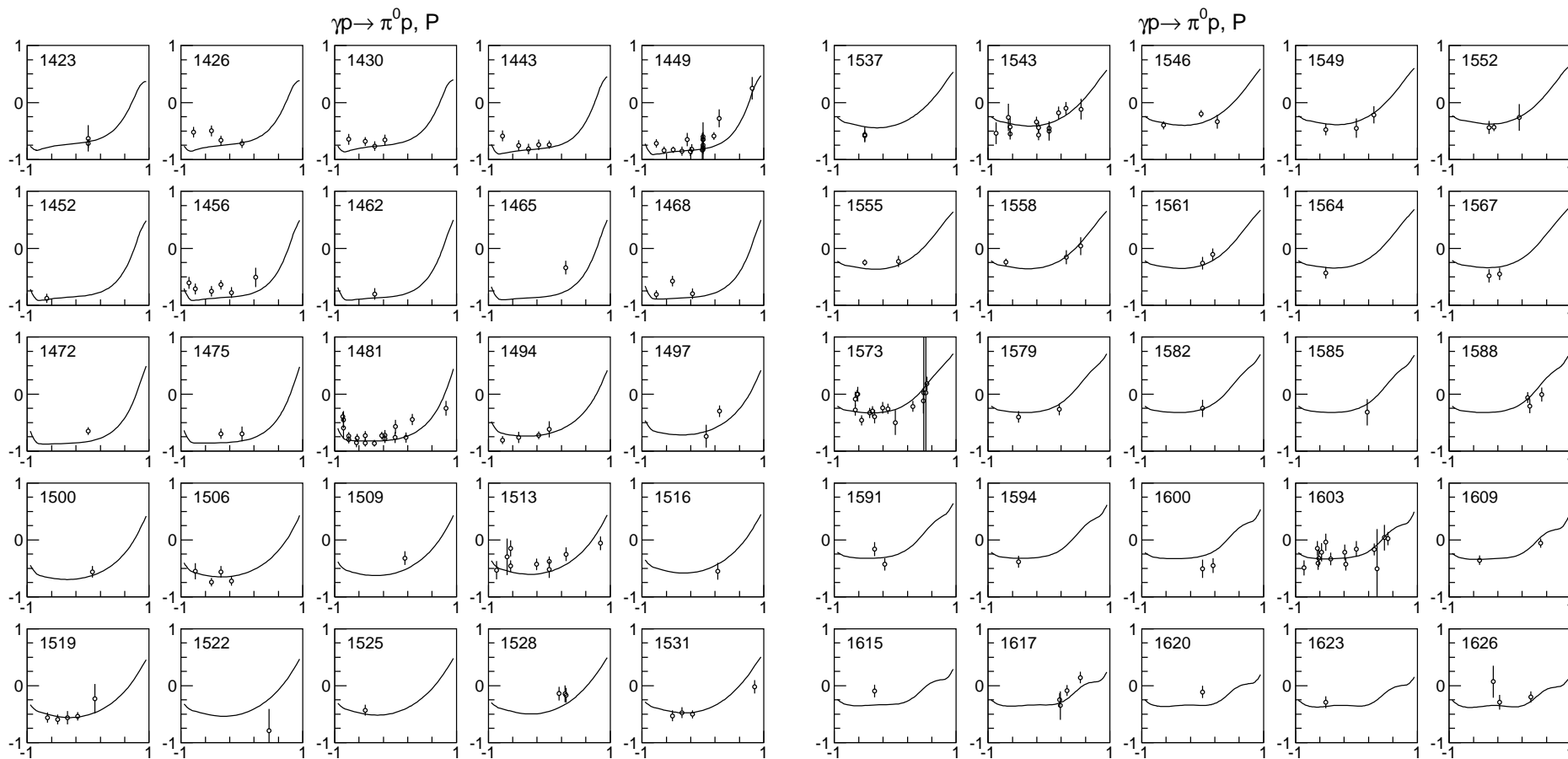


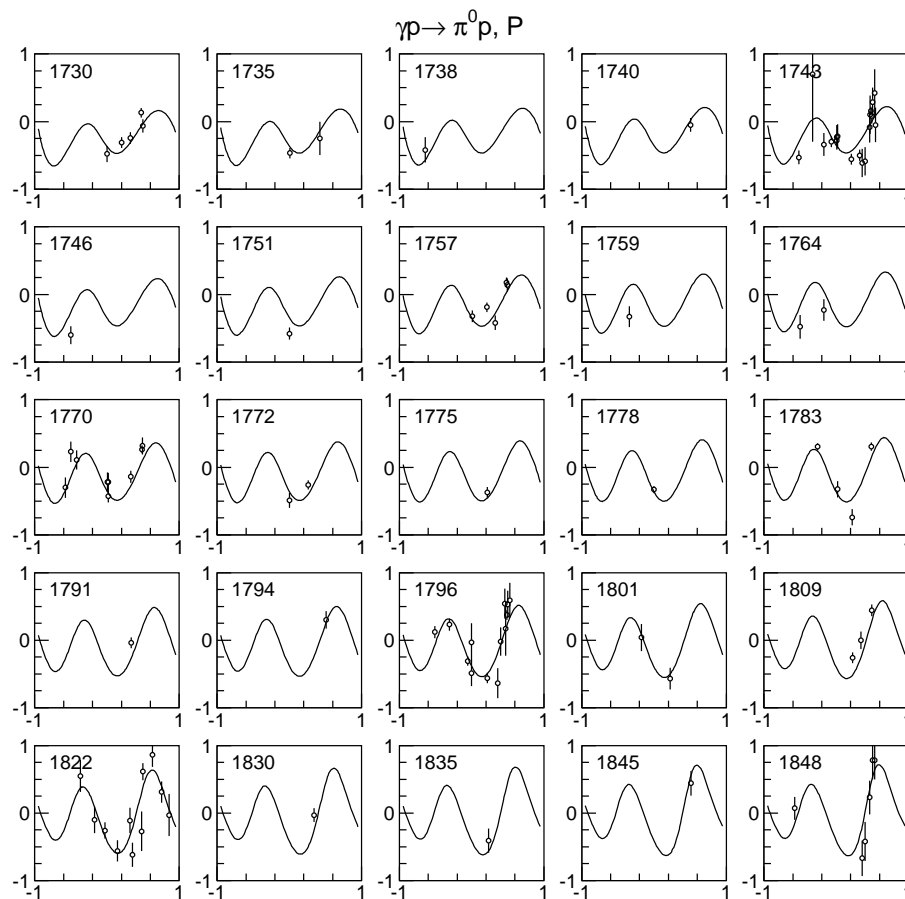
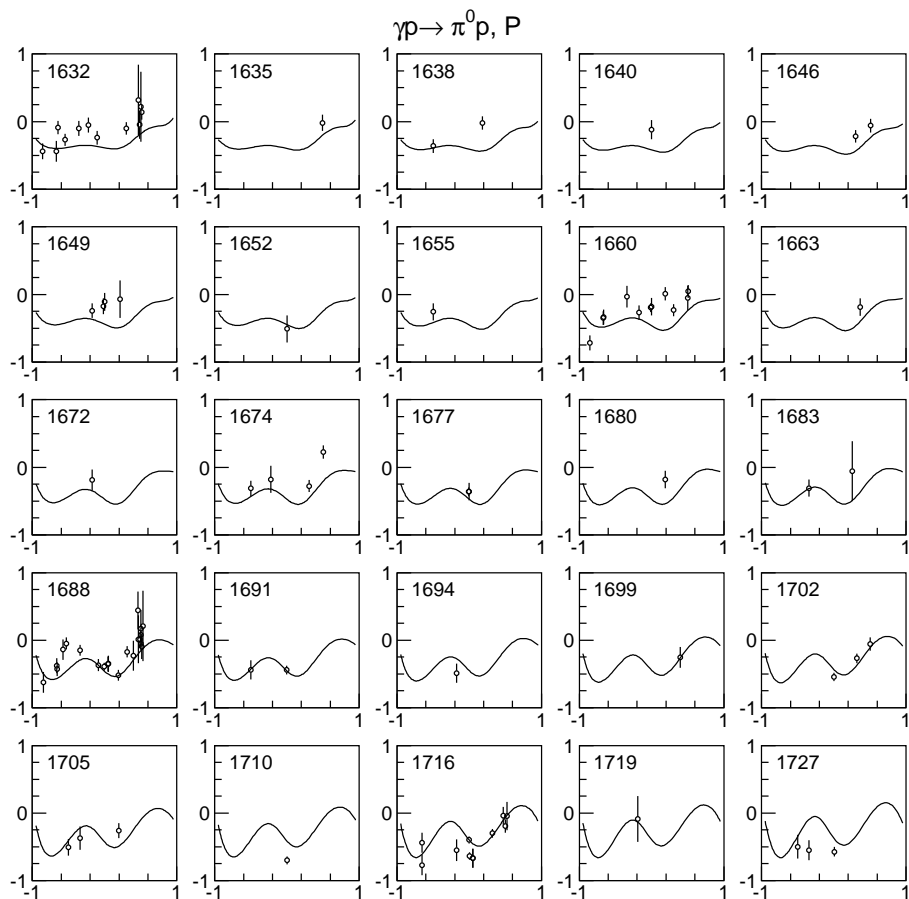


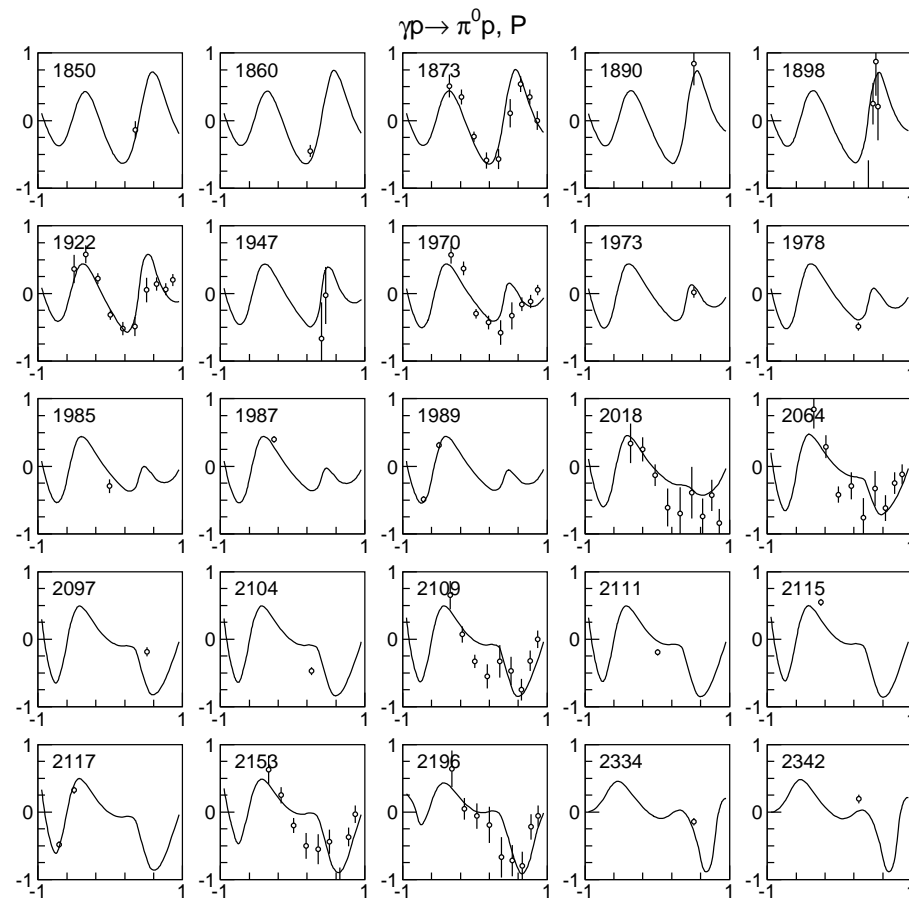


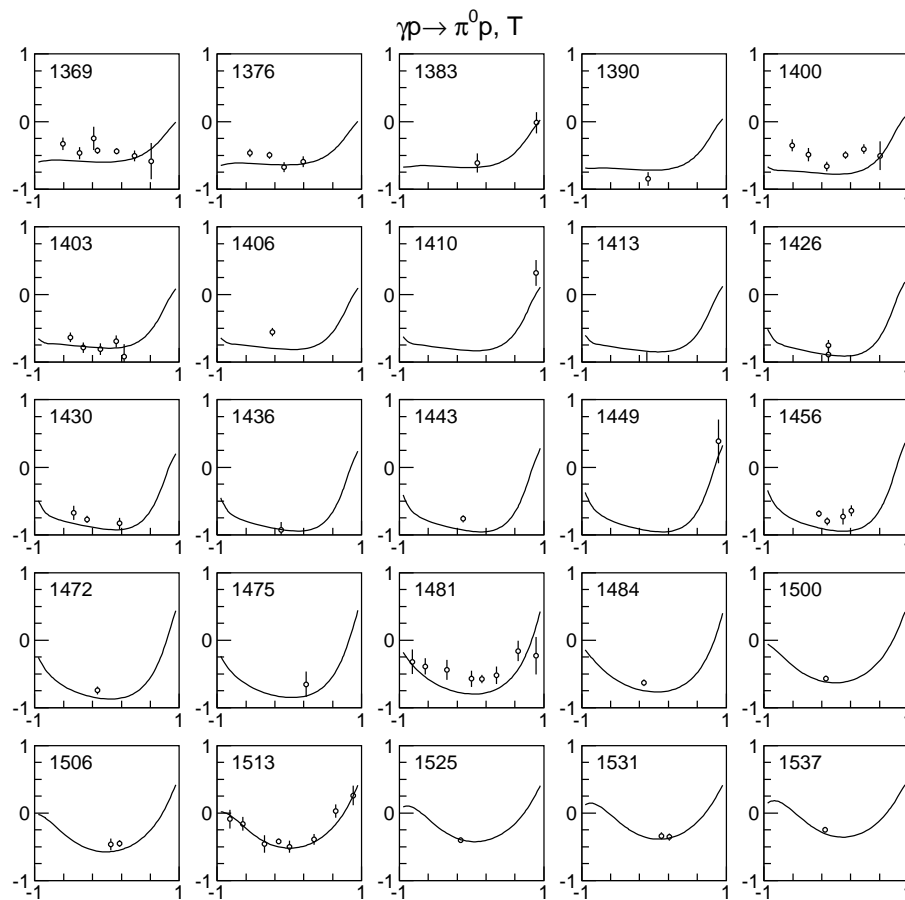
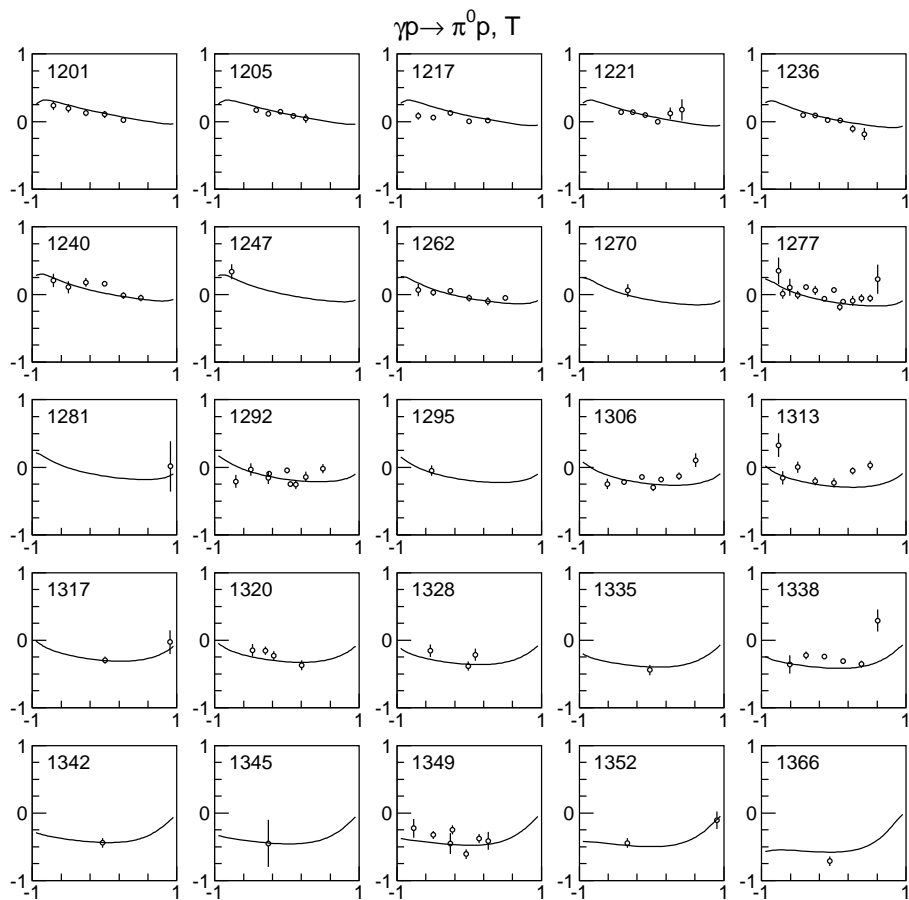


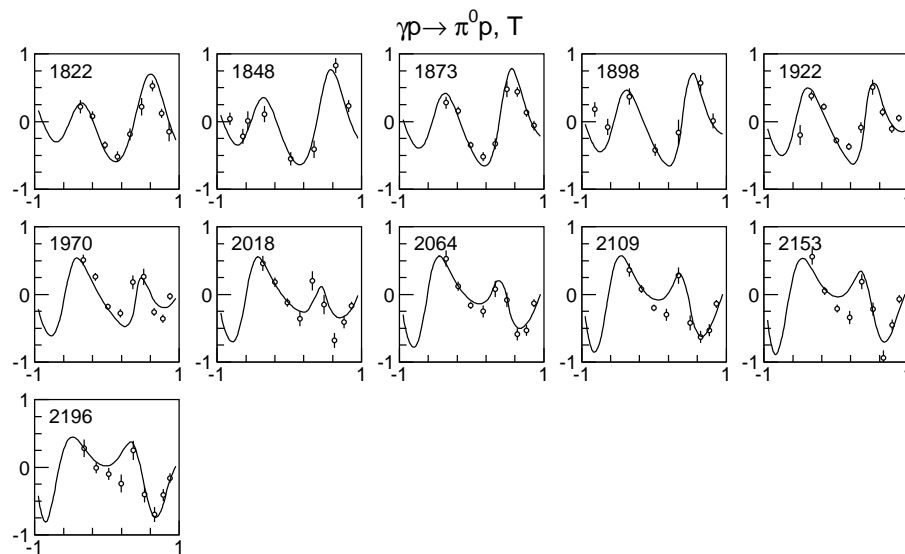
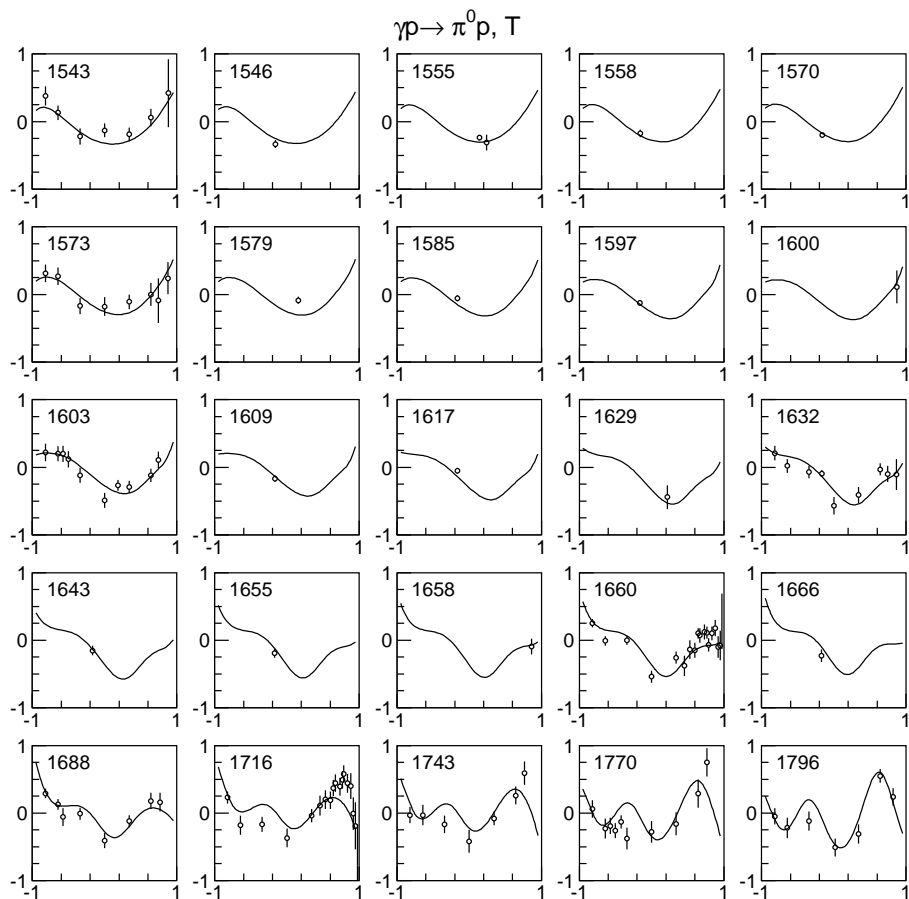


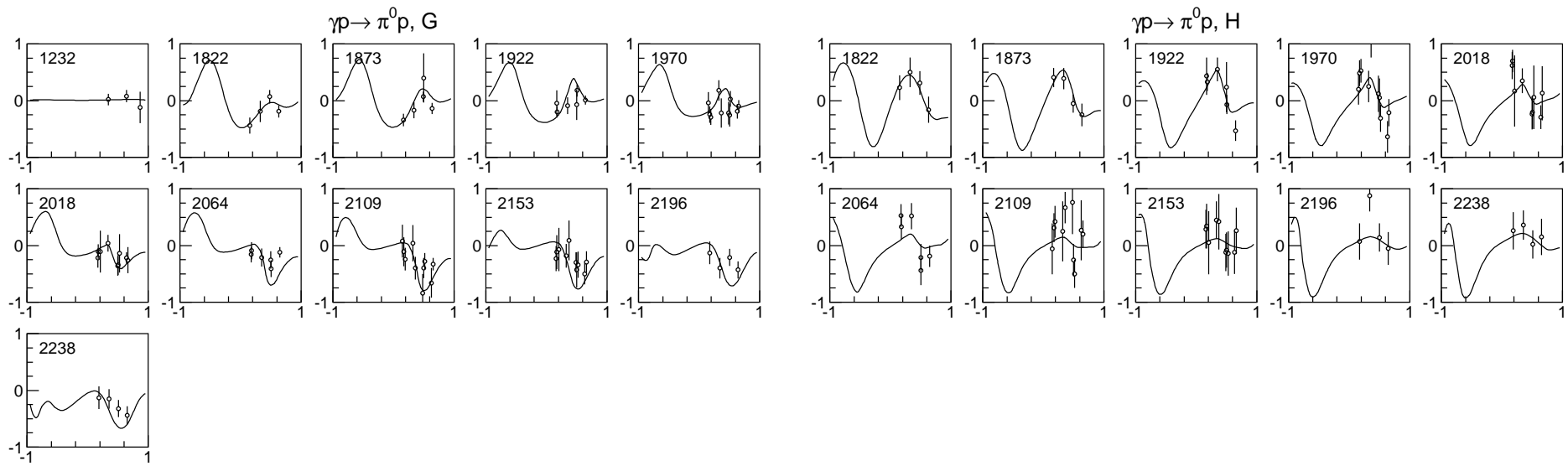


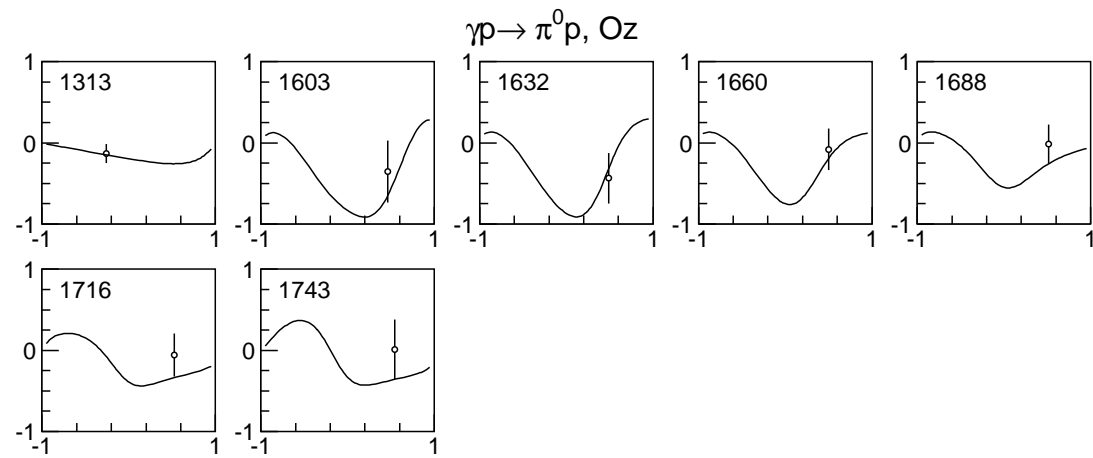
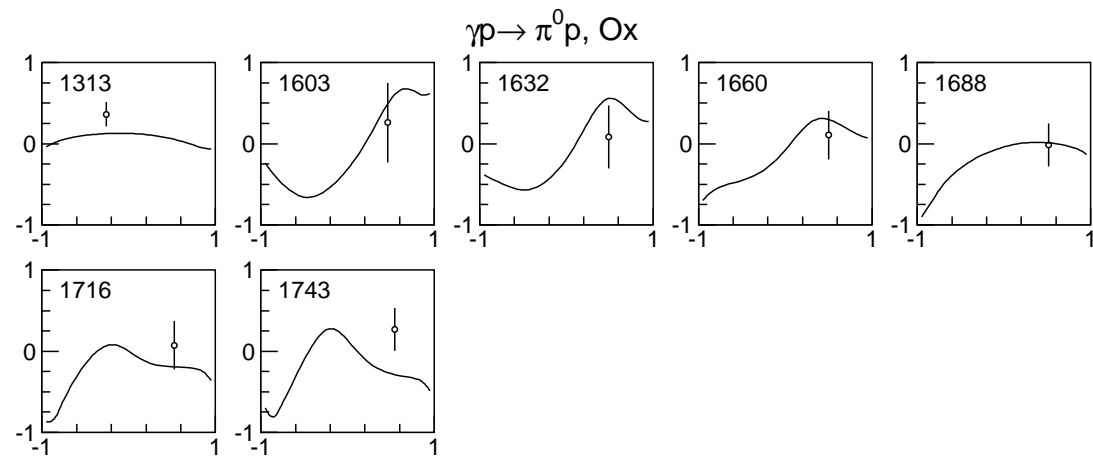


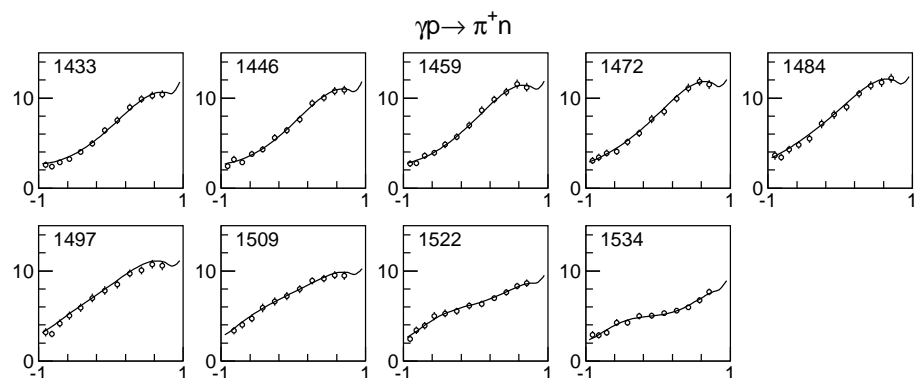
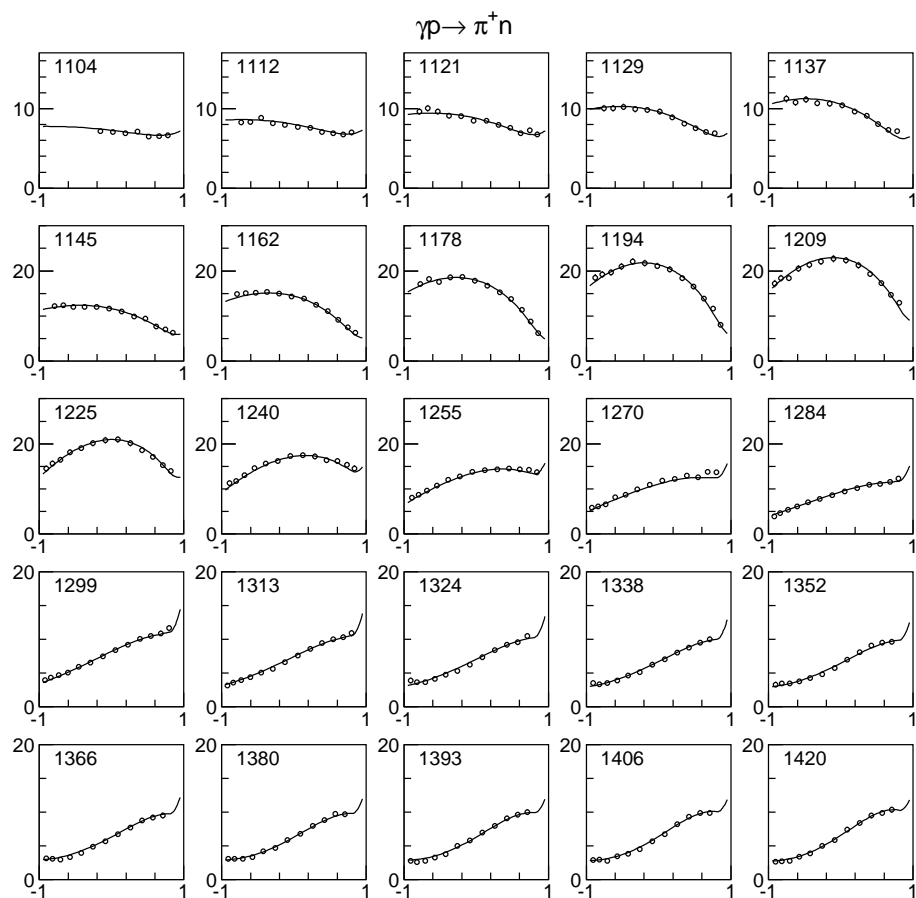


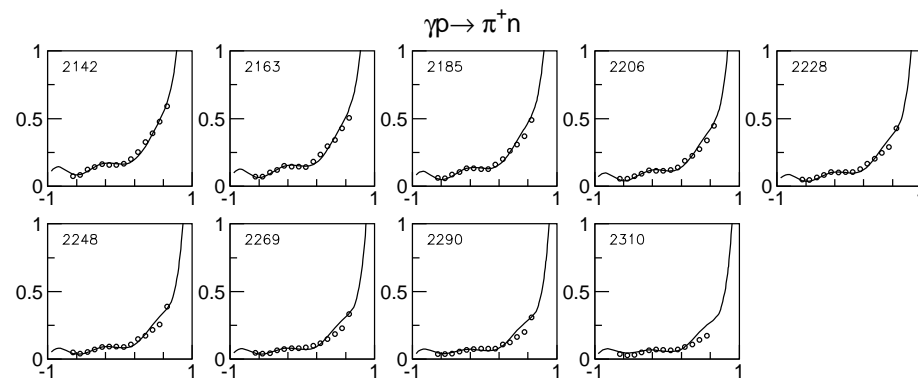
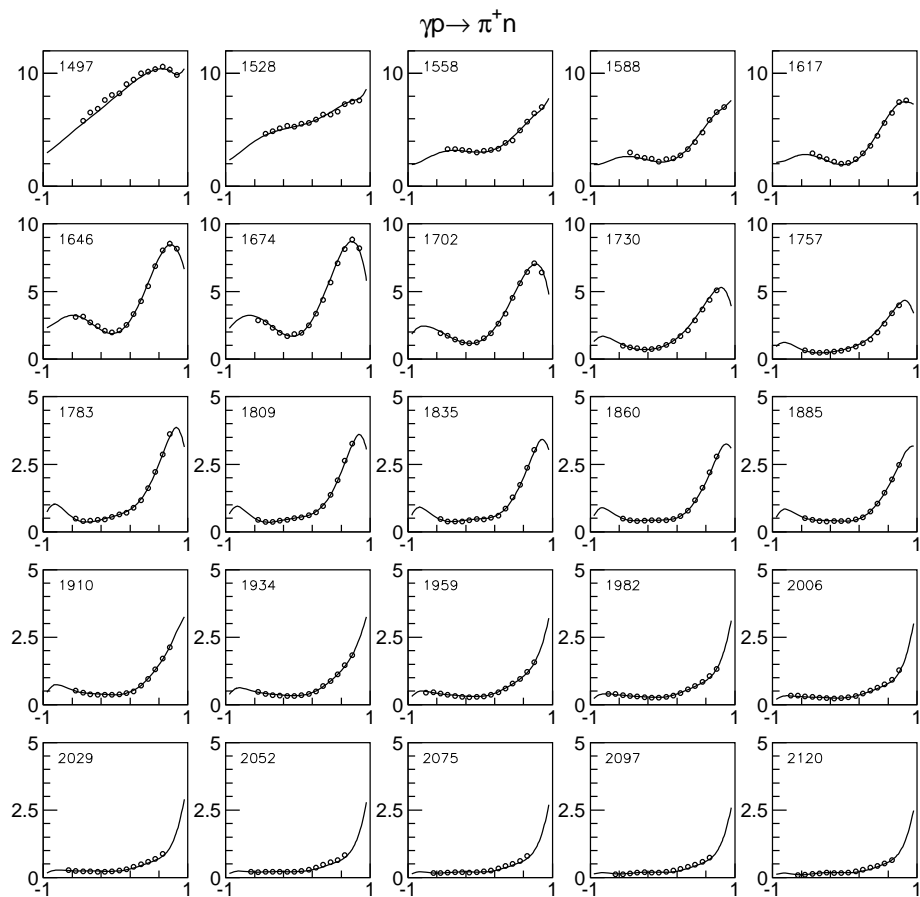


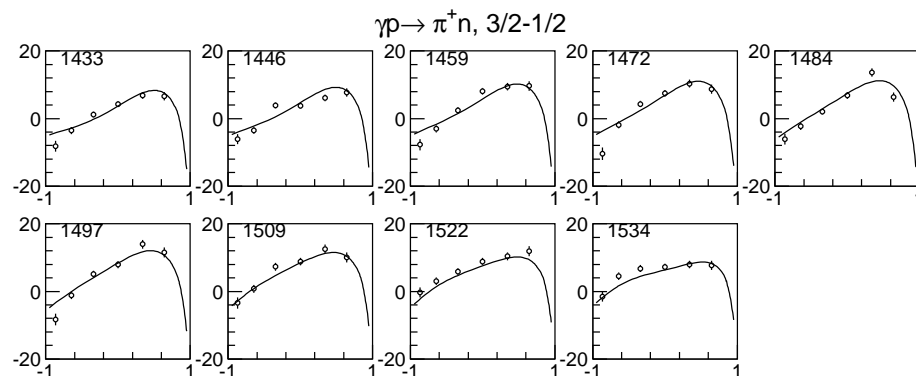
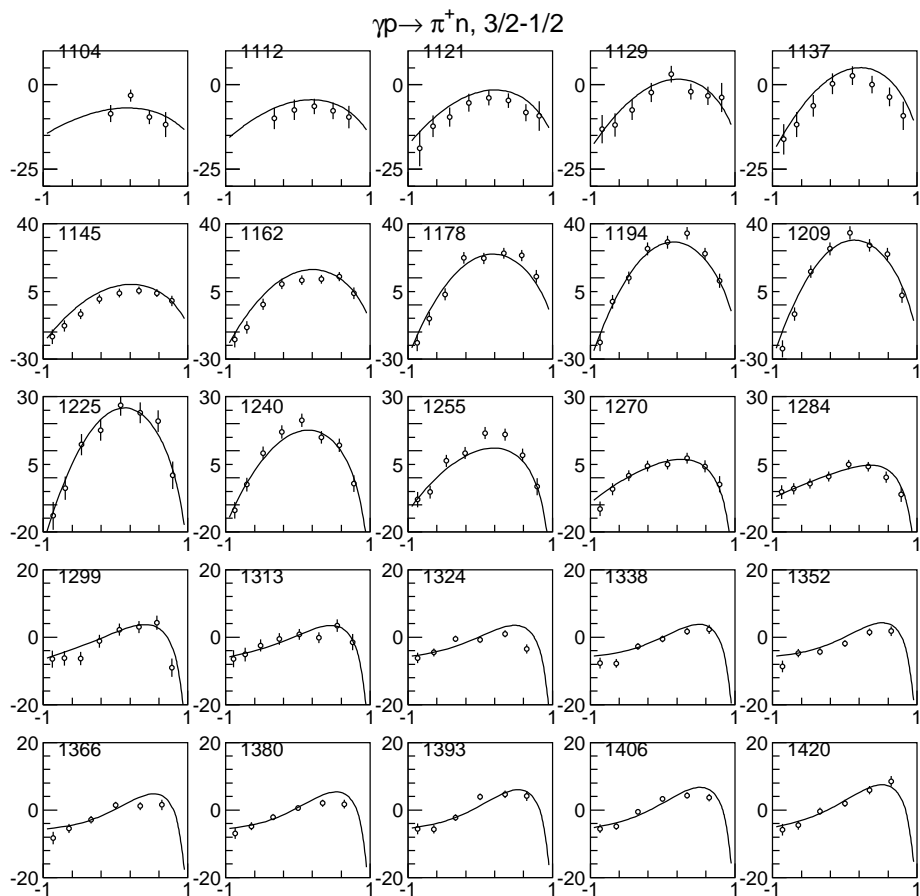


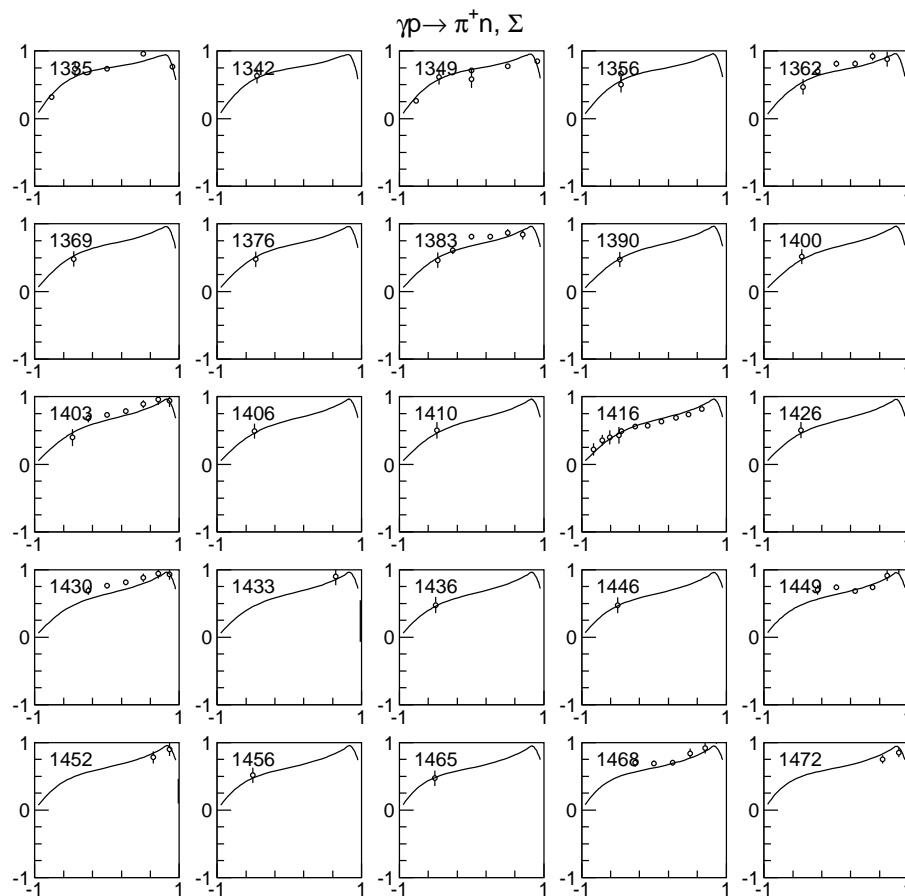
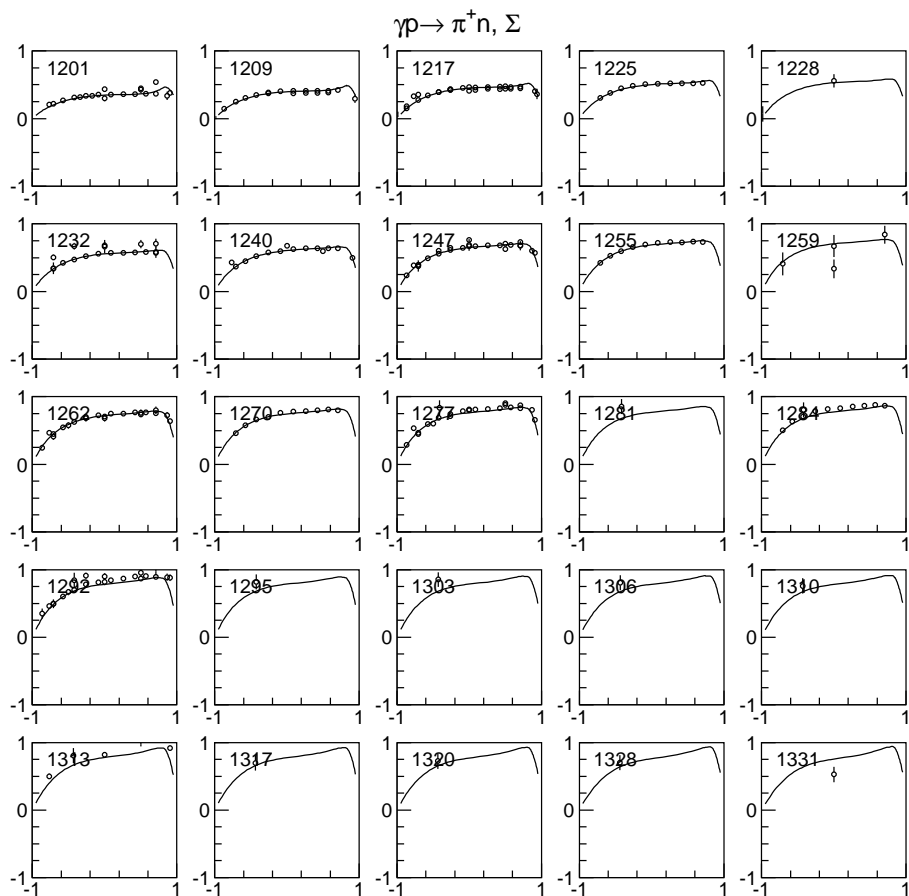


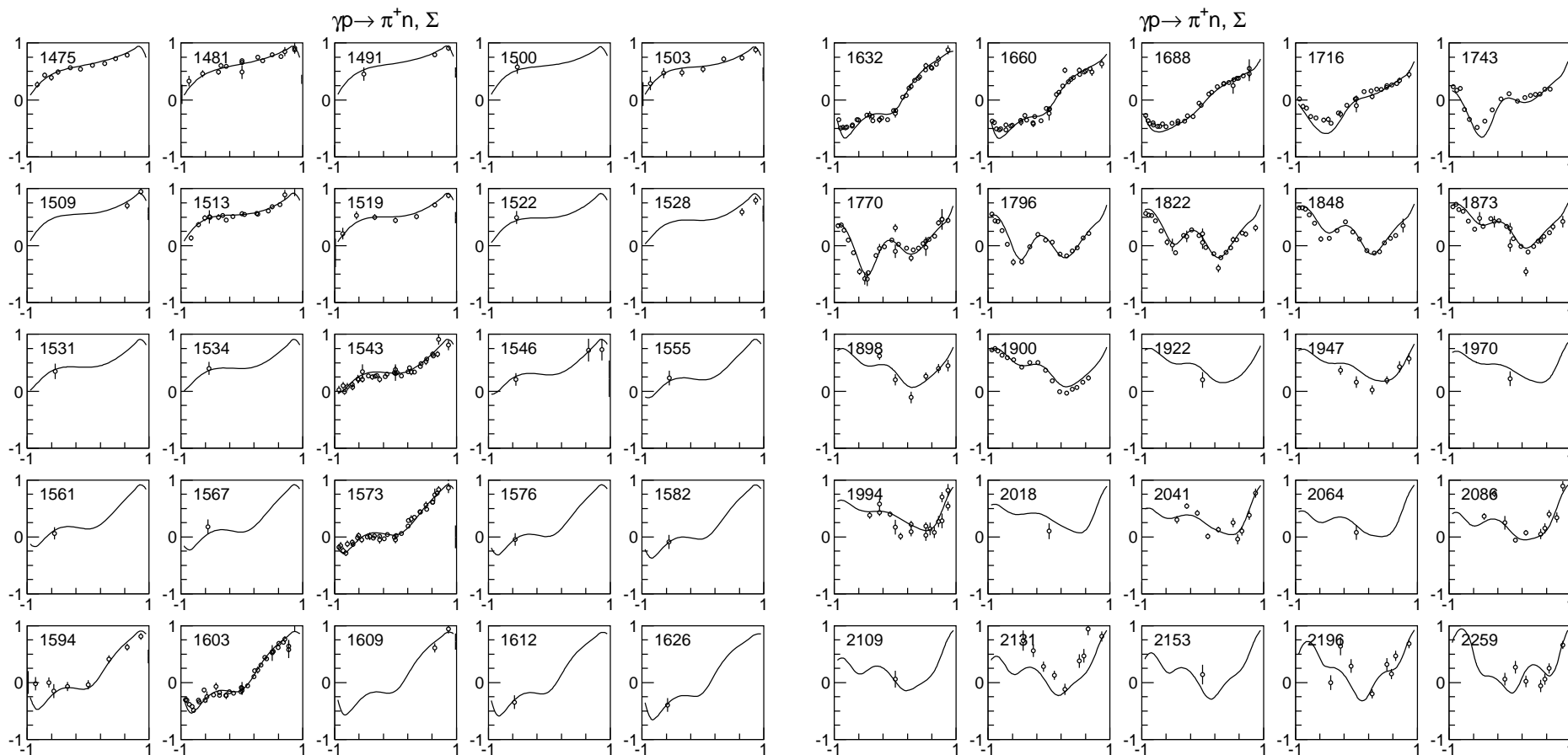


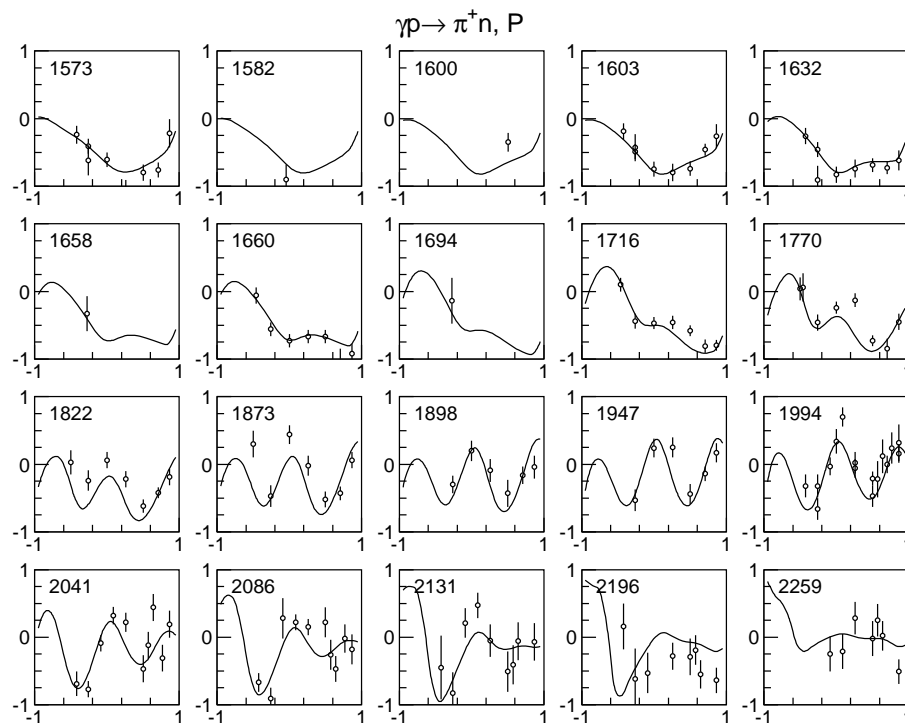
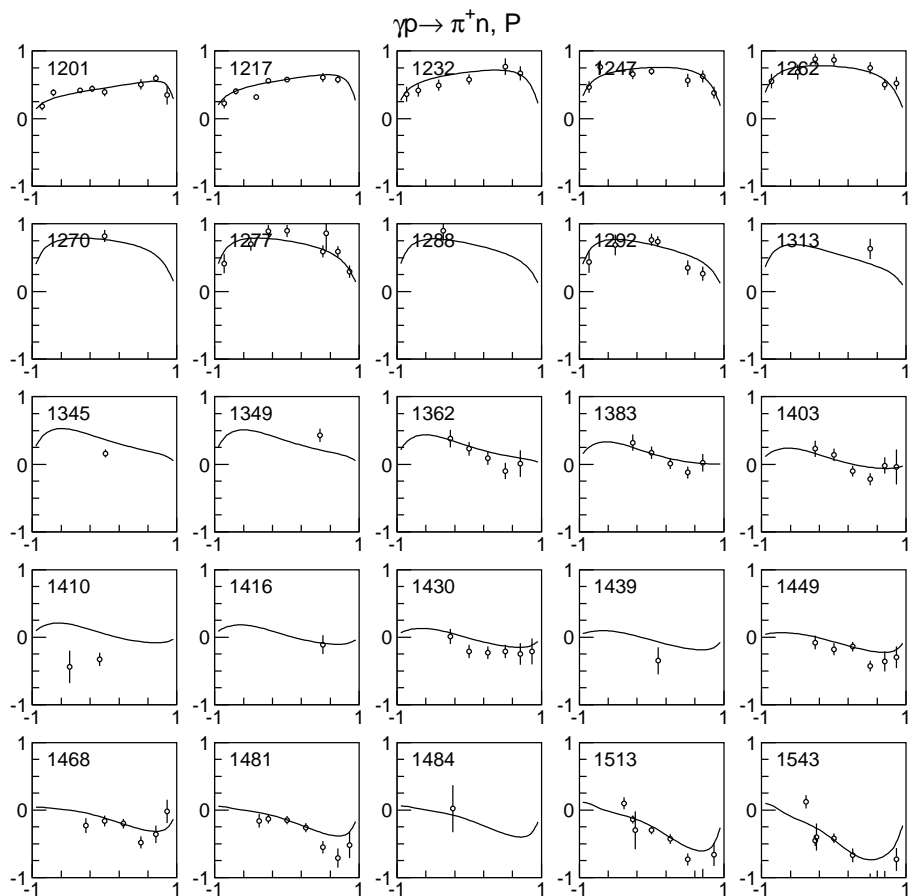


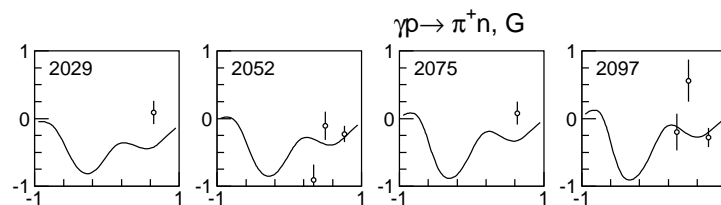
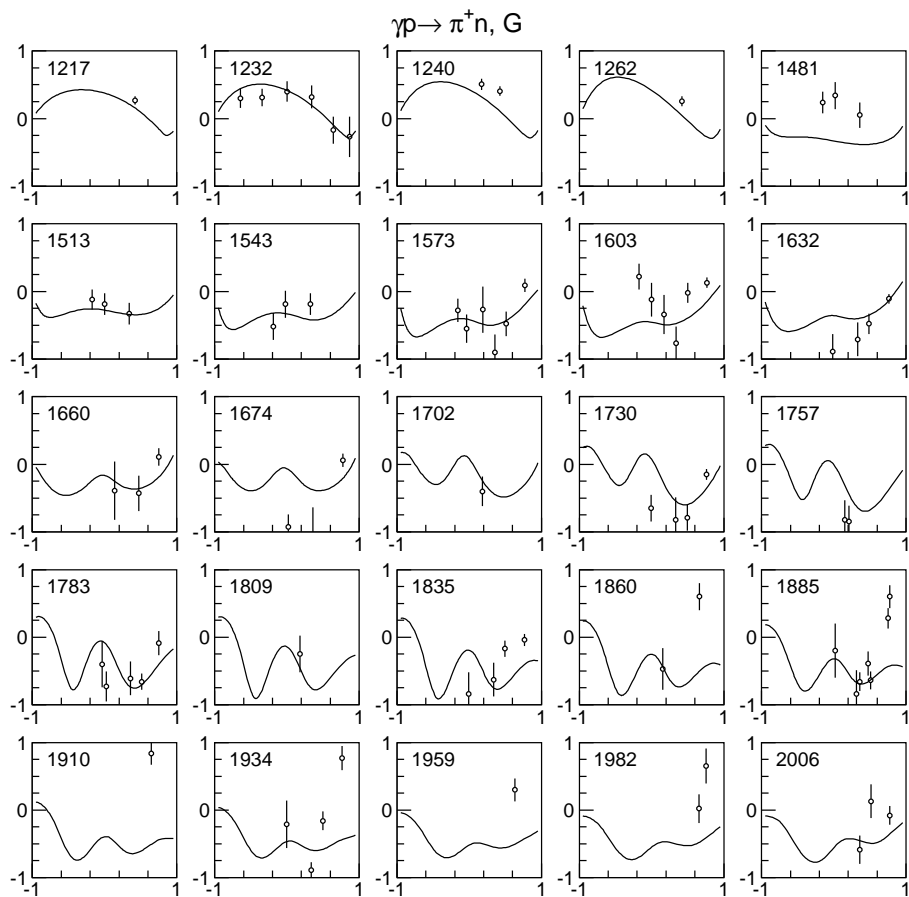


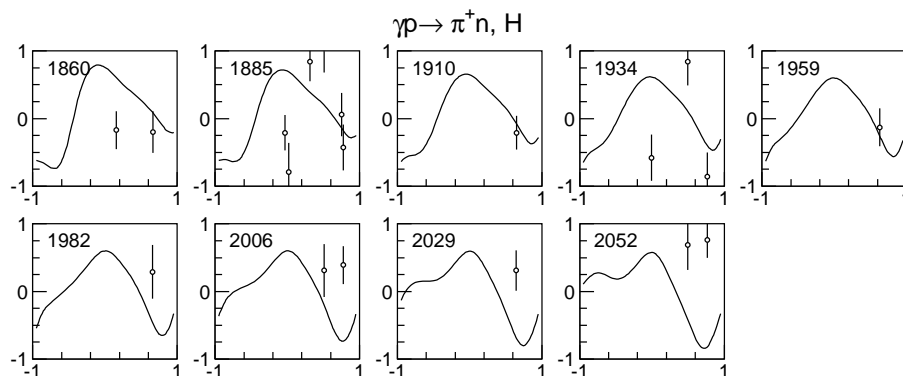
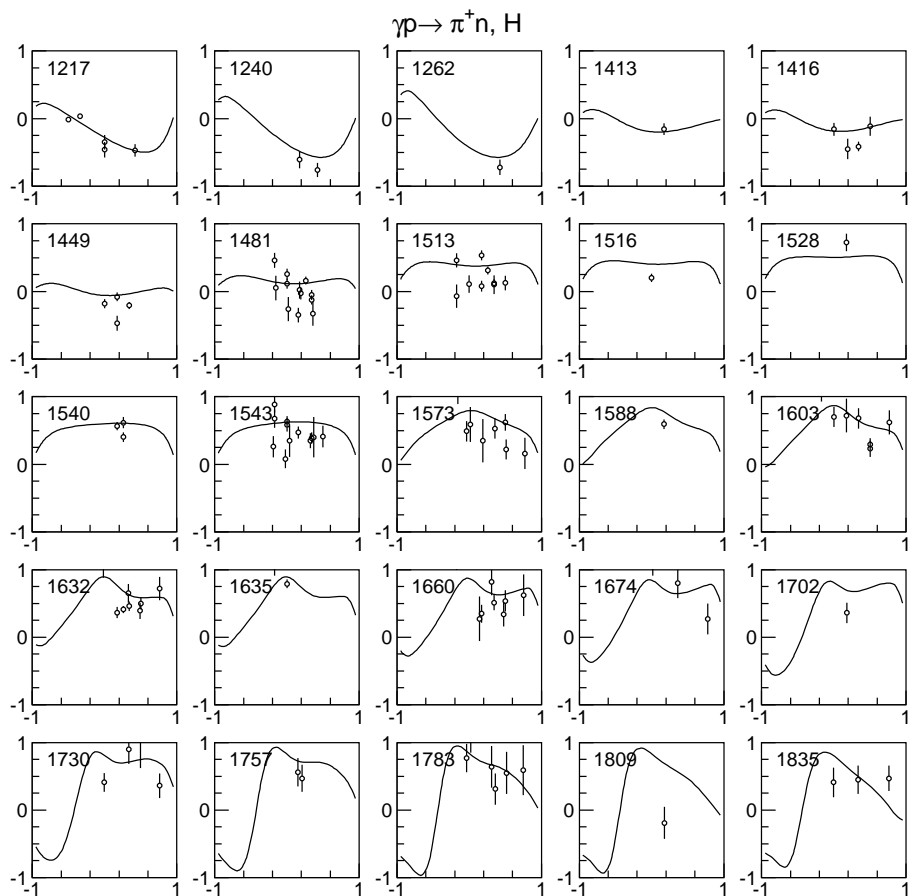


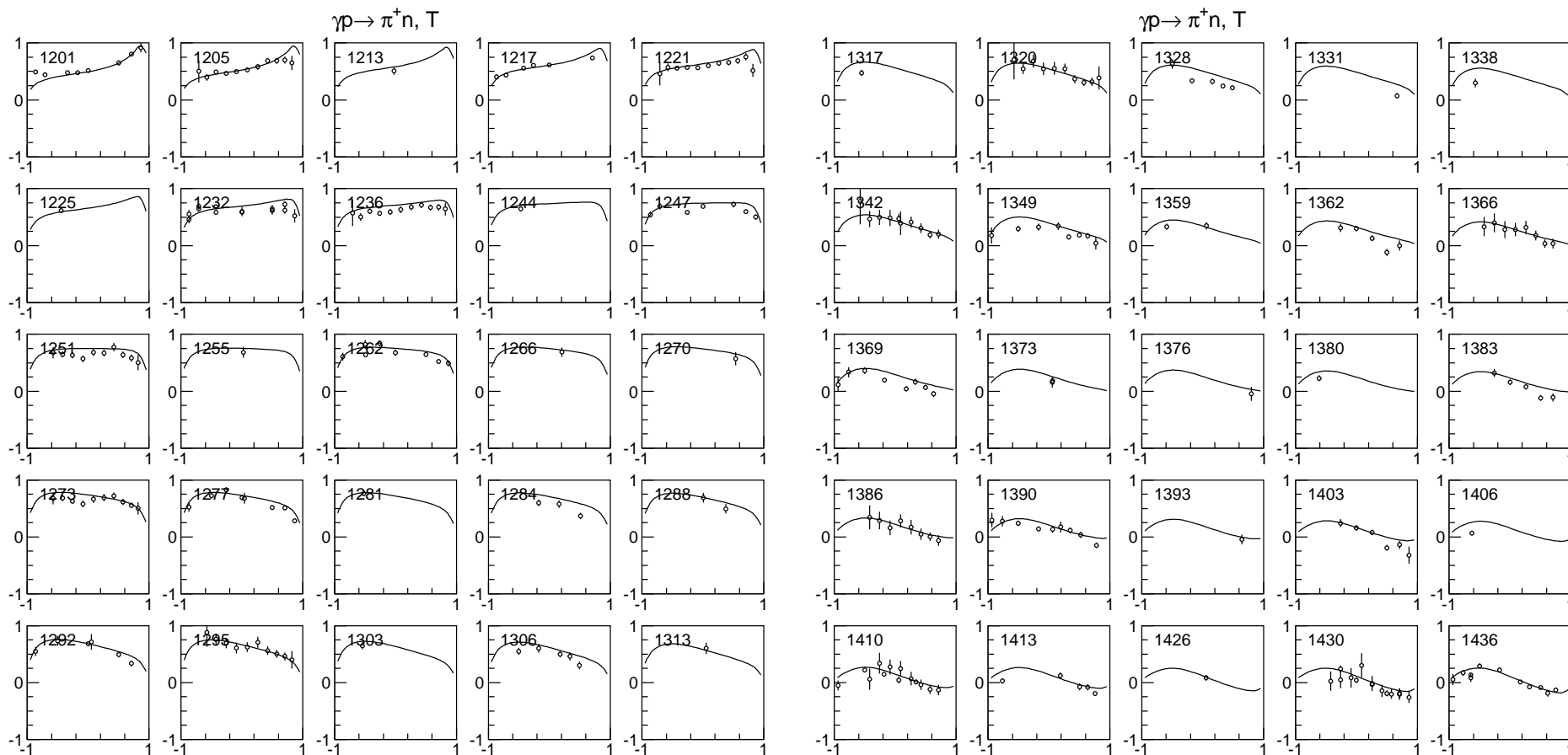


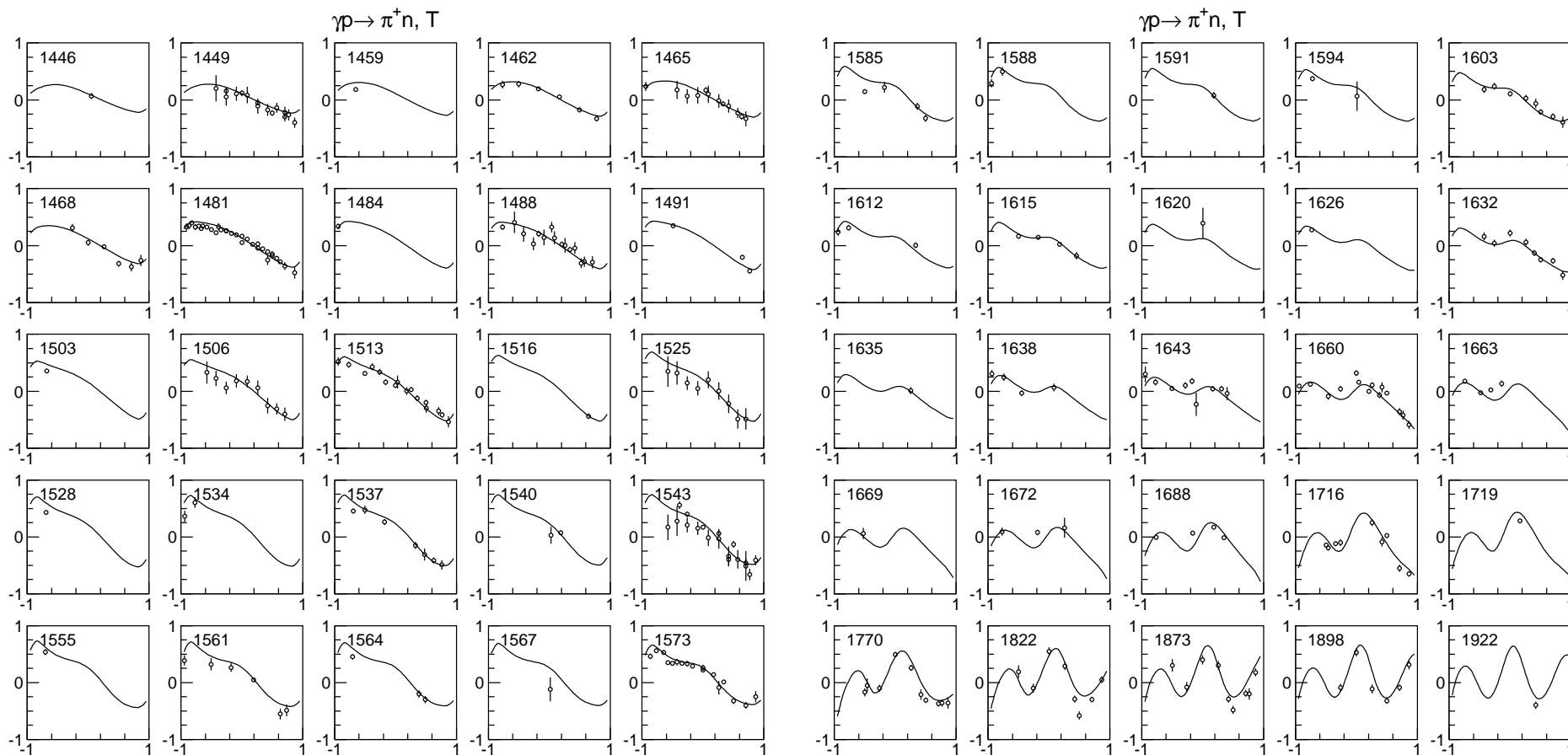




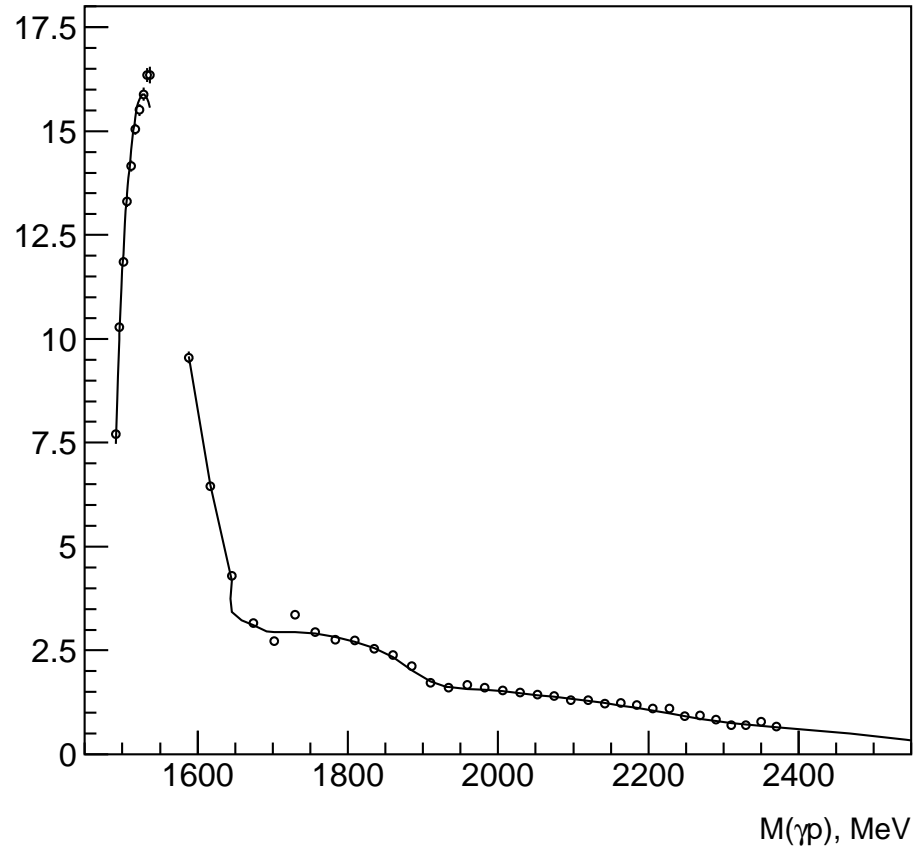




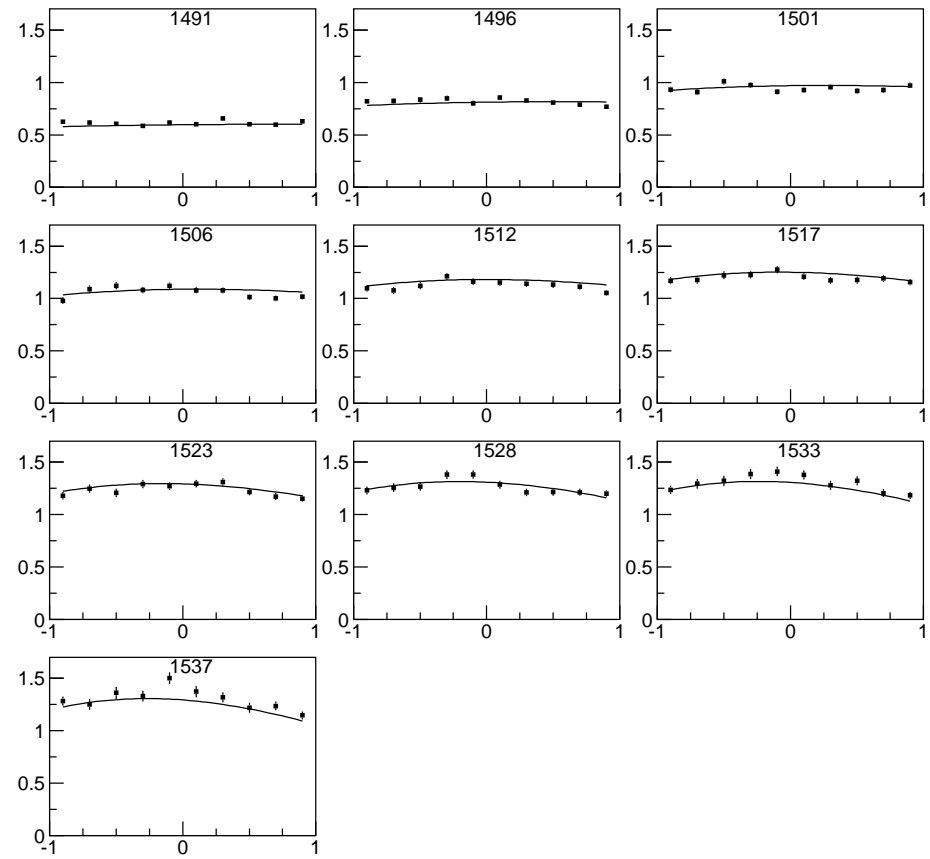


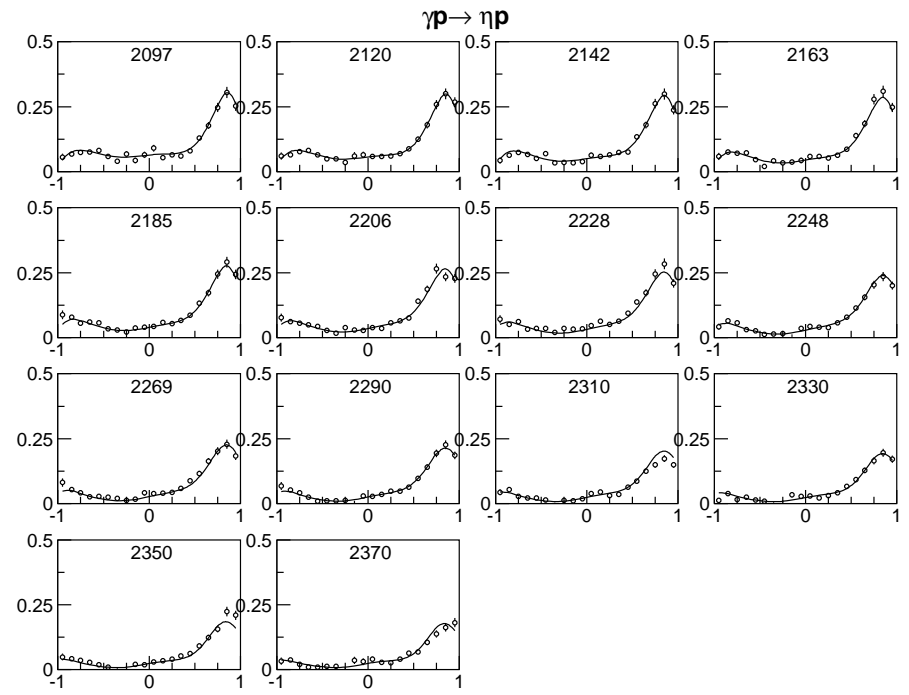
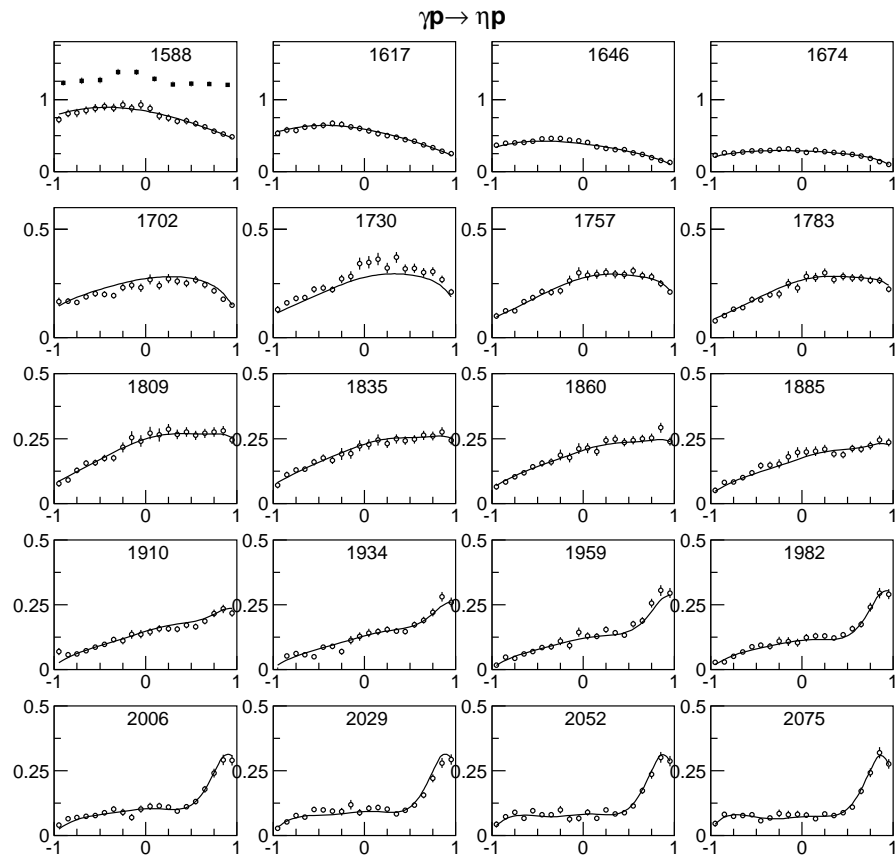


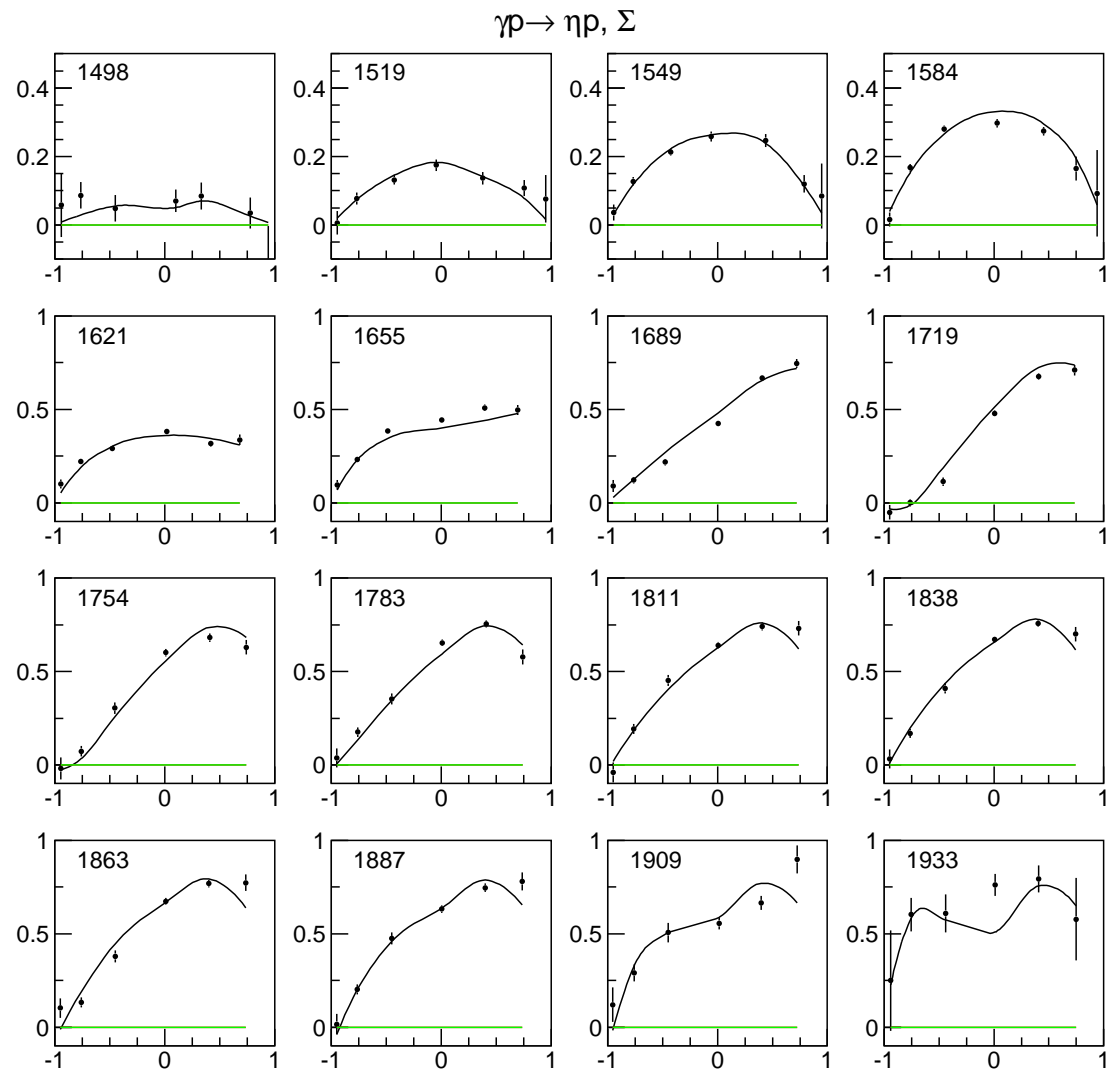
$\gamma p \rightarrow \eta p$

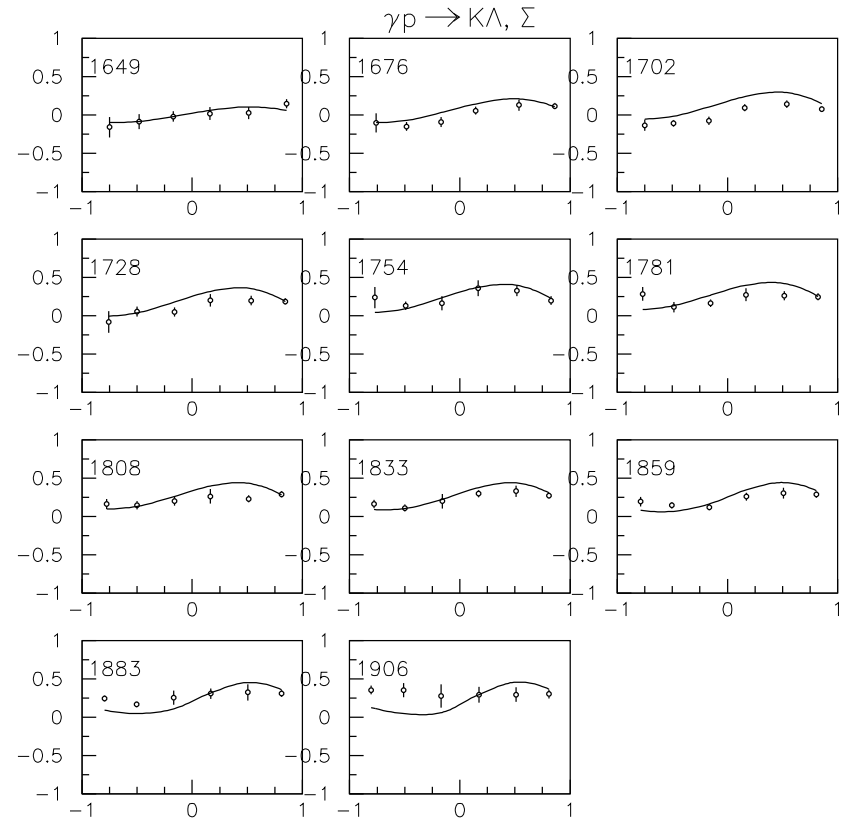
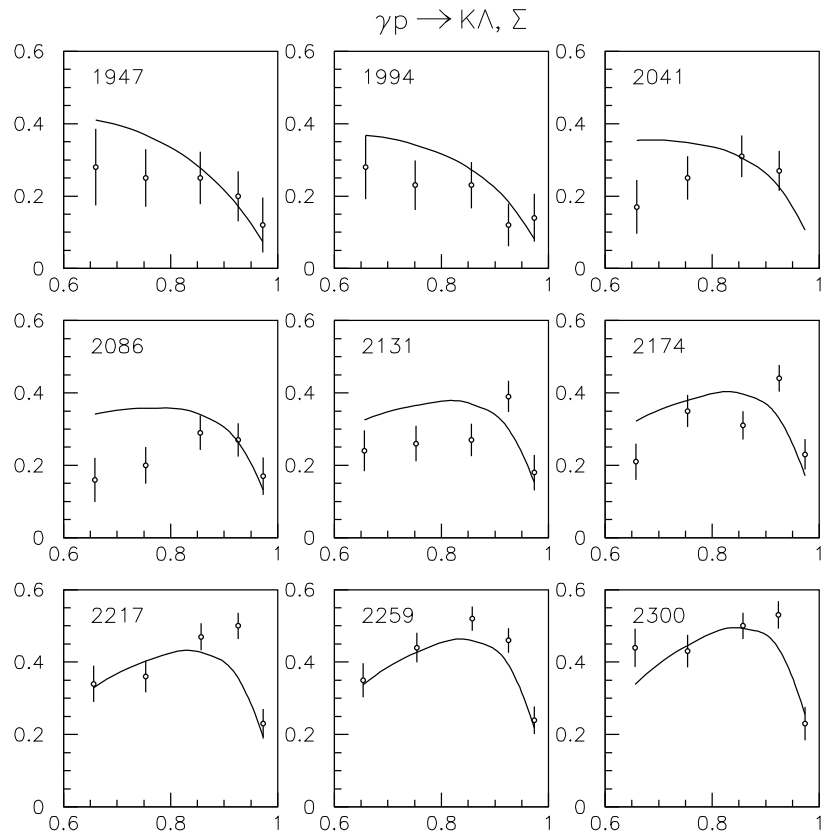


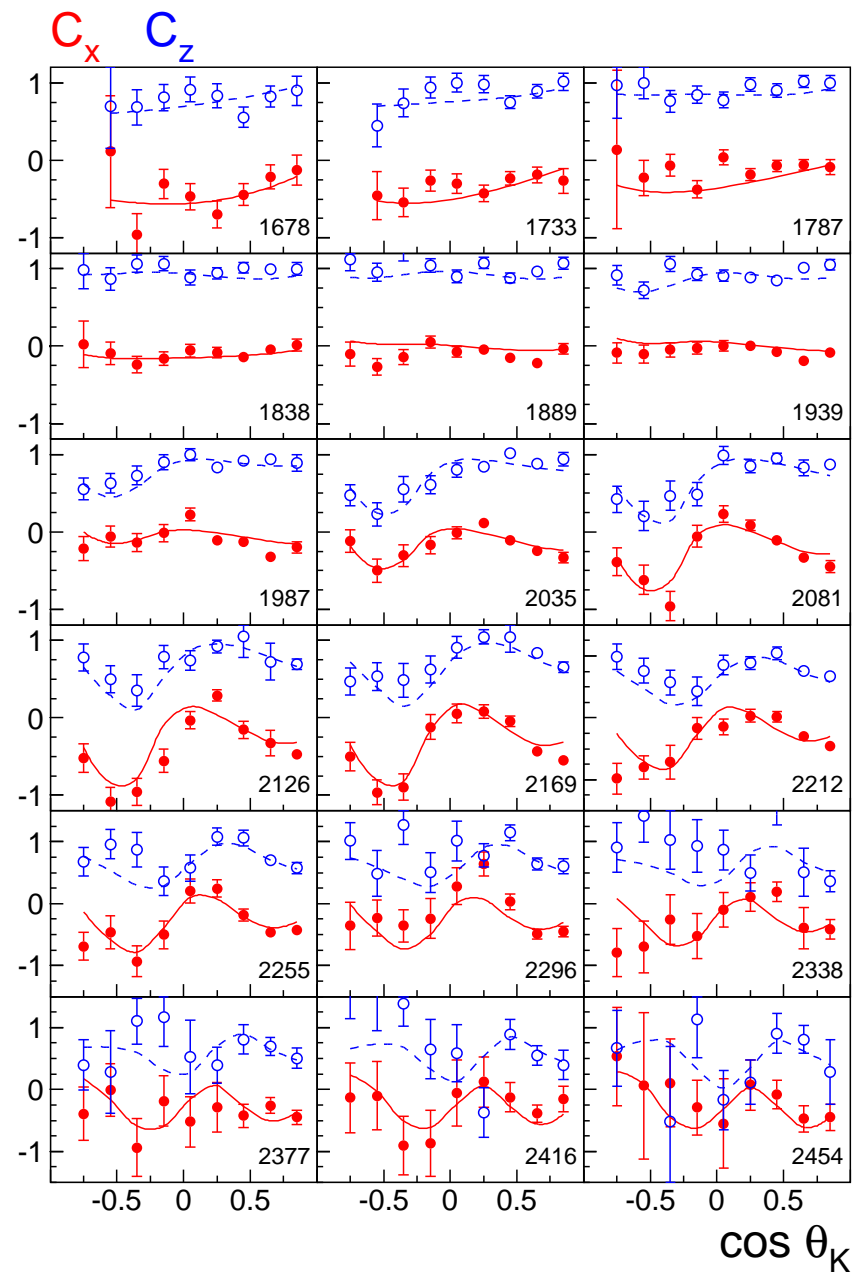
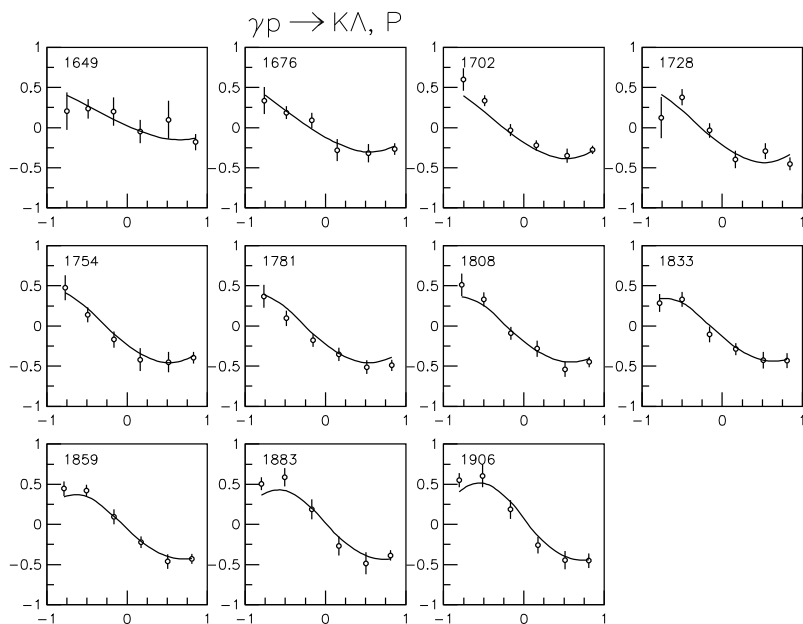
$\gamma p \rightarrow \eta p$

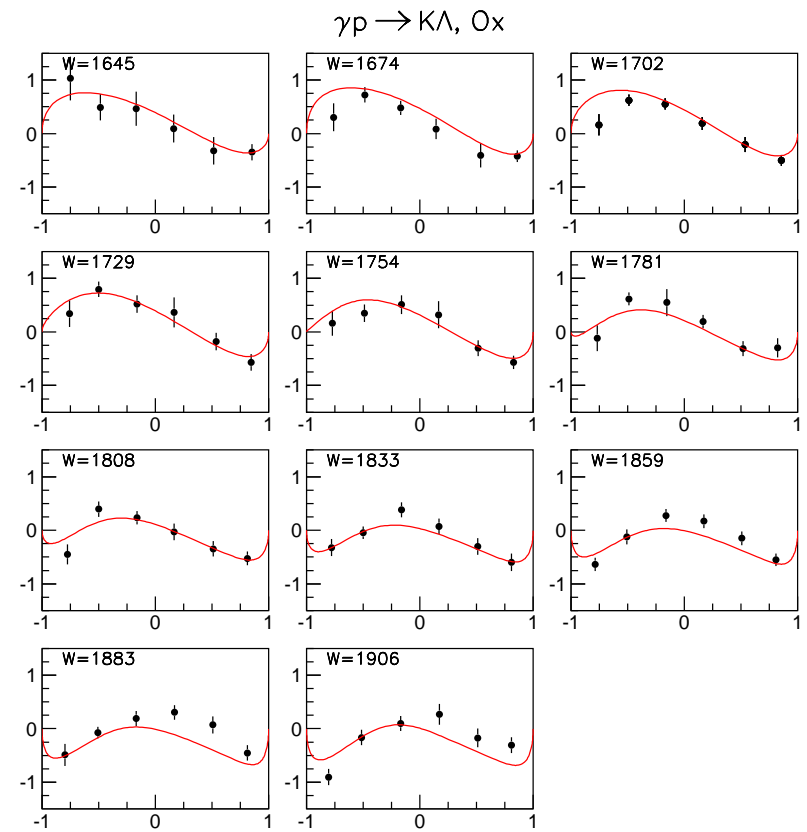
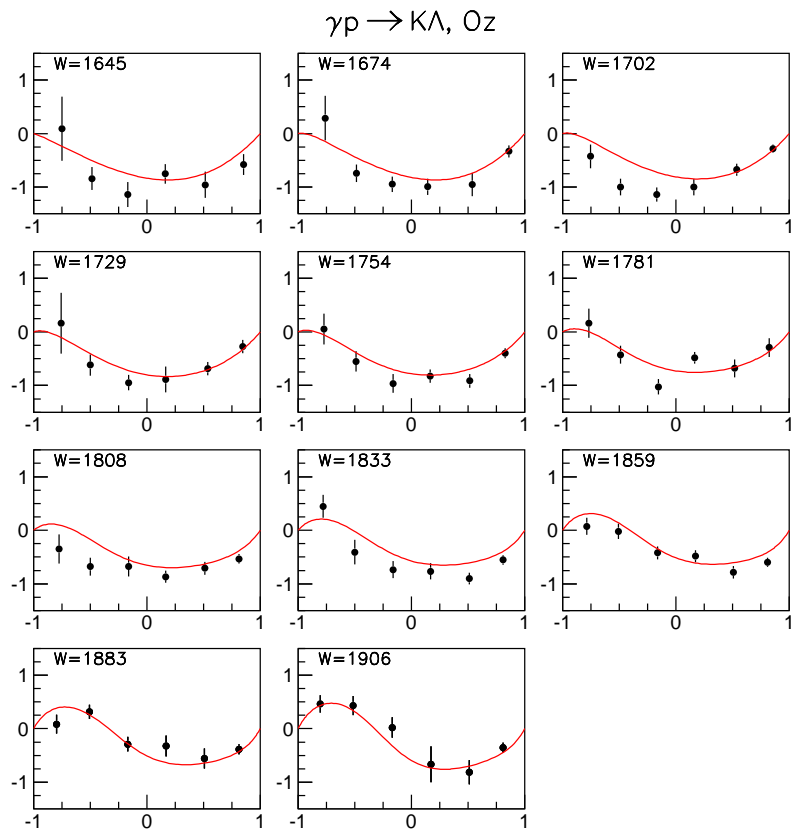


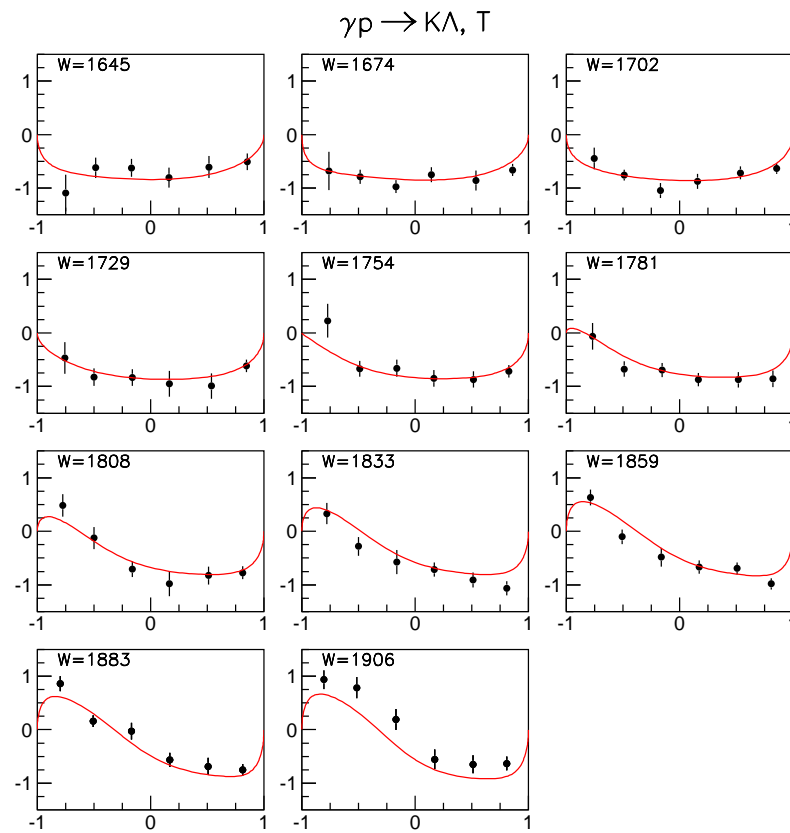


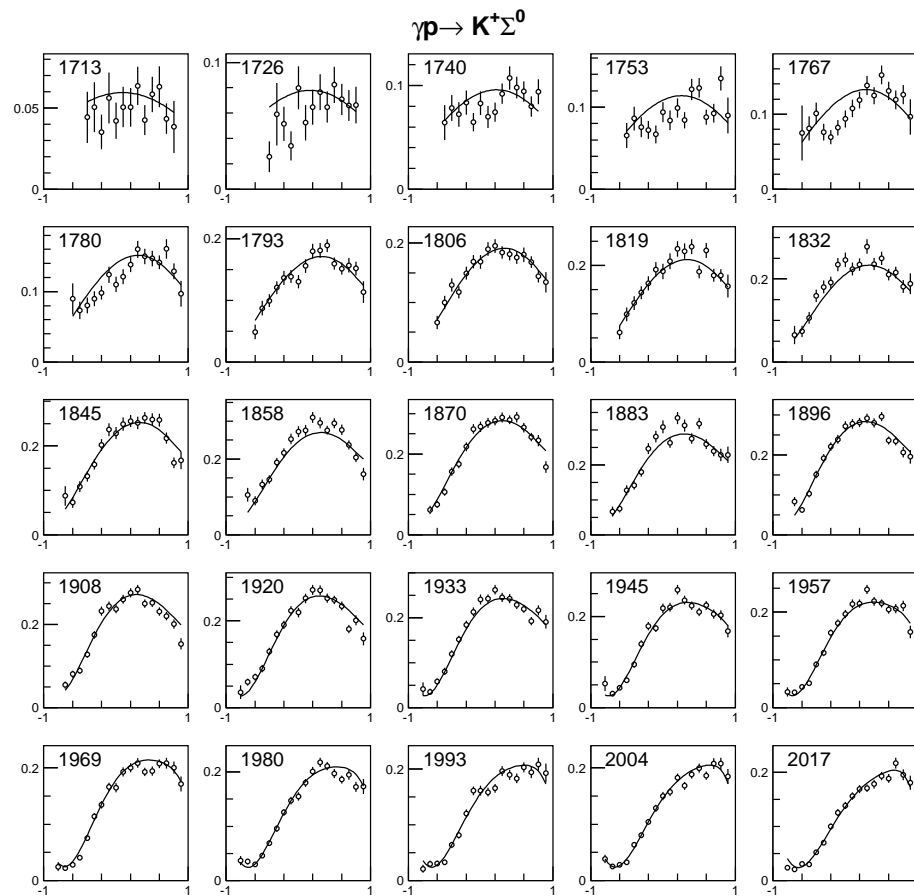
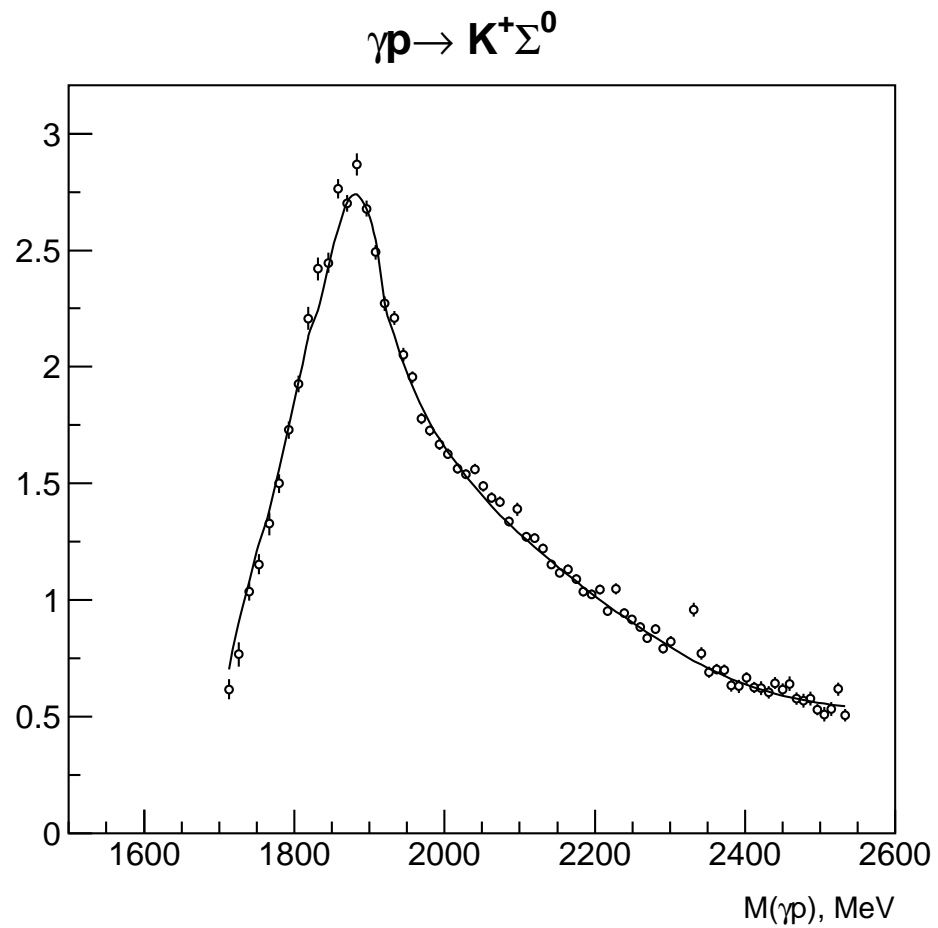


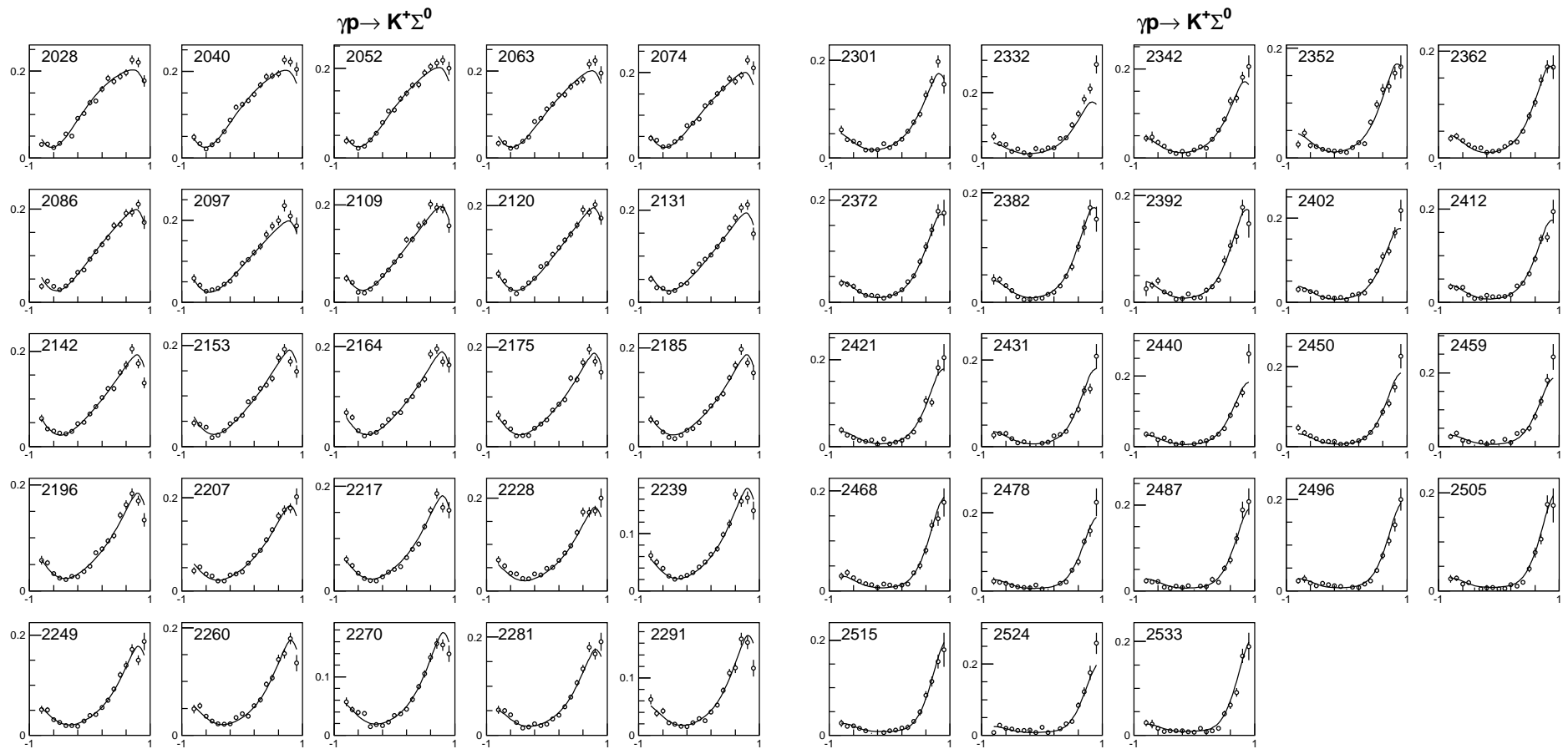


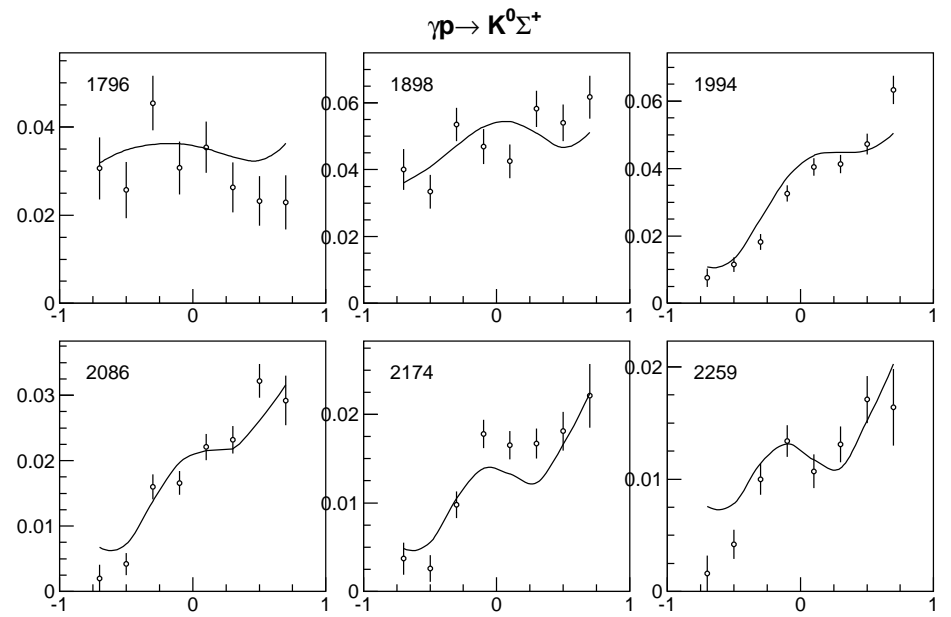
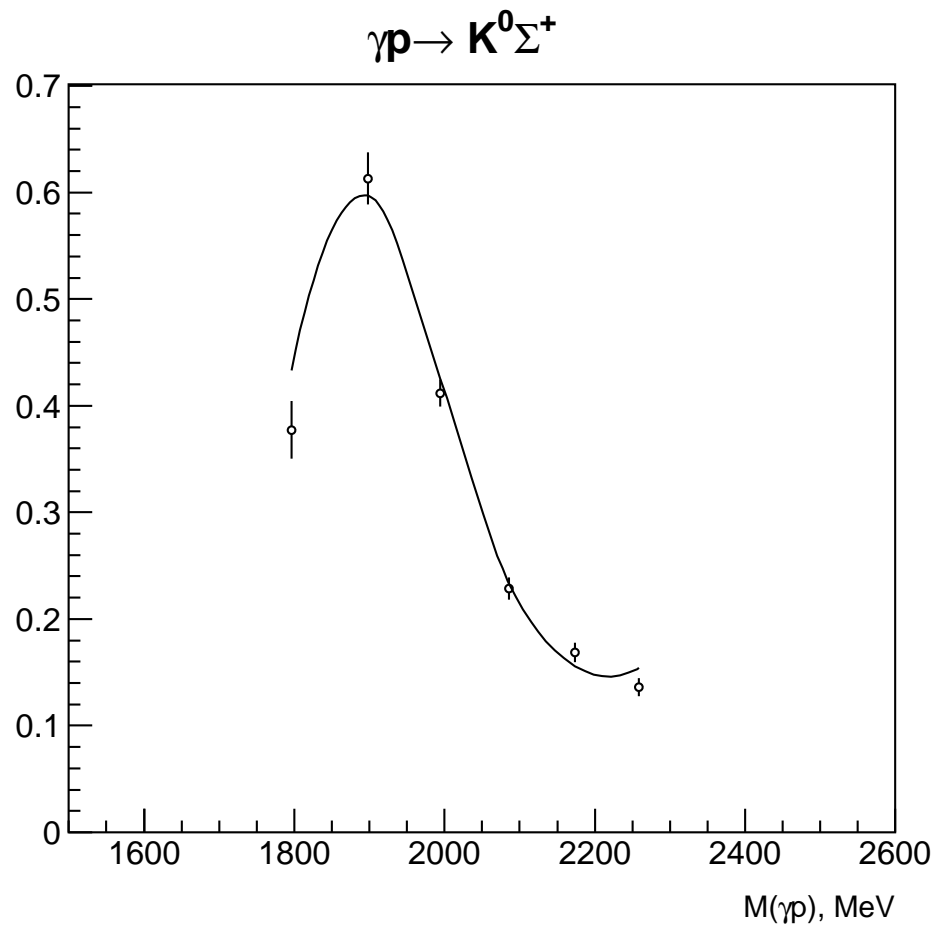


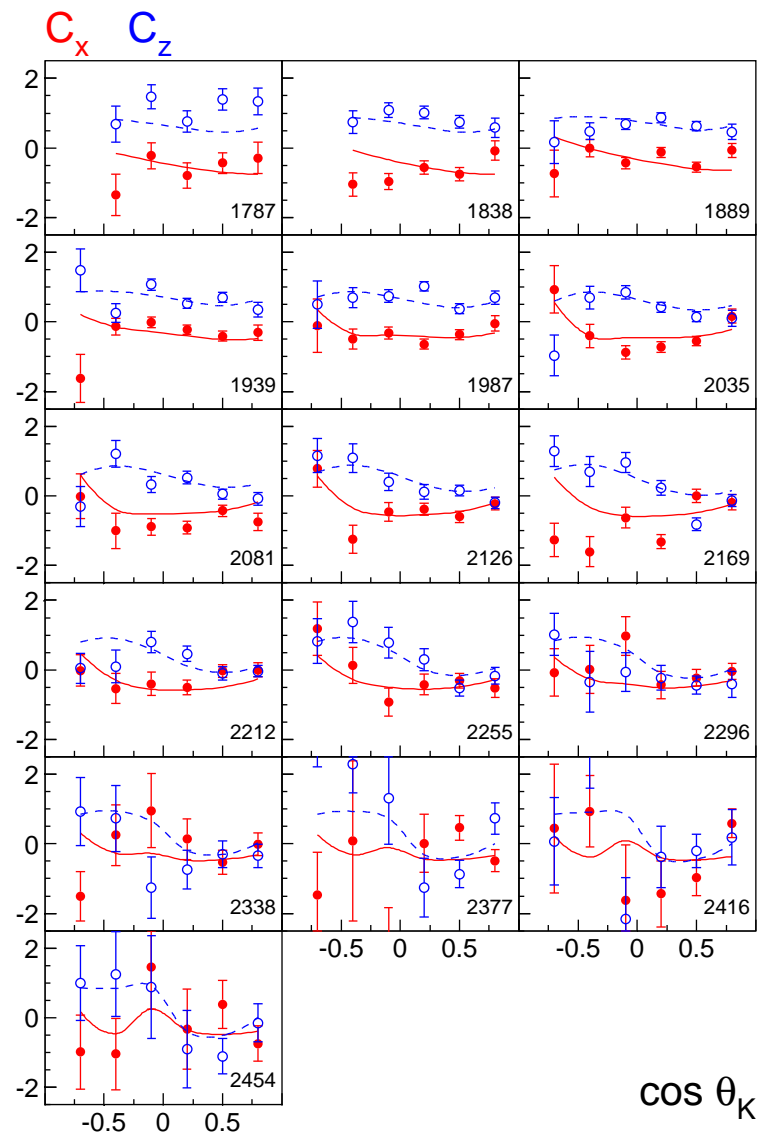
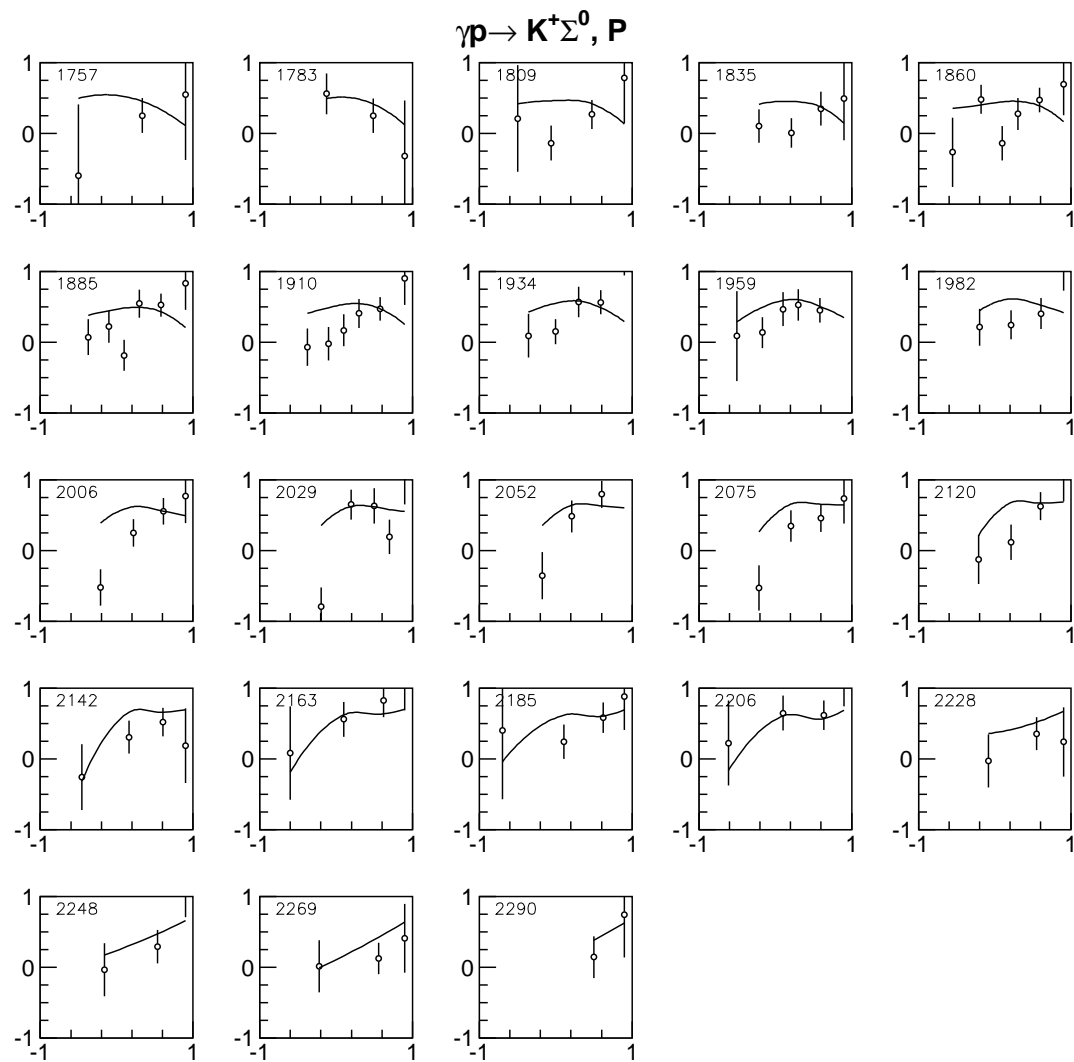


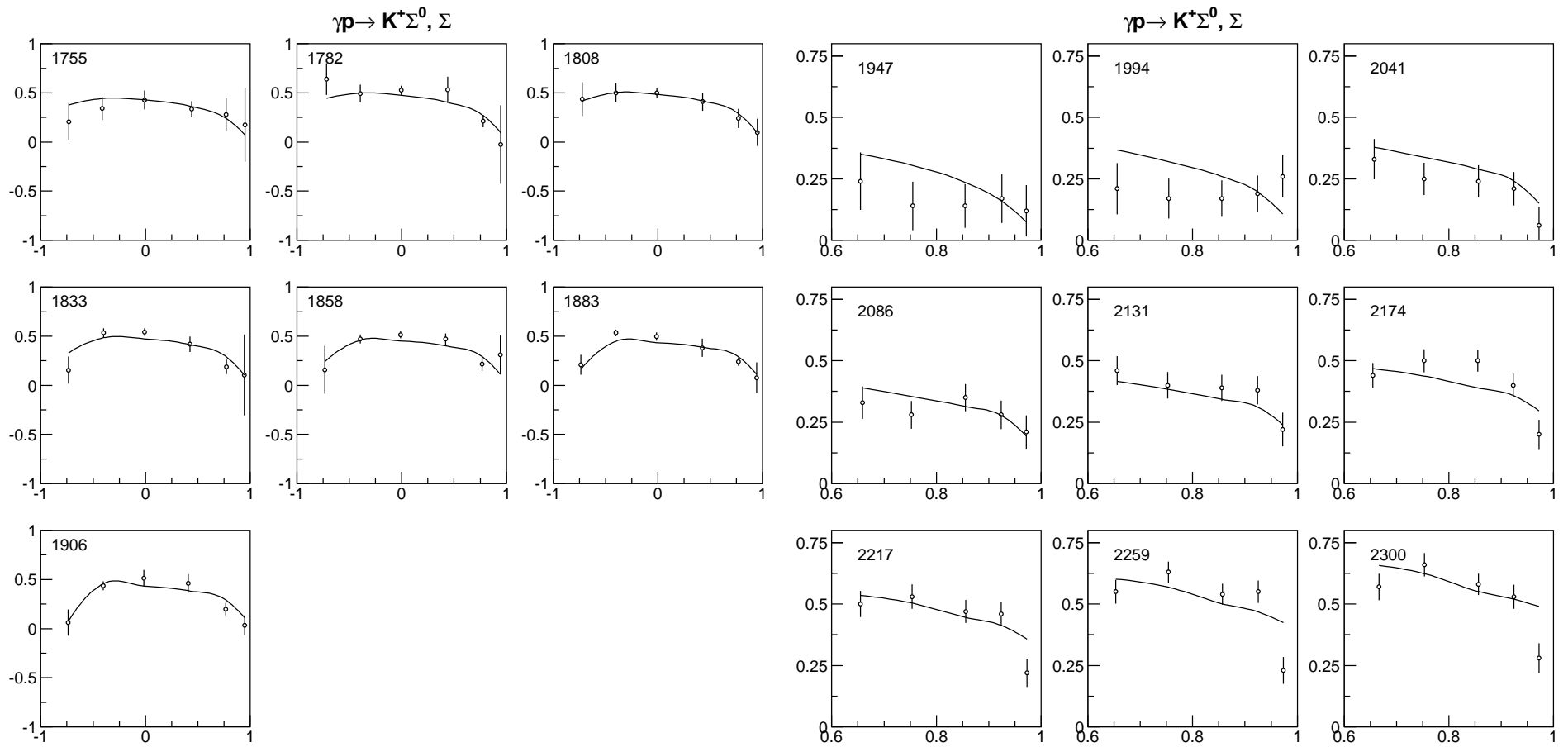


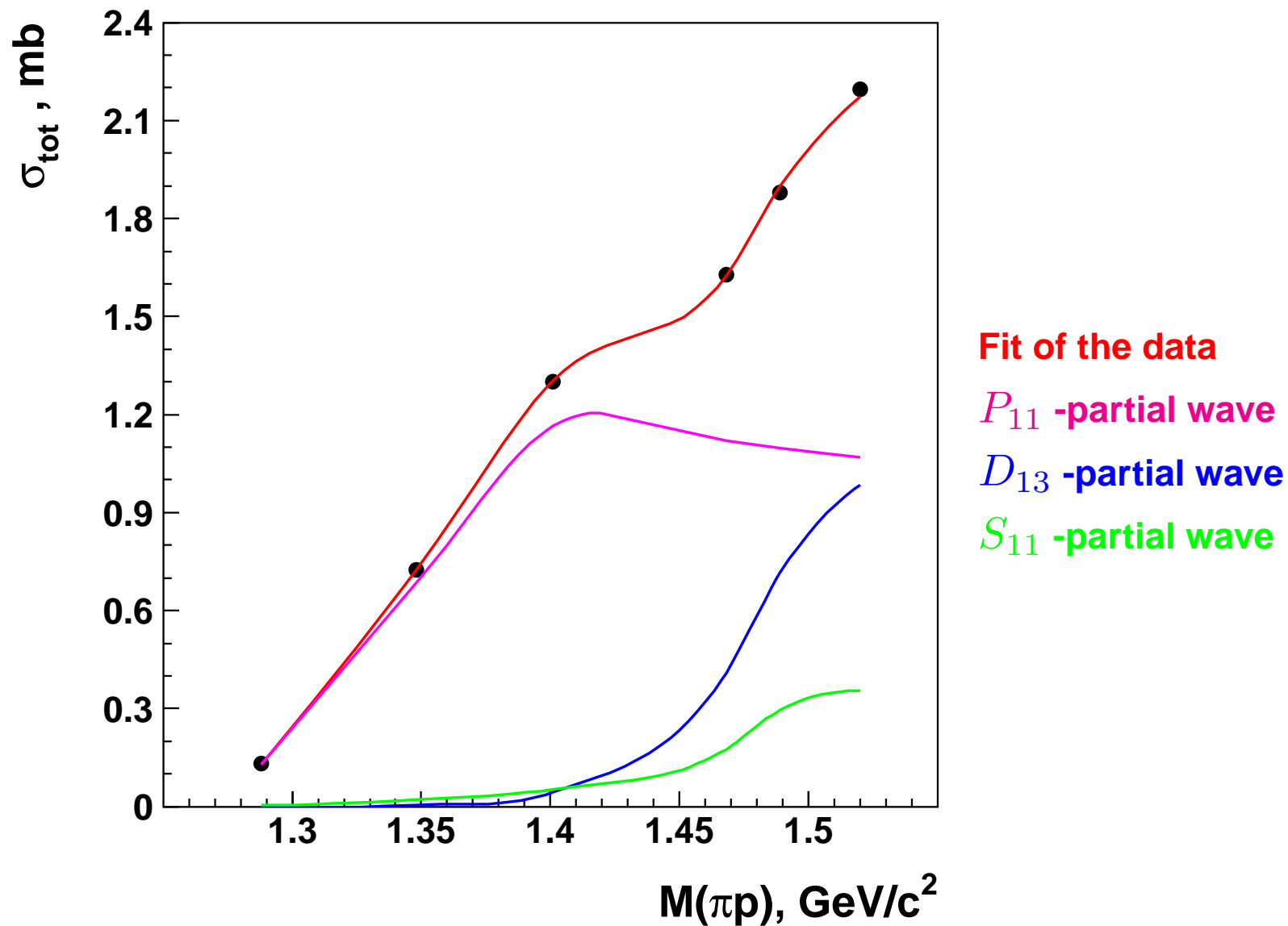






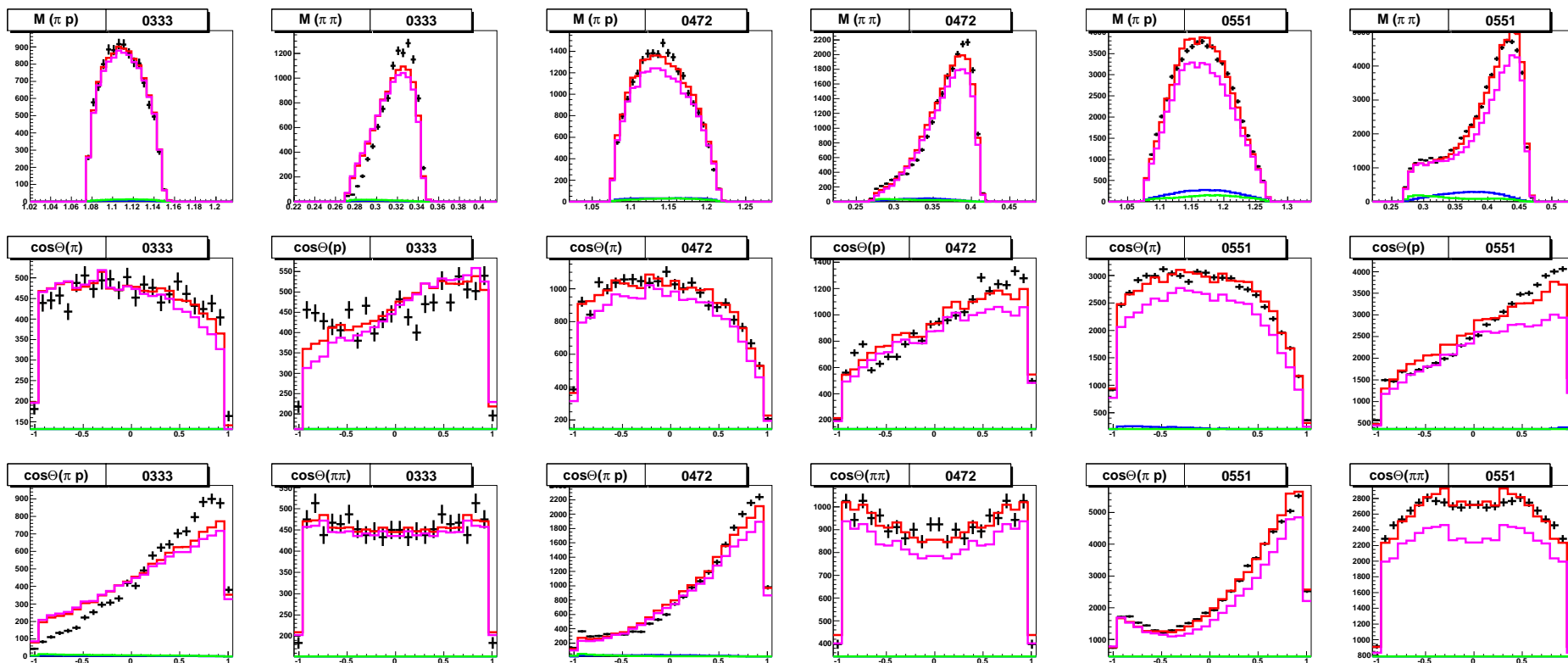




$\pi^- p \rightarrow n\pi^0\pi^0$ (Crystal Ball) total cross section

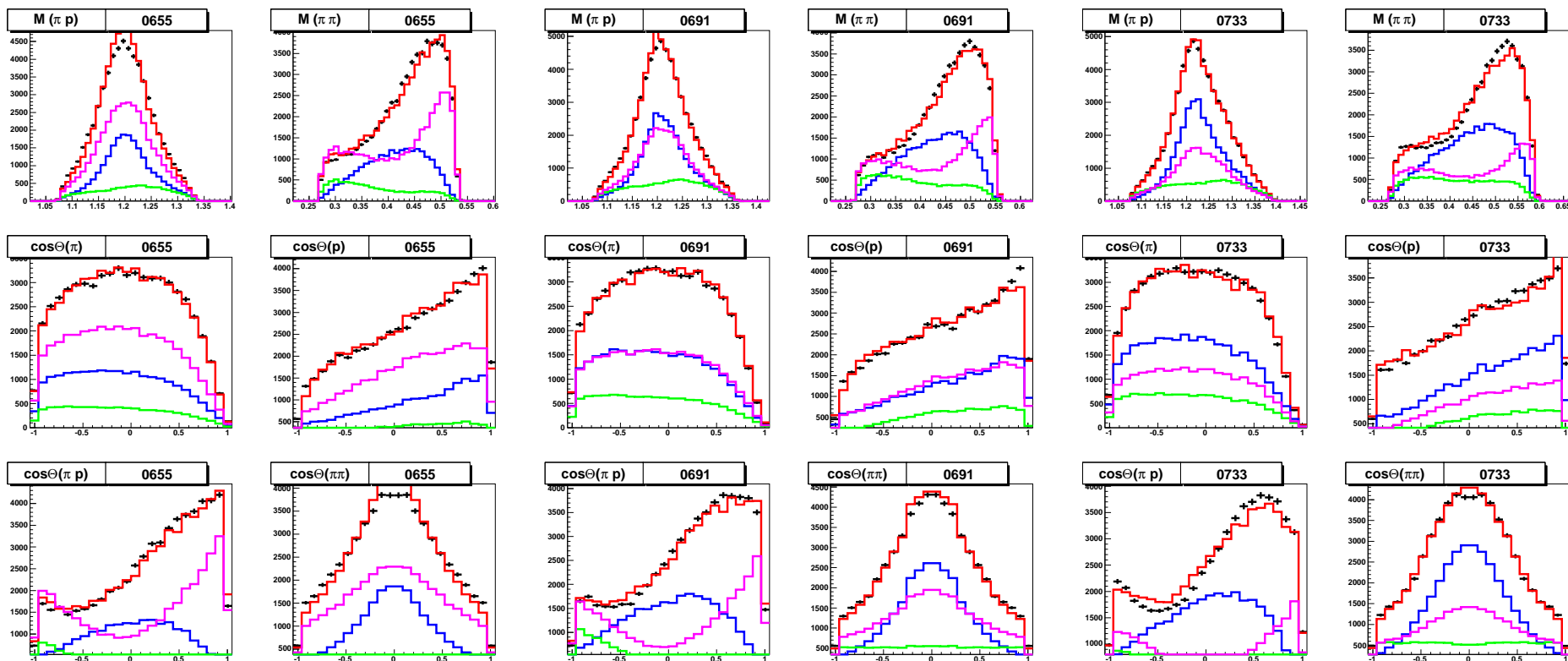
$\pi^- p \rightarrow n\pi^0\pi^0$ (Crystal Ball)

Differential cross sections for 333,472 and 551 MeV/c data.



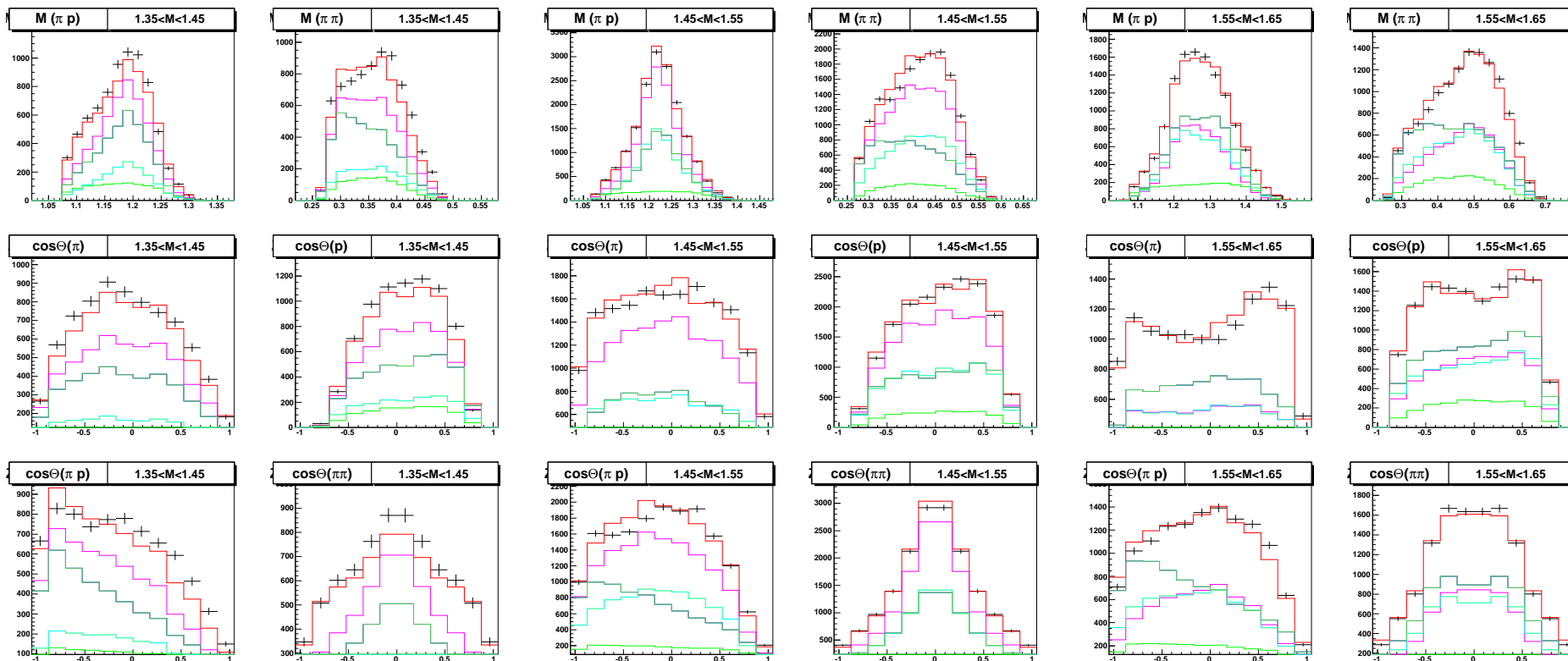
$\pi^- p \rightarrow n\pi^0\pi^0$ (Crystal Ball)

Differential cross sections for 655, 691 and 733 MeV/c data.



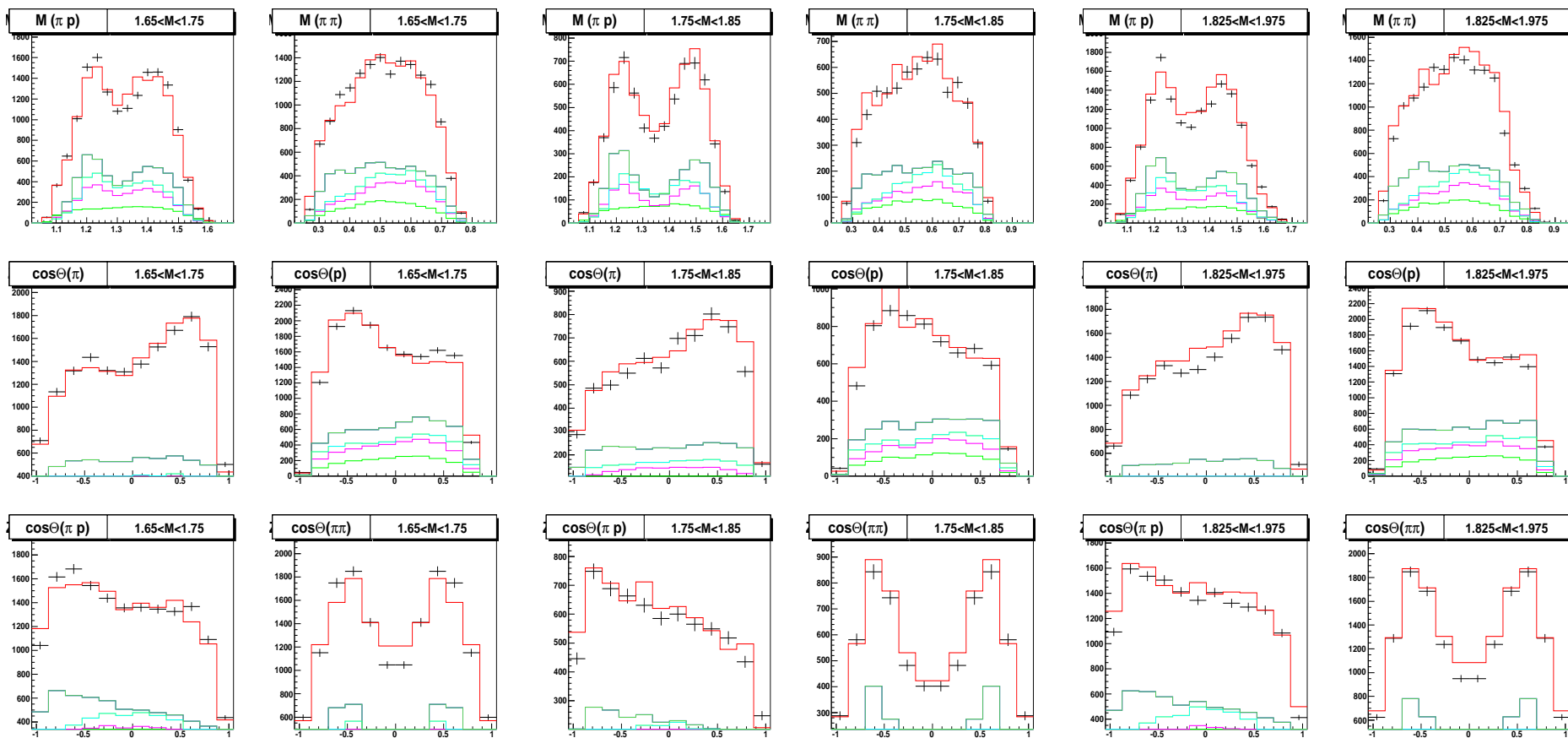
$\gamma p \rightarrow p\pi^0\pi^0$ (CB-ELSA)

Differential cross sections for W=1400, 1500 and 1600 MeV data.



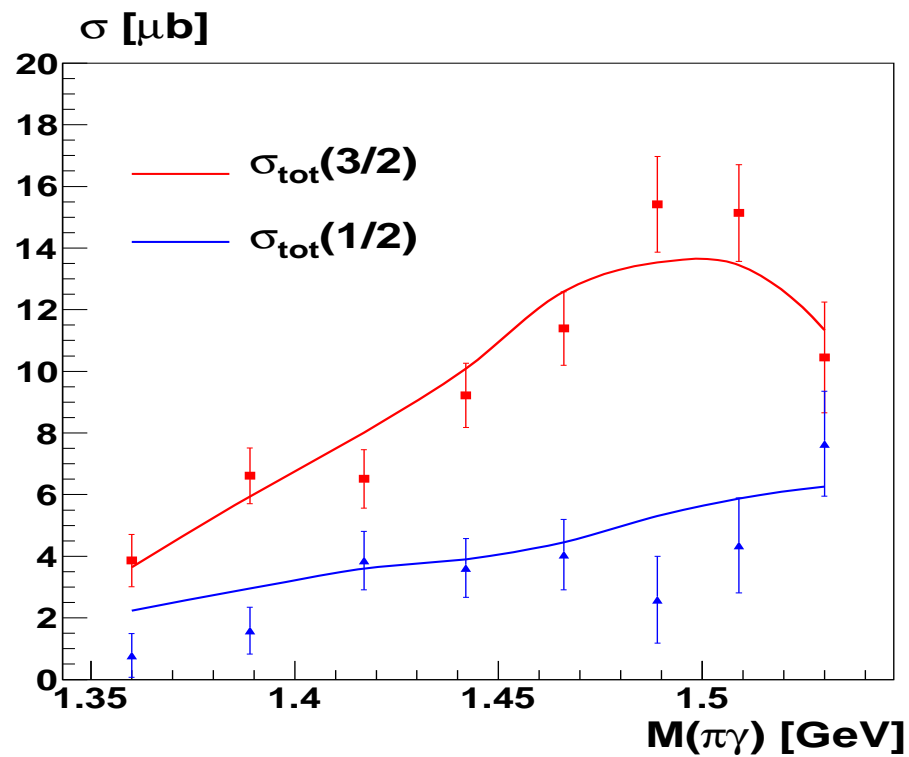
$$\gamma p \rightarrow p\pi^0\pi^0 \text{ (CB-ELSA)}$$

Differential cross sections for W=1700, 1800 and 1900 MeV data.



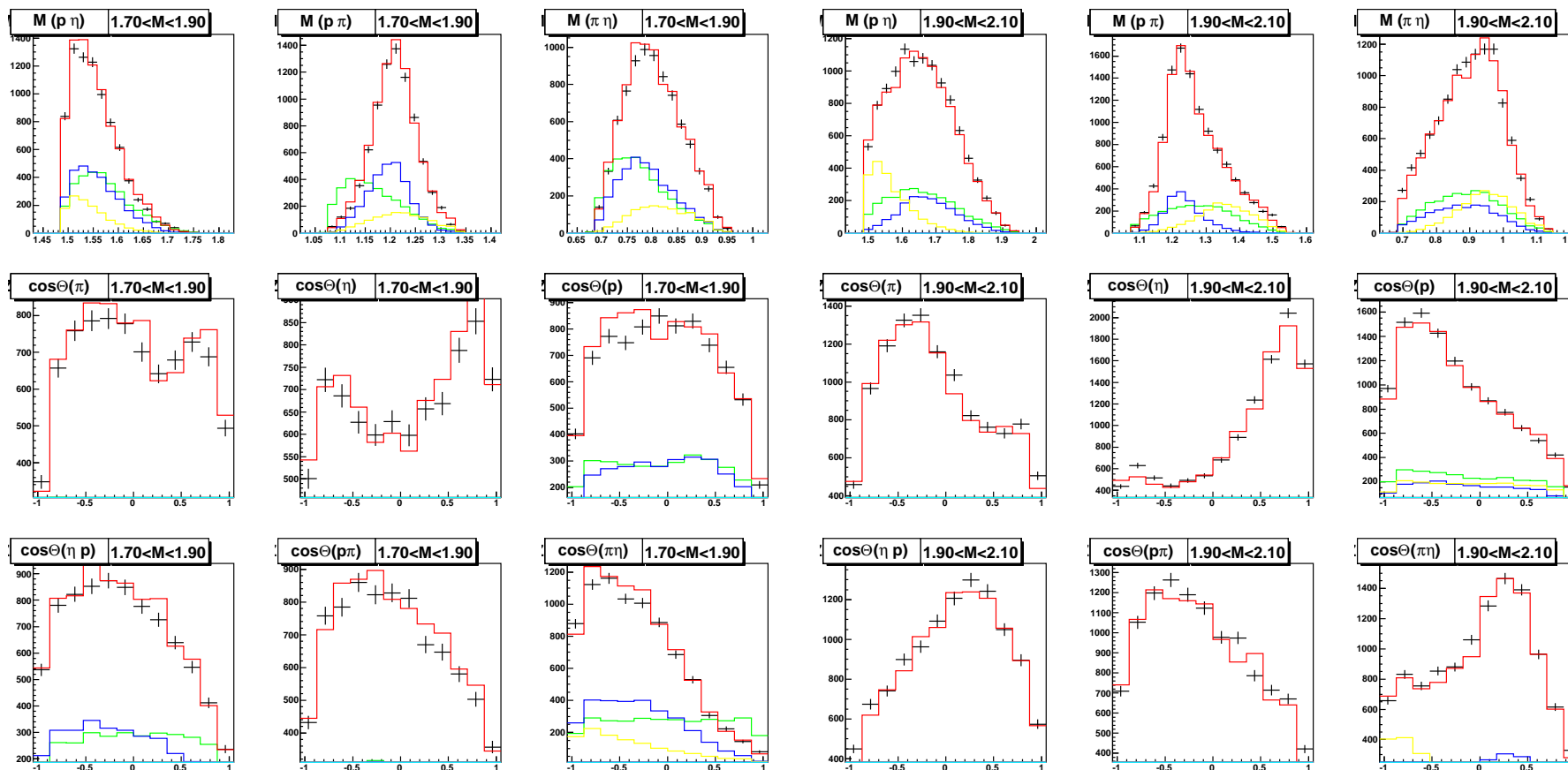
$$\gamma p \rightarrow p\pi^0\pi^0 \text{ (MAMI)}$$

Differential cross sections $S = 3/2$ and $S = 1/2$.



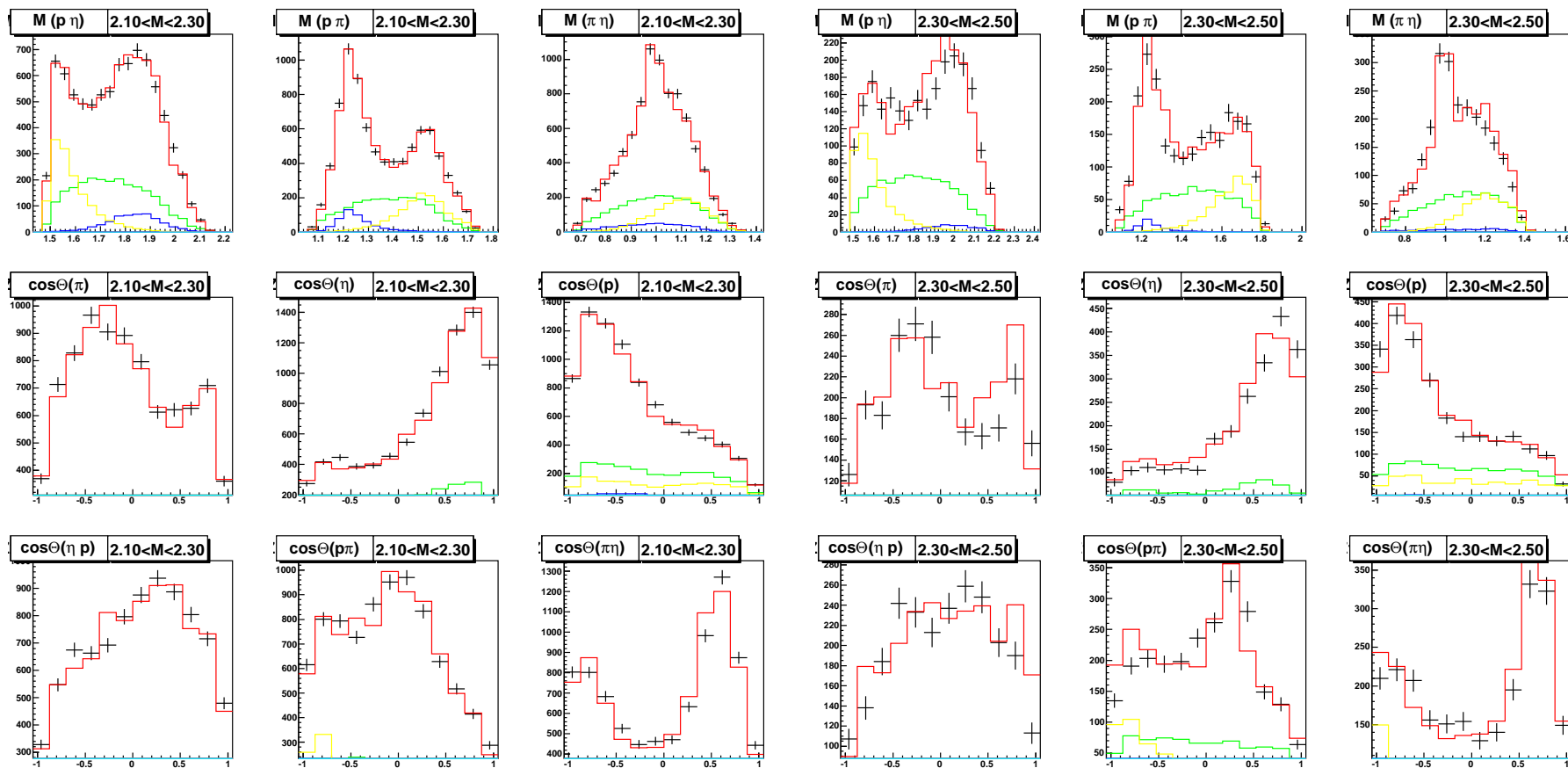
$\gamma p \rightarrow p\eta\pi^0$ (CB-ELSA)

Differential cross sections for W=1700 and 1800 MeV data.



$$\gamma p \rightarrow p \eta \pi^0 \text{ (CB-ELSA)}$$

Differential cross sections for W=1900 and 2000 MeV data.



$\gamma p \rightarrow p\eta\pi^0$ (CB-ELSA)

Beam asymmetry data.

